

การกักเก็บและการปล่อยแบบควบคุมของไฟเพอรินโดยใช้อนุภาคระดับนาโนเมตรของไฮโดรเจล  
ไคโตซาน

นางสาวพรรณิไท เฟื่องผ่อง

วิทยานิพนธ์นี้เป็นส่วนหนึ่งของการศึกษาตามหลักสูตรปริญญาวิทยาศาสตรมหาบัณฑิต  
สาขาวิชาปิโตรเคมีและวิทยาศาสตร์พอลิเมอร์  
คณะวิทยาศาสตร์ จุฬาลงกรณ์มหาวิทยาลัย  
ปีการศึกษา 2555

ลิขสิทธิ์ของเอกสารฉบับนี้สงวนไว้โดย  
บัณฑิตยและแฟ้มข้อมูลฉบับเต็มของวิทยานิพนธ์ฉบับนี้สงวนไว้โดย  
เป็นแฟ้มข้อมูลของนิสิตเจ้าของวิทยานิพนธ์ที่ส่งผ่านทางบัณฑิตวิทยาลัย

The abstract and full text of theses from the academic year 2011 in Chulalongkorn University Intellectual Repository (CUIR)  
are the thesis authors' files submitted through the Graduate School.

ENCAPSULATION AND CONTROLLED RELEASE OF PIPERINE USING  
HYDROGEL CHITOSAN NANOPARTICLES

Miss Thatthai Pengpong

A Thesis Submitted in Partial Fulfillment of the Requirements  
for the Degree of Master of Science Program in Petrochemistry and Polymer Science

Faculty of Science

Chulalongkorn University

Academic Year 2012

Copyright of Chulalongkorn University

Thesis Title	ENCAPSULATION AND CONTROLLED RELEASE OF PIPERINE USING HYDROGEL CHITOSAN NANOPARTICLES
By	Miss Thatthai Pengpong
Field of Study	Petrochemistry and Polymer Science
Thesis Advisor	Associate Professor Polkit Sangvanich, Ph.D.

---

Accepted by the Faculty of Science, Chulalongkorn University in  
Partial Fulfillment of the Requirements for the Master's Degree

.....Dean of the Faculty of Science  
(Professor Supot Hannongbua, Dr.rer.nat.)

#### THESIS COMMITTEE

.....Chairman  
(Professor Pattarapan Prasassarakich, Ph.D.)

.....Thesis Advisor  
(Associate Professor Polkit Sangvanich, Ph.D.)

.....Examiner  
(Associate Professor Wimonrat Trakarnpruk, Ph.D.)

.....External Examiner  
(Assistant Professor Nalena Praphairaksit, D.V.M., Ph.D.)

พรรณไพ เพิ่งผ่อง: การกักเก็บและการปล่อยแบบควบคุมของไพเพอรีนโดยใช้อนุภาคระดับนาโนเมตรของไฮโดรเจลไคโตซาน (ENCAPSULATION AND CONTROLLED RELEASE OF PIPERINE USING HYDROGEL CHITOSAN NANOPARTICLES) อ.ที่ปรึกษาวิทยานิพนธ์หลัก: รศ.ดร.พลกฤษณ์ แสงวณิช, 96 หน้า.

วัตถุประสงค์ของงานวิจัยชิ้นนี้คือการเพิ่มคุณสมบัติการยึดติดเยื่อเมือกของไคโตซานและประเมินผลสำหรับการประยุกต์ใช้พอลิเมอร์ในระบบการนำส่งยาประเภทไฮโดรโฟบิก ไทโอเลเทคไคโตซานสังเคราะห์โดยโควาลেন্টครดพาราควาริกเพื่อเพิ่มส่วนไฮโดรโฟบิกและคอนจูเกตไฮโมซิสเตอิน-ไทโอแลกโตนเพื่อปรับปรุงคุณสมบัติการยึดติดเยื่อเมือกของไคโตซาน พิสูจน์เอกลักษณ์ไคโตซานที่ดัดแปรแล้วด้วยเทคนิค NMR, FTIR และ TGA ศึกษาสมบัติการยึดติดเยื่อเมือกและการบวมตัวในระบบทางเดินอาหารจำลอง (pH 1.2, 4.0 และ 6.4) สมบัติการยึดติดเยื่อเมือกของไทโอเลเทคไคโตซานสูงกว่าไคโตซานประมาณ 9.87, 2.01 และ 1.58 เท่า ในการทดสอบทั้งสามพีเอช นอกจากนี้ไทโอเลเทคไคโตซานยังเป็นพอลิเมอร์สำหรับนำส่งยาประเภทไฮโดรโฟบิก งานวิจัยนี้ใช้ไพเพอรีนเป็นยาไฮโดรโฟบิกซึ่งช่วยเพิ่มการดูดซึมสารอาหารและยาในระบบทางเดินอาหารบริเวณลำไส้เล็กเตรียมอนุภาคโดยใช้เทคนิคอิเล็กทออสเปรย์ อนุภาคมีรูปร่างเป็นทรงกลมขนาดใกล้เคียงกัน มีขนาดเฉลี่ย 3-4 ไมโครเมตร สามารถกักเก็บไพเพอรีนได้มากกว่า 80 เปอร์เซ็นต์ และมีคุณสมบัติยึดติดเยื่อเมือกสูงกว่าไคโตซาน 5.72, 1.59 และ 1.55 เท่า ในการทดสอบที่พีเอช 1.2, 4.0 และ 6.4 ตามลำดับสุดท้ายอนุภาคไทโอเลเทคไคโตซานสามารถปลดปล่อยไพเพอรีนได้นานถึง 12 ชั่วโมง

สาขาวิชา ปิโตรเคมีและวิทยาศาสตร์พอลิเมอร์ ลายมือชื่อนิสิต.....

ปีการศึกษา.....2555..... ลายมือชื่อ อ.ที่ปรึกษาวิทยานิพนธ์หลัก.....

## 5372251723: MAJOR PETROCHEMISTRY AND POLYMER SCIENCE

KEYWORDS: THIOLATED CHITOSAN / PIPERINE / ENCAPSULATION / CONTROLLED RELEASE

THATTHAI PENG PONG: ENCAPSULATION AND CONTROLLED RELEASE OF PIPERINE USING HYDROGEL CHITOSAN NANOPARTICLES. ADVISOR: ASSOC. PROF. POLKIT SANGVANICH, Ph.D., 96 pp.

The objective of this research was to increase the mucoadhesive property of chitosan and evaluate for its application in mucoadhesive hydrophobic drug delivery systems. Thiolated chitosan (pCA-HT-chitosan) was synthesized by the covalent attachment of *p*-coumaric acid (pCA) to increase hydrophobic part and conjugated homocysteine thiolactone (HT) to improve mucoadhesive property of chitosan. The modified chitosan was characterized by NMR, FTIR and TGA. The mucoadhesive and swelling properties were studied at the simulated gastric tract (pH 1.2, 4.0, and 6.4). The mucoadhesive properties of pCA-HT-chitosan higher than chitosan about 9.87-, 2.01- and 1.58-fold in all tested three pHs. Furthermore, the thiolated chitosan as hydrophobic drug carrier systems. This research used piperine (PIP) as hydrophobic drug that was investigated in order to increase the nutrients/drug adsorption in intestinal fluid. The microspheres were fabricated using electrospray ionization technique. The particles were nearly spherical in shape with an average size of 3 - 4  $\mu\text{m}$ , entrapped piperine (PIP) over than 80% EE and the mucoadhesive properties displayed 5.72-, 1.59- and 1.55-fold stronger than the unmodified chitosan at pH 1.2, 4.0, and 6.4 respectively. Final the formulations could sustain release of piperine with % cumulative drug over within 12 h in vitro.

Field of Study : Petrochemistry and Polymer Science Student's Signature.....

Academic Year : .....2012..... Advisor's Signature.....

## ACKNOWLEDGEMENTS

I would like to express my deepest appreciation and gratitude to my advisor, Associate Professor Dr. Polkit Sangvanich, for his excellent suggestion, guidance, encouragement and supportiveness throughout the entire period of conducting this thesis. I would like to thank Associate Professor Dr. Nongnuj Muangsin for their suggestion, helping and teaching me the experimental techniques throughout this work.

Additionally, I wish to express my grateful thank to Dr. Krisana Siraleartmukul for her valuable advice. Furthermore, the author also thank the Center for Petroleum, Petrochemicals and Advanced Materials, Chulalongkorn University, Bangkok 10330, Thailand and the center of Chitin-Chitosan Biomaterial, Metallurgy and Materials Science Research Institute of Chulalongkorn University for providing the equipment, chemicals, and facilities.

I would also like to thank Associate Professor Dr. Pattarapan Prasassarakich, Associate Professor Dr. Wimonrat Trakarnpruk and Assistant Professor Dr. Nalena Praphiraksit attending as the chairman and members of my thesis committee, respectively, for their kind guidance and valuable suggestions and comments.

Finally, I would like to express thanks to my family for their care and supports to make my study successful. Thanks are also due to everyone who has contributed suggestions and supports throughout my research.

# CONTENTS

	<b>Page</b>
ABSTRACT (THAI).....	iv
ABSTRACT (ENGLISH).....	v
ACKNOWLEDGEMENTS.....	vi
CONTENTS.....	vii
LIST OF TABLES.....	xi
LIST OF FIGURES.....	xiii
LIST OF ABBREVIATIONS.....	xv
CHAPTER I INTRODUCTION.....	1
1.1 Introduction.....	1
1.2 The objectives of this research.....	8
1.3 The scope of research.....	8
1.4 Flow chart of methodology.....	10
CHAPTER II THEORY AND LITERATURE REVIEWS.....	11
2.1 Controlled release.....	11
2.2 Mucoadhesion.....	13
2.3 Thiolated polymer.....	18
2.4 Coronary heart disease.....	19
2.5 Piperine.....	20
2.6 Electrospray ionization technique.....	21
CHAPTER III EXPERIMENTAL.....	25
3.1 Materials.....	25
3.2 Methods.....	26
3.2.1 Synthesis of thiolated chitosan.....	26
3.2.2 Characterization.....	27

	<b>Page</b>
3.2.2.1 FTIR.....	27
3.2.2.2 NMR.....	28
3.3.2.3 TGA.....	28
3.2.3 In vitro bioadhesion.....	29
3.2.4 Swelling study.....	30
3.3 Pharmaceutical applications.....	31
3.3.1 Preparation of drugs-loaded polymer microspheres.....	31
3.3.2 Characterization of microspheres.....	31
3.3.2.1 SEM.....	32
3.3.2.2 Particle size measurement.....	32
3.3.2.3 Zeta potential.....	33
3.3.2.4 FTIR.....	33
3.3.3 Study of the drug behavior of the microspheres.....	34
CHAPTER IV RESULTS AND DISCUSSION.....	35
4.1 Synthesis of pCA-CS-chitosan and pCA-HT-chitosan.....	35
4.2 Characterization.....	36
4.2.1 NMR.....	36
4.2.2 FTIR.....	39
4.2.3 TGA.....	39
4.3 Degree of substitution of phenolic and thiol contents.....	41
4.4 Mucoadhesive properties.....	42
4.5 Swelling study.....	44
4.6 Fabrication microspheres.....	47
4.6.1. Morphology.....	47
4.6.2. Characterization of microspheres.....	51
4.6.3. Evaluation of drug encapsulation efficiency.....	54
4.6.4. In vitro drug release.....	55



	<b>Page</b>
CHAPTER V CONCLUSION.....	64
REFERENCE.....	66
APPENDICES.....	71
APPENDIX A .....	72
APPENDIX B.....	73
APPENDIX C.....	75
APPENDIX D.....	77
APPENDIX E .....	80
APPENDIX F .....	84
VITA.....	96

## LIST OF TABLES

<b>Table</b>		<b>Page</b>
2.1	The relative bioadhesive property of various polymers.....	18
3.1	Instruments.....	24
3.2	The conditions for the microspheres preparation.....	31
4.1	Comparison of the levels of their phenolics content in modified chitosan.....	40
4.2	Comparison of the levels of their thiol and disulfide contents in thiolated chitosan.....	41
4.3	Comparison of the different reaction time to mucoadhesive property.....	43
4.4	Effect of composition on morphology of the microsphere.....	56
4.5	Encapsulation of PIP loaded polymer microspheres.....	56
4.6	Effect of composition on mucoadhesive property of the chitosan and modified chitosan microspheres.....	57

## LIST OF FIGURES

Figure	Page
1.1 Structures of chitin and chitosan .....	2
1.2 Structure of <i>p</i> -coumaric acid .....	3
1.3 Structure of homocysteine thiolactone .....	3
1.4 Structure of piperine (a), hydrolysis of piperine (b) and oxidation of piperic acid (c) .....	4
1.5 Influence of polymer to mucoadhesive properties .....	5
1.6 Synthesis scheme of pCA-chitosan (step A) and pCA-HT chitosan (step B) .....	7
1.7 Schematic of drug loaded mucoadhesive particle .....	8
1.8 Flow chart of methodology .....	10
2.1 A schematic drawing illustrating the controlled .....	12
2.2 The two steps of the mucoadhesion .....	15
2.3 Structure of piperine .....	20
2.4 The droplet is generated by electrical force .....	21
3.1 Reaction scheme of the covalent attachment of pCA and HT onto chitosan .....	26
3.2 Preparation of PIP loaded chitosan and modified chitosan microspheres..	31
4.1 Synthesis scheme of pCA-chitosan (step A) and pCA-HT chitosan (step B) .....	34
4.2 Representative <sup>1</sup> H NMR spectra of (a) chitosan, (b) pCA-chitosan and (c) pCA-HT-chitosan .....	36
4.3 Representative FTIR spectra of (a) chitosan, (b) pCA, (c) pCA-chitosan and (d) pCA-HT-chitosan .....	37
4.4 Representative TG and DTG curves of (a) chitosan, (b) pCA-chitosan and (c) pCA-HT-chitosan .....	39
4.5 Adsorption of mucin on CS, pCA-CS and pCA-HT-CS of different reaction time at pH 1.2, 4.0 and 6.4 .....	42

<b>Figure</b>	<b>Page</b>
4.6 Swelling behaviors of the chitosan and modified chitosan.....	44
4.7 Representative swelling mechanism of pCA-HT-chitosan in pH 1.2, 4.0 and 6.4.....	46
4.8 Scanning electron micrographs of (a) chitosan, (b) pCA-chitosan and (c) pCA-HT-chitosan without PIP.....	47
4.9 Scanning electron micrographs of (a) chitosan, (b) pCA-chitosan and (c) pCA-HT-chitosan loading PIP.....	48
4.10 Representative FTIR spectra of (a) PIP, (b) chitosan/PIP, (c) pCA-chitosan/PIP and (d) pCA-HT-chitosan/PIP.....	52
4.11 TGA thermogram of (a) PIP, (b) chitosan/PIP, (c) pCA-chitosan/PIP and pCA-HT-chitosan/PIP microspheres.....	53
4.12 Release profiles of piperine (PIP) from chitosan and modified chitosan in pH 1.2.....	60
4.13 Release profiles of piperine (PIP) from chitosan and modified chitosan in pH 4.0.....	61
4.14 Release profiles of piperine (PIP) from chitosan and modified chitosan in pH 4.0.....	62
4.15 Release profiles of 5%wt piperine (PIP) from pCA-HT- chitosan in different pHs.....	63

## LIST OF ABBREVIATIONS

%	percentage
μg	microgram
μL	microliter
μmol	micromole
aq	aqueous
cm	centimeter
cm <sup>-1</sup>	unit of wave number
conc.	concentration
HT	homocysteine-thiolactone
pCA	<i>p</i> -Coumaric acid
°C	degree Celsius (centigrade)
PIP	piperine
TGA	thermogravimetric analysis
%DD	degree of deacetylation
EE	entrapment efficiency
FTIR	Fourier Transform Infrared Spectrophotometer
g	gram
h	hour
kDa	kilodalton
kV	kilovolt
M	concentration in molar
mg	milligram
min	minute
mL	milliliter
mL/h	milliliter per hour
MW	molecular weight
nm	nanometer
PDI	polydispersity index

pH	power of hydrogen ion or the negative logarithm (base ten)
ppm	part per million
KBr	potassium bromide
rpm	round per minute
S.D.	standard deviation
SEM	Scanning Electron Microscope
t	time
T <sub>m</sub>	melting temperature
UV	ultraviolet
v/v	volume/volume
w/w	weight/weight
PAS	periodic acid schiff

# CHAPTER I

## INTRODUCTION

### 1.1 Introduction

Controlled release drug delivery system is a field of importance to medicine and healthcare. Controlled drug delivery improves bioavailability by preventing premature degradation and enhancing uptake, maintains drug concentration within the body at an optimum level, reduces side effects by targeting to target site, controlled release dosage forms enhance the safety, efficacy and reliability of drug therapy [1-3].

Nowadays, mucoadhesive polymers have received considerable attention for various drug delivery systems due to their ability to prolong the residence time at the site of drug absorption, the frequency of dosing can be reduced and as a result the patient compliance improved. Due to these advantages, many attempts have been made to improve the mucoadhesive properties of polymeric carriers. Mucoadhesive polymers which can be used in drug carrier are chitosan, sodium alginate, tragacanth, gelatin and guar gum, etc. [4-7].

Chitosan was used as mucoadhesive polymer due to its unique physicochemical properties, biological functions, excellent biocompatibility and hydrophilic polymer of low toxicity. The most easily exploited sources are the protective shells of crabs and shrimps. Chitosan contains primary amino groups in the main backbone that make the surfaces positively charged in biological fluids. This a natural cationic amino polysaccharide copolymer of glucosamine and N-acetylglucosamine obtained by partial deacetylation of chitin (Figure 1.1). The cationic polymer of chitosan contains OH and NH<sub>2</sub> groups, the potential reactive groups make it an attractive biopolymer for many biomedical and pharmaceutical applications. Chitosan has also demonstrated that it possesses mucoadhesive properties due to the formation, depending on environmental pH, the chemical bonds such as hydrogen bonds and ionic interactions between the positively charged amino

groups of chitosan and the negatively charged sialic acid residues of mucus glycoproteins. This non-covalent interaction results in weak mucoadhesion [8-12].

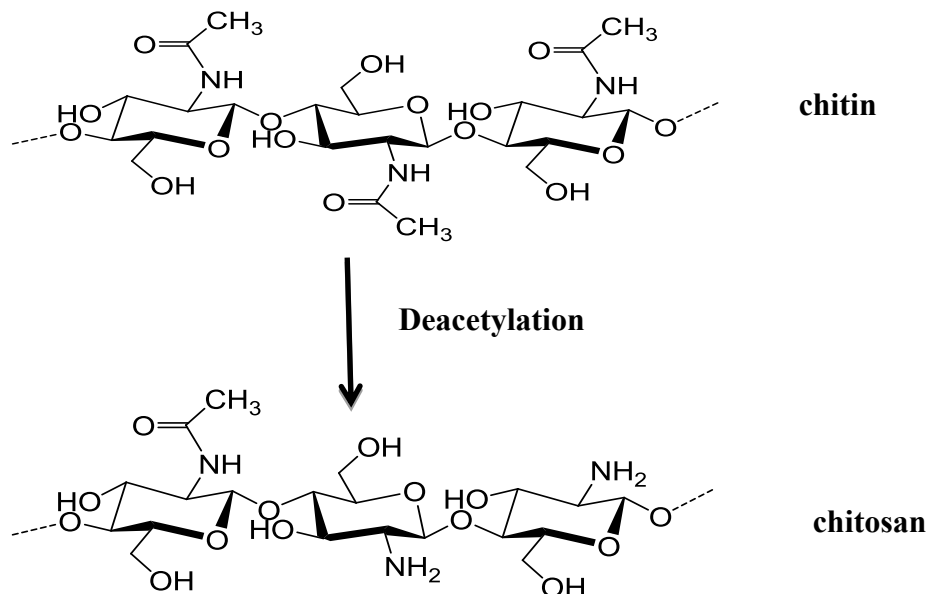


**Figure 1.1 Structures of chitin and chitosan.**

A presumptive new generation of thiolated mucoadhesive polymers has been introduced into the pharmaceutical application. Thiolated polymers display strongly improved mucoadhesive properties, thiol side chain interacts with cysteine rich subdomains of mucus glycoprotein forming via thiol/disulfide exchange reactions as covalent bonds. However, the poor interaction of these thiolated polymers with hydrophobic drug molecules often resulted in a faster drug release, which will affect their potential applications in pharmaceutical fields [13-14]. Hydrophobic mucoadhesive polymers for hydrophobic drug delivery system have been developed, An example of thiolated carboxymethyl chitosan-g-β-cyclodextrin (CMC-g-β-CD) [15], N-(4-N, N-dimethylaminocinnamyl) chitosan chloride (MDMCMChC) with improved mucoadhesive properties may potentially become an effective hydrophobic drug delivery system with controlled drug release capability [16].

The aims of this work was to design and evaluate delivery hydrophobic drug being based on a thiolated polymer, by conjugated *p*-coumaric acid (pCA) as a hydrophobic part onto the amino groups of chitosan and then grafted homocysteine thiolactone (HT) to the pCA-chitosan to increase the mucoadhesive property.



The *p*-coumaric acid (Figure 1.2) is present in esterified or free acid forms in many fruits and vegetables such as peanuts, navy beans, tomatoes, carrots, and garlic. It's widely used in the chemical, food, health, cosmetic, and pharmaceutical industries [17].

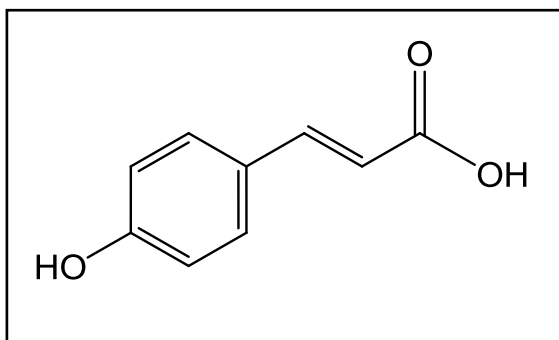


**Figure 1.2 Structure of *p*-coumaric acid (pCA).**

Homocysteine thiolactone (Figure 1.3) is known to be cytotoxic in experimental animals and in cell cultures. HT is a sulfur-containing amino acid that is produced of the demethylation of methionine and is a critical intermediate in several metabolic cycles [18].

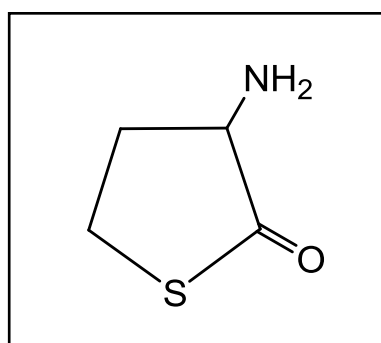


**Figure 1.3 Structure of homocysteine thiolactone (HT).**

Piperine is the major alkaloid of black and long peppers, the well know spice obtained from *Piper nigrum* L. (*Piperaceae*), which herbs and spices are important part of the human diet. There are structural features of piperine. There is an aromatic ring, a trans, trans diene and an amide (Figure 1.4a). This compound is known to possess several pharmacological actions such as reduces inflammation and pain, possesses anticonvulsant and antiulcer activity, protects the liver and has deleterious effects on testis function, antimicrobial, antifungal, anti-inflammatory and antioxidant

effects. The most important property of piperine is that it significantly enhances the bioavailability of various supplemental nutrients through increased absorption [19].

Piperine has functional groups such as lactam, it was hydrolyzed by alkalis into a base and acid which were named as piperidine and piperic acid (Figure 1.4b). The structure of piperic acid was oxidized by potassium permanganate to yield Oxalic acid, Piperonal, and Piperonylic acid (Figure 1.4b) [20]. The chemical interaction leads to degradation of piperine. These systems we use of polymer to prevent drug for delivery hydrophobic drug to target site.

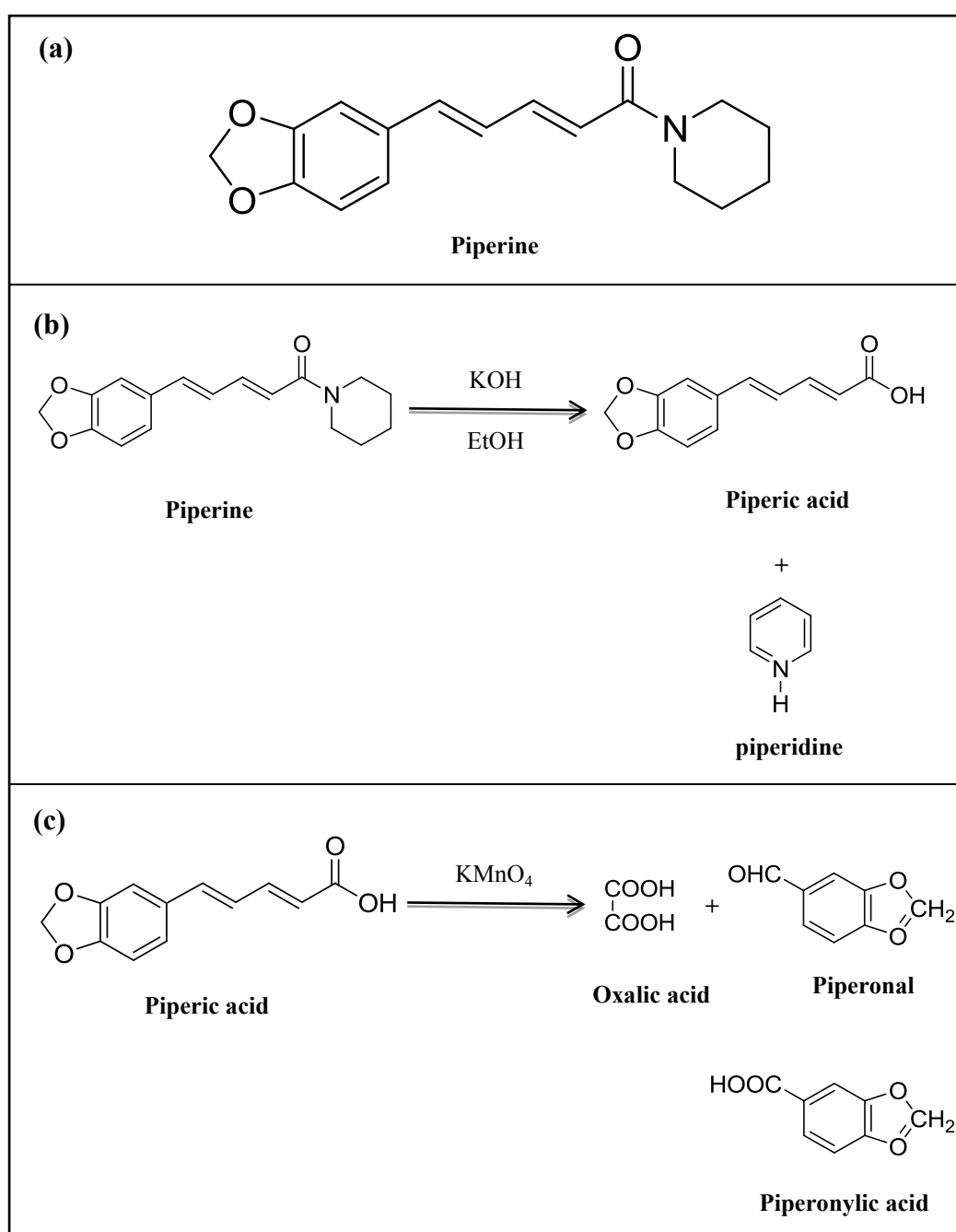


**Figure 1.4 Structure of piperine (a), hydrolysis of piperine (b) and oxidation of piperic acid (c).**

In the research, the amino groups within the chitosan backbone were partially substituted with pCA and HT (Figure 1.5). The *p*-coumaric acid (pCA) increase hydrophobic part onto chitosan side chains, so as to make chitosan can be encapsulated hydrophobic drug. In addition, the homocysteine thiolactone (HT) has thiol groups that can form disulfide covalent bond with cysteine rich-subdomain of mucus glycoprotein. There are increase mucoadhesive properties of chitosan.

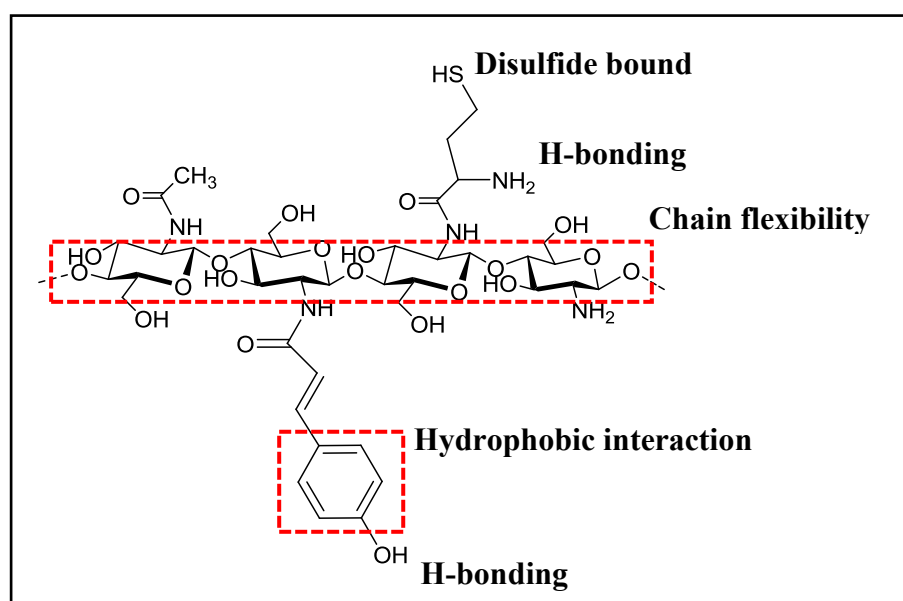


**Figure 1.5 Influence of polymer to mucoadhesive properties**

Polymers have been used extensively in these drug delivery systems, including systems such as nanoparticles microcapsules, laminates, matrices, and microporous powders. In all these delivery systems, the drug is dispersed or incorporated into the system with the formation of a hydrophobic interaction between the drug and polymer [21].

Chitosan particles can be fabricated using a number of techniques such as solvent evaporation, double emulsion, phase-inversion nanoencapsulation, polymer precipitation and polycondensation, and soft lithography [22]. Electrospraying is a novel technique for the generation of micro/nanoparticles for pharmaceutical applications. The principles of electrospraying are based on the ability of an electric field to deform the interface of a liquid drop. An electric field is applied to a polymeric solution contained within a syringe. The applied high voltage potential

forces the polymer to come out of the syringe in the form of a jet that eventually enables the formation of micro/nanoparticles [23].

The electrospraying has some advantages over other methods for particle productions such as the droplets have size small and the size distribution is usually narrow, charged droplets are self-dispersing in absence of droplet agglomeration and coagulation and the motion of charged droplets can be easily controlled [24].

The purpose of the present work was to demonstrate the mucoadhesive polymer for delivery hydrophobic drug, different pH environment. The thiolated chitosan has been chemically modified by covalent attachment *p*-coumaric acid (pCA) and homocysteine thiolactone (HT) onto chitosan using EDAC as a coupling reagent with carboxylic group and amine group of chitosan. This modified chitosan was characterized by FTIR, NMR and TGA. Degree of phenol and thiol substitution was found using Folin-Ciocalteu and Ellman's method, respectively. Moreover, the in vitro mucoadhesion properties was evaluated by periodic-acid schiff (PAS) method and the swelling properties of modified chitosan were investigated in biological fluids such as 0.1 N HCl buffer pH 1.2 for simulated gastric fluid, 0.1 N sodium acetate buffers pH 4.0 for simulated intestinal fluid and 0.1 N phosphate buffer saline pH 6.4 for simulated intestinal fluid.

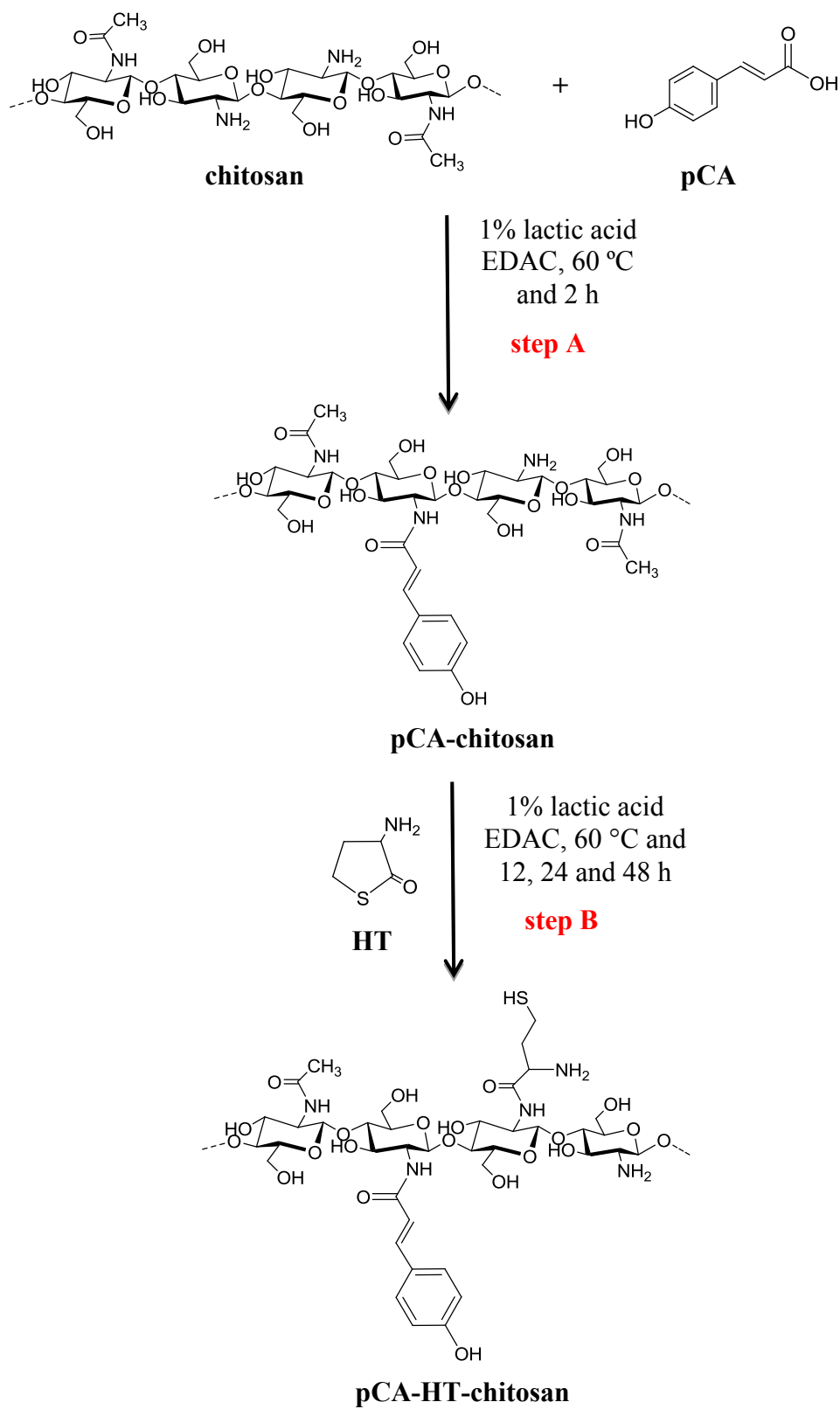
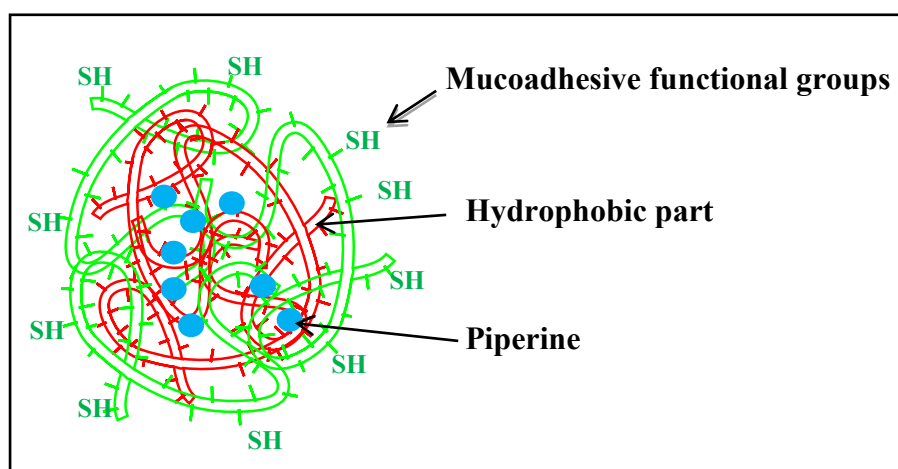


Figure 1.6 Synthesis scheme of pCA-chitosan (step A) and pCA-HT chitosan (step B).

Additionally, the purpose of work was to evaluate the feasibility of preparing controlled release of microspheres encapsulating piperine. The microspheres were prepared by electrospray ionization technique (Figure 1.7). Furthermore, a preliminary characterization of microspheres in terms of morphology, particle size and size distribution, zeta potential, chemical analysis and thermal behavior were investigated. Finally, the in vitro release behavior of the spheres was studied in various pH buffers (pH 1.2, 4.0 and 6.4).



**Figure 1.7 Schematic of drug loaded mucoadhesive particle**

## 1.2 The objectives of this research

- 1) To improve mucoadhesive property of chitosan
- 2) To investigate the possibility of using modified chitosan as hydrophobic drug carrier

## 1.3 The scope of research

The scope of this research was divided into 2 main parts:

- Literature review of related research works

### Part I Modifying chitosan

- a. Preparation of thiolated chitosan
- b. Characterization of the physical and chemical properties of chitosan and modified chitosan using FTIR,  $^1\text{H-NMR}$ , and TGA
- c. Determination degree of substitution phenol, thiol and disulfide
- d. In vitro investigation of mucoadhesive property and swelling behavior in various pH conditions

**Part II Fabrication and evaluation of the thiolated chitosan as a hydrophobic drug delivery carrier**

- a. Preparation of the microspheres with and without drug
  - b. Characterization of the obtained microspheres in terms of morphology size and size distribution, zeta potential, chemical analysis and thermal behavior
  - c. Determination of the drug encapsulation efficiency
  - d. Study the in vitro release behavior of the spheres by using UV-Vis method
- Report, discussion and writing up thesis

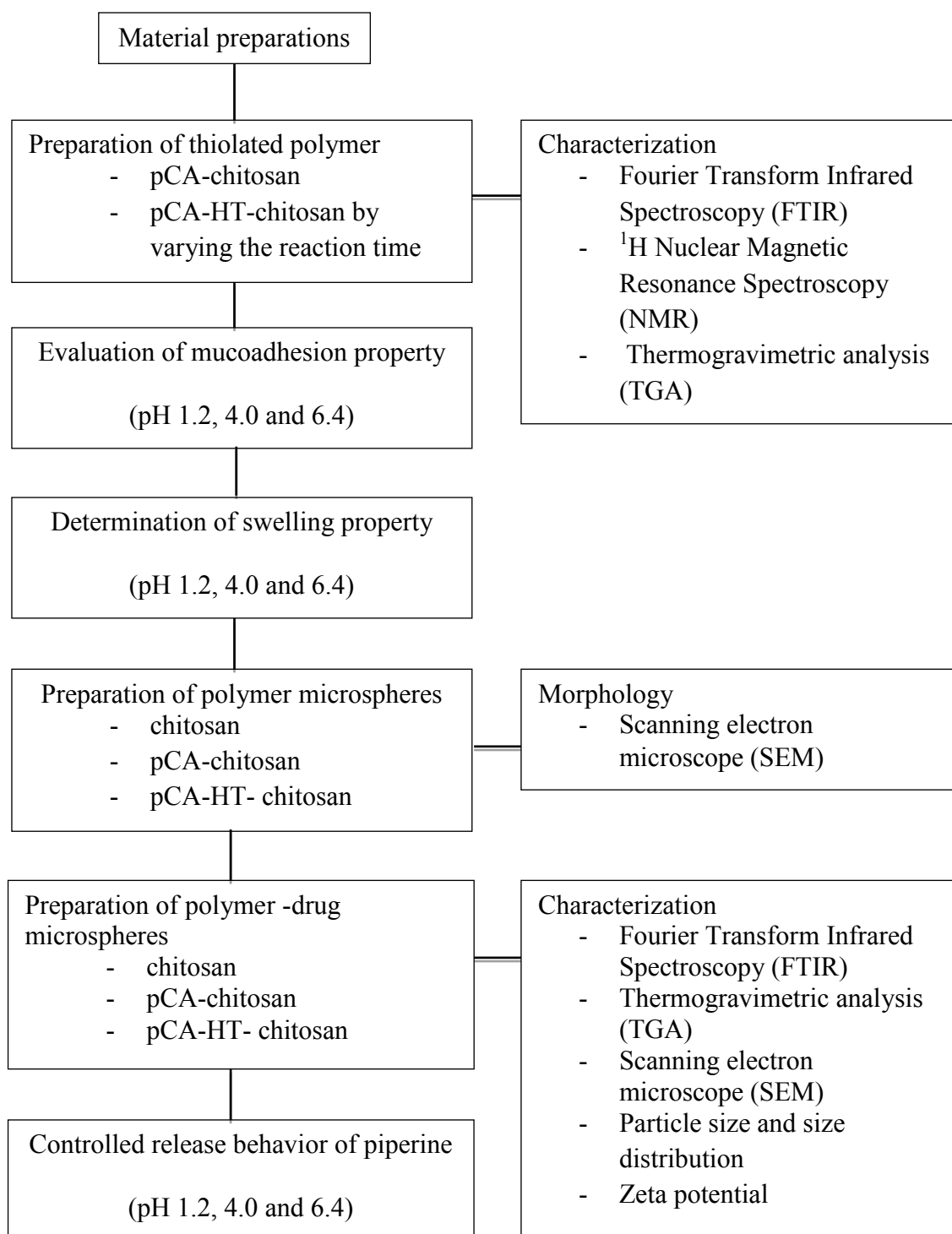


**Figure 1.8 Flow chart of methodology**



## **CHAPTER II**

### **THEORY AND LITERATURE REVIEWS**

#### **2.1 Controlled release drug delivery systems**

Controlled release drug delivery systems consisting of a drug encapsulated within a suitable polymer carrier are designed to enhance drug therapy, to shield drug from premature degradation or elimination, and enables drugs to be delivered of drugs directly to various organs or tissues. The drug can be released from the system by 3 mechanisms [25].

##### **2.1.1 Diffusion-controlled drug release**

Diffusion of a drug molecule through a polymeric membrane forms the basis of this controlled drug delivery system. These are manufactured either by encapsulating the drug particle in a polymeric membrane or by dispersing the drug in a polymeric matrix.

##### **2.1.2 Swelling-controlled release**

Swelling-controlled release occurs when diffusion of drug is faster than hydrogel swelling. The modeling of this mechanism usually involves moving boundary conditions where molecules are released at the interface of rubbery and glassy phases of swollen hydrogels.

##### **2.2.3 Erosion Controlled Release**

The drug can be released from the matrix due to erosion of polymers, which can be classified into 2 types.

Bulk erosion: The polymer degrades in a fairly uniform manner throughout the polymer matrix.

Surface erosion: The degradation occurs only at the surface of the polymer device.

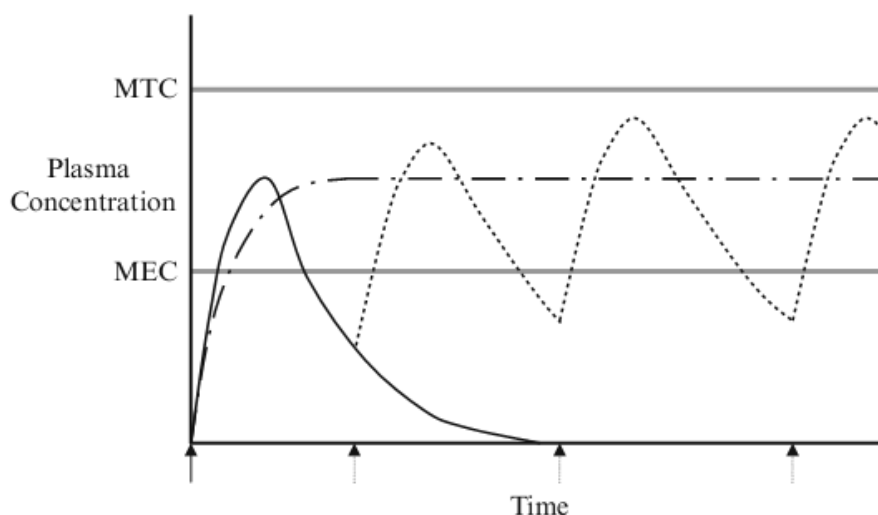


**Figure 2.1 A schematic drawing illustrating the controlled [26]**

Indeed the controlled release system employed plays a vital role in controlling the rate of drug release, duration of drug action and the side effect profile. Figure 2.1 showing the drug plasma concentration profile after oral administration of a drug from rapid release dosage forms. A rapid increase in concentration is followed by a rapid decrease and little time is spent inside the so-called therapeutic range, which is bounded below by the drug concentration at the appropriate site should be above the minimal effective concentration (MEC) and below the minimal toxic concentration (MTC). Frequent repetitive dosing is required to maintain concentration within these limits, and compliance and control are difficult.

Dosage forms that prolong release can maintain drug concentration within the therapeutic range for extended periods and minimize episodes of underexposure or toxicity. A well designed system displays a narrow, predictable residence time distribution in the gastrointestinal (GI) tract, and releases drug by a controlled mechanism [26].

## 2.2 Mucoadhesion

Mucoadhesion is the ability of materials to adhere to mucosal membranes in the human body for extended period of time by the help of interfacial forces. Mucoadhesion is the attachment of the drug along with a suitable carrier to the mucous membrane. The advantages associated with the use of mucoadhesives in drug delivery include [27-29]:

- Prolongs the residence time of the dosage form at the site of absorption
- Increased drug concentration gradient at the absorption site and therefore improved bioavailability of systemically delivered drugs.
- Reduce side effect that may be caused by systemic administration of drugs.

### 2.1.1 Mucoadhesive/mucous interaction

A mucous membrane is a layer of epithelial tissue, in which mucins are the major component. Most mucins carry a net negative charge due to the presence of carboxylate groups (sialic acid) and ester sulfates at the terminus of some sugar units. The approximate pKa of these acidic groups is 1.0–2.6 resulting in their complete ionization under physiological conditions [30-31].

For adhesion to occur, molecules must bond across the interface. These bonds can arise in the following way.

(1) Ionic bonds where two oppositely charged ions attract each other via electrostatic interactions to form a strong bond

(2) Covalent bonds where electrons are shared, in pairs, between the bonded atoms in order to “fill” the orbitals in both. These are also strong bonds.

(3) Hydrogen bonds here a hydrogen atom, when covalently bonded to electronegative atoms such as oxygen, fluorine or nitrogen, carries a slight positive charge and is therefore attracted to other electronegative atoms. The hydrogen can therefore be thought of as being shared, and the bond formed is generally weaker than ionic or covalent bonds.

(4) Van -der-Waals bonds these are some of the weakest forms of interaction that arise from dipole–dipole and dipole-induced dipole attractions in polar molecules, and dispersion forces with non-polar substances.

5) Hydrophobic bonds more accurately described as the hydrophobic effect, these are indirect bonds (such groups only appear to be attracted to each other) that occur when non-polar groups are present in an aqueous solution. Water molecules adjacent to non-polar groups form hydrogen bonded structures, which lowers the system entropy. There is therefore an increase in the tendency of non-polar groups to associate with each other to minimise this effect.

### 2.1.2 Mechanism mucoadhesion

The mucoadhesive must spread over the substrate to increase attachment of the drug along with a suitable carrier to the mucous membrane. In considering the mechanism of mucoadhesion is a complex phenomenon in two steps, the contact stage and the consolidation stage (Figure 2.2).

The contact stage: An intimate contact occurs between the mucoadhesive and mucous membrane, with wetting and swelling of the formulation, initiating its deep contact with the mucus layer. In some case, such as oral cavity, eye or vagina, the delivery system is mechanically held with the membrane. In other cases, the deposition is encouraged by the aerodynamics of the organ such as for the nasal cavity. The gastrointestinal tract is an example of an inaccessible mucosal surface where the adhesive material cannot be placed directly onto the target mucosal surface, but an adhesion in the esophagus can occur. It can be explained by Brownian motion that peristalsis and other gastrointestinal movement would help to repulsive forces (osmotic pressure, electrostatic re-pulsion, etc.) and attractive forces (van der Waals forces and electrostatic attraction) the dosage form into contact with the mucosa [32].

The consolidation stage: The mucoadhesive materials are activated by the presence of moisture. Moisture will effectively plasticize the system permission mucoadhesive molecules to become free and to link up by weak van der Waals and hydrogen bonding. In the case of cationic material s such as chitosan, electrostatic

interactions with the negatively charged groups (such as carboxyl or sulphate) on the mucin or cell surfaces is also possible [33].

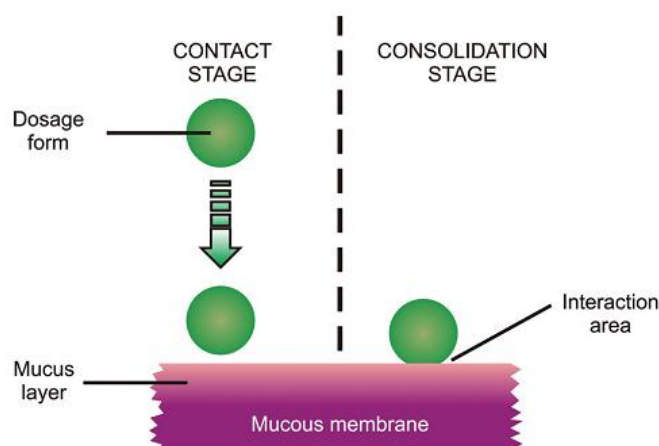


**Figure 2.2 The two steps of the mucoadhesion [32].**

### 2.1.3 Factors affecting mucoadhesion

The mucoadhesion of a drug carrier have been several factors the below mentioned

#### 1. Polymer-Related Factors

- **Molecular weight:** Larger molecular weight polymers will not hydrate readily to free the binding groups to interact with a substrate, while lower molecular weight polymers will form weak gels and readily dissolve. It is generally understood that the threshold required for successful bioadhesion is least 100,000 molecular weight.
- **Concentration of active polymers:** In highly concentrated systems, above the optimal level the adhesive strength drops significantly because the coiled molecules become separated from the medium so that the chains available for interpenetration become limited.
- **Flexibility of polymer chains:** The flexibility of polymer chains is believed to be critical for interpenetration and entanglement, mobility of individual polymer chains decrease, allowing binding groups to

come together and thus the effective length of the chain that can penetrate into the mucus layer decreases.

## 2. Environment Related Factors

- pH: It can influence the formal charge on the surface of mucus as well as certain ionisable bioadhesive polymers. Mucus will have a different charge density depending on pH due to difference in dissociation of functional groups on the carbohydrate moiety and the amino acids of the polypeptide backbone. pH of the medium is important for the degree of hydration of cross-linked polyacrylic acid, showing consistently increased hydration from pH 4 to 7 and then a decrease as alkalinity and ionic strength increases.
- Swelling: It depends on the polymer concentration, ionic concentration, as well as the presence of water. Over hydration results in the formation of a slippery mucilage without adhesion.

### 2.1.4 Polymer used for oral mucoadhesive drug delivery

Polymers with hydroxyl or carboxyl groups on their surface had been earlier claimed as the most desirable candidates for bioadhesion. The characteristics of an ideal polymer such as [34-35]

- Polymer and its degradation products should be non-toxic, non-irritant and free from leachable impurities
- Should have good spread ability, wetting, swelling, solubility and biodegradability properties
- Form a strong non covalent bond with mucin epithelial cell surfaces
- Should adhere quickly to moist tissue and should possess site specificity
- Allow easy incorporation of the drug and offer no hindrance to its release
- Polymer must not decompose on storage or during shelf life of dosage form

- Cost effective.

There are two broad classes of mucoadhesive polymers: hydrophilic polymer and hydrogels. In the large classes of hydrophilic polymers those containing carboxylic group exhibit the best mucoadhesive properties, poly vinyl pyrrolidone (PVP), methyl cellulose (MC), sodium carboxy methylcellulose (SCMC), hydroxy propyl cellulose (HPC) and other cellulose derivative. Hydrogels are the class of polymeric biomaterial that exhibit the basic characteristics of an hydrogels to swell by absorbing water interacting by means of adhesion with the mucus that covers epithelia.

- Anionic group- Carbopol, polyacrylates and their crosslinked modifications
- Cationic group- Chitosan and its derivatives

**Table 2.1** The relative bioadhesive property of various polymers [35]

<b>Polymer</b>	<b>Bioadhesive property</b>
Poly(acrylic acid) (neutralized)	+++
Carbomer (neutralized)	+++
Hyaluronan	+++
Chitosan	++
Sodium carboxymethylcellulose	++
Poly(galacturonic acid)	++
Sodium alginate	++
Pectin	++

NOTE: +++ : Excellent

++ : Good

### 2.3 Thiolated polymer

A new generation of mucoadhesive polymer drug delivery system is thiomers. These are hydrophilic polymers, which display thiol bearing side chains. Disulphide bonds between thiolated polymers and cysteine-rich subdomains of mucus glycoproteins are supposed to be responsible for the enhanced mucoadhesive properties of polymer [13]. The thiolated polymer have been developed drug delivery systems, Self-assembled nanoparticles between TMC-Cys and negatively charged



protein drugs could be a promising vehicle for oral delivery and enhancing mucoadhesive properties [14]. The N,N,N-trimethyl-chitosan were synthesized and then grafted with homocysteine thiolactone (HT) exerted higher mucoadhesive property [41].

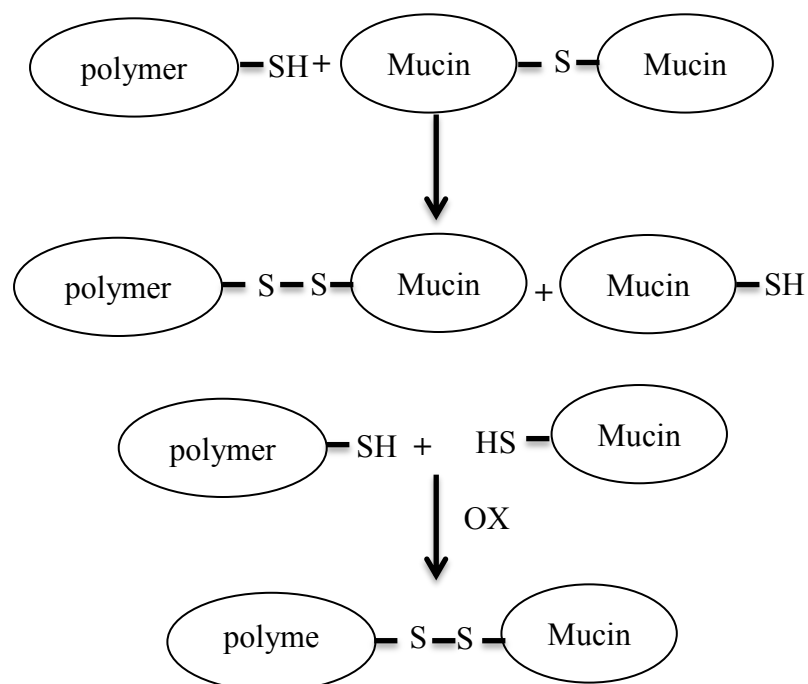


**Figure 2.3 the formation of covalent bond between thiolated polymer and mucin**

## 2.4 Coronary heart disease

Coronary heart disease is a reduction of blood flow which a waxy substance called plaque building up inside the coronary arteries. These substances are composed mostly of cholesterol, other lipids, and fibrous tissue, such as collagen, allowing a blood clot to form. A complete cut off of the blood supply results in the death of heart cells, and a heart attack occurs. A common symptom of coronary heart disease is angina chest pain or discomfort when an area of the heart muscle doesn't get enough oxygen. There are several treatments available such as bypass surgery, Balloon

angioplasty and drugs. Drugs are very useful in the treatment of disease. These medicines may slow the disease's progress or ease its symptoms such as [36]

- Nitroglycerin (nitro) can dilate the arteries and improve blood flow.
- Beta blockers slow of heart rate and reduce the heart's demand for oxygen.
- Aspirin or Cholesterol-lowering medications. Statins and other medications are often very effective in lowering blood levels of LDL (the "bad" cholesterol). Other medications may be used to raise levels of HDL (the "good" cholesterol). Together, these two steps can slow or stop plaque build-up in arteries.
- Calcium channel blockers relax blood vessels, which reduces high blood pressure and lightens heart's workload as it pumps blood throughout the body.

The elderly have a higher rate of heart disease than any other age group. The prevalence of heart disease increased with age (5-year age groups, from 65 to 69 to 85 and older). Although pharmacotherapy for the elderly can treat diseases and improve well-being, its benefits can be compromised by drug-related problems. Pharmacotherapy in the elderly is complicated by multifactorial issues, including age related physiologic changes, the presence of multiple chronic disease states, functional changes in neuropsychiatric and physical abilities, and the patient's desire versus ability to comply with recommended therapy [37].

The absorption of orally administered agents may be affected by increased gastric pH and the slowing of gastric emptying and intestinal transit. The diminution of total body water, circulating volume, and plasma proteins, as well as increases in body fat, will affect the volume of distribution of a drug, depending on its protein binding and aqueous and lipid solubility characteristics. Age-related decreases in hepatic and renal function will impair drug metabolism, clearance, and excretion.

## **2.5 Piperine**

Piperine is an alkaloid present as the major pungent ingredient in various parts of the plants from the family Piperaceae which has a number of medicinal properties.

Piperine, the trans-trans isomer of 1-piperoyl piperidine has been shown in Figure 2.3. The structures consist of aromatic moiety, aliphatic chain and amide substitution. This compound is known to possess several pharmacological actions such as antimicrobial, antiinflammatory, hepatoprotective, antimutagenic, etc. Piperine enhances the bioavailability of structurally and therapeutically different drugs, either by increasing the absorption or by delaying the metabolism of the drug or by a combination of both processes [38-39].

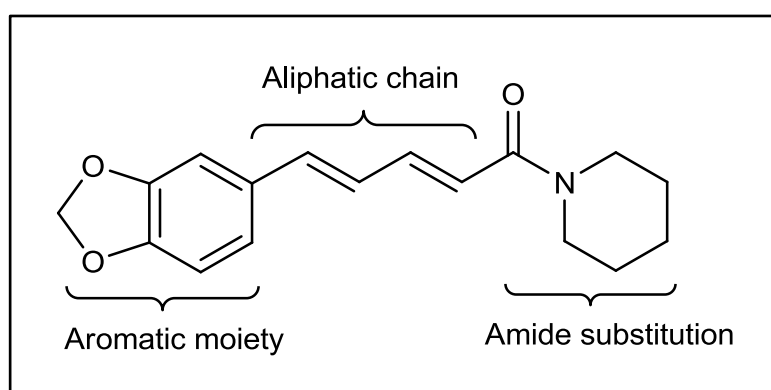


**Figure 2.3 Structure of piperine**

It is evident that black pepper fruits have been used to enhance the bioavailability of co-administered drugs. The ability of piperine to enhance the bioavailability of propranolol and theophylline is reported in this and previous studies, the co-administration of piperine and curcumin, which may act as a useful and potent combination in the treatment of depressive disorders, to enhance the serum response of a fat soluble nutrient [40].

## 2.6 Electrospray ionization technique

Electrospraying process is conceptually simple. A polymer solution becomes spherical because of surface tension at the capillary tip. When a high voltage is applied, the liquid changes its shape into a form called the Taylor cone because the charged liquid is pulled toward the counter electrode. When the charged repulsion of the surface is greater than the surface tension, the liquid is

separated into smaller droplets and these droplets fly toward the counter electrode. A highly charged droplet at the capillary tip splits into micro- or nano-scale droplets, and the charged fine liquid aerosol is accelerated by the high voltage electric field [41-42].

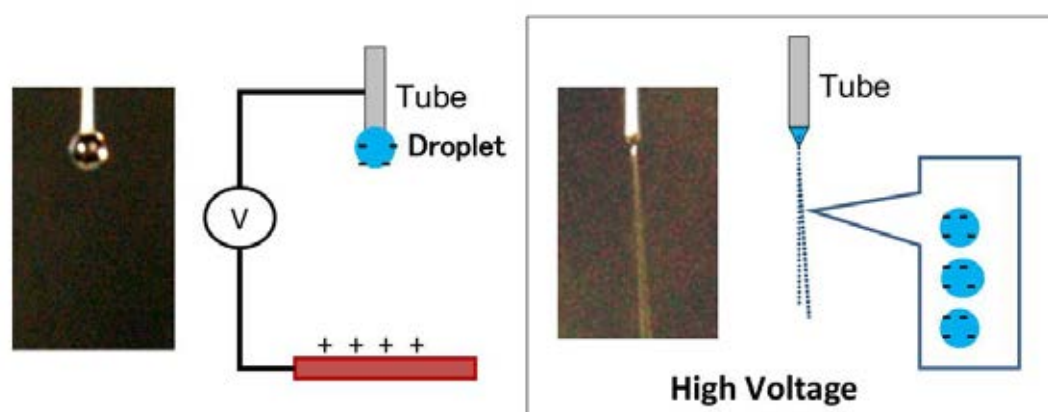


**Figure 2.4 the droplet is generated by electrical force**

Electrospray ionization is widely used in many important fields, such as biochemistry, the food industry, and pharmacy, and is still under fast development. The applications of electrospraying have been reported, such as the particles of pure thiolated chitosan and its PECs with alginate and carrageenan were fabricated using the electrospray ionization technique (EI). The EI technique could be a promising technique for the fabrication of particle-based drug delivery carriers, at least as microparticles. The size distribution of microparticles was relatively narrow (PDI of 0.69–0.88) [43].

The electrospraying has some advantages over conventional mechanical spraying systems with droplet charged by induction such as

1. Droplet size is smaller than that available from conventional mechanical atomisers, and can be smaller than 1  $\mu\text{m}$ .
2. The size distribution of the droplets is usually narrow, with small standard deviation that allows production of particles of nearly uniform size.
3. Charged droplet is self-dispersing in space (due to their mutual repulsion), resulting also in the absence of droplet coagulation.
4. The motion of charged droplets can be easily controlled (including deflection or focusing) by electric fields.

5. The deposition efficiency of a charged spray on an object is order of magnitudes higher than for uncharged droplets.

# CHAPTER III

## EXPERIMENTAL

### 3.1 Materials

The following materials were obtained from commercial suppliers.

#### 3.1.1 Model drug

Piperine (CAS Number: 94-62-2,  $\geq 97\%$  FG, powder obtained by Sigma Aldrich, USA)

#### 3.1.2 Polymer

- Chitosan, food grade, w M 100 kDa., Deacetylation 95 %, Lot No. 497613, (Bonafides, Thailand)

#### 3.1.3 Chemicals

- Ethanol 95 %, commercial grade (Merck, Germany)
- Acetone, commercial grade (Merck, Germany)
- Hydrochloric acid fuming 37%, AR grade (Merck, Germany)
- Lactic acid, AR grade (Union chemicals, Thailand)
- Mucin from porcine stomach (type 2), AR grade (Sigma-Aldrich, USA)
- Potassium dihydrogen phosphate, AR grade (Merck, Germany)
- Potassium bromide, AR grade (Merck, Germany)
- Potassium iodide, AR grade (Merck, Germany)
- Sodium chloride, AR grade (Merck, Germany)
- Sodium hydrogen phosphate, AR grade (Merck, Germany)
- Sodium hydroxide, AR grade (Merck, Germany)
- Sodium tripolyphosphate, AR grade (Sigma-Aldrich, USA)
- Folin & Ciocalteu's phenol reagent (Sigma-Aldrich, USA)
- 5, 5'-Dithiobis (2-nitrobenzoic acid), DTNB (Sigma-Aldrich, USA)

- Dialysis membrane with  $M_w$  cut off at 12,000 – 14,000 Da (Spectrum Laboratories Inc.)

**Table 3.1 Instruments**

<b>Instrument</b>	<b>Manufacture</b>	<b>Model</b>
Freeze dryer	Labconco	Freeze 6
FTIR spectrometer	Nicolet	6700
High voltage	Ormond beach	GAMMA
Horizotal shaking water-bath	Lab-line instrument	3575-1
Micropipette	Mettler Toledo	Volumate
Microtiterplate	BIOTEX	Powerwave xs2
NMR spectrometer	Varian	400 Hz
Scanning Electron Microscope	Philips	XL30CP
Particle size	Malvern Instruments	Zetasizer nanoseries
Syringe pump	Pennyful	kdScience
TGA	PerkinElmer	Pyris Diamond
UV-VIS spectrometer	PerkinElmer	Lambda 800
Ultrasonic bath	Ney Ultrasonik	28

## 3.2 Methods

### 3.2.1 Synthesis of thiolated chitosan

#### 3.2.1.1. Synthesis of pCA-chitosan

The pCA-chitosan was prepared by conjugating *p*-coumaric acid onto the amino groups of chitosan following the reaction scheme presented in Figure 3.1 step A. The coupling reaction of chitosan with pCA was mediated by a carbodiimide (EDAC). To a solution 1 g of chitosan was dissolved in 100 ml 1% (v/v) of lactic acid. After all the soluble chitosan, added 0.2 g of *p*-coumaric acid into ethanol and then added with a EDAC at mole ratio of 1:1.5(pCA:EDAC). The reaction is completed after stirred at 60°C for 2 h, precipitated with excess 1 M NaOH and re-dissolved in water. The product dialysis in ethanol and air dried.

#### 3.2.1.2 Synthesis of pCA-HT-chitosan

The pCA-HT-chitosan was synthesized based on the method by covalent attachment as summarized in Figure 3.2 step B, using different reaction time Briefly, 100 mL of 1% (w/v) of pCA-chitosan in 1% (v/v) lactic acid was added an aqueous solution of imidazole (0.68 g in 2.5 mL water), followed by the dropwise addition of HT 0.5 g in 100 mL water and was added the solution of EDAC at mole ratio 1:2 (HT:EDAC). The reaction mixture was stirred at 60°C in a nitrogen atmosphere for either 12, 24 and 48 h. The reaction mixture was adjusted to pH 7 with 1 M NaOH, precipitated with excess acetone. The suspension was re-dissolved in water and harvested by centrifugation (12,000 rpm for 2 min), dialysis (MW cut-off 12–14 kDa) against 1 L of water for 2 days and freeze-dried. The products were stored at 4 °C and found stable towards air oxidation during the course of the study [44].

The thiolated chitosan was prepared by the above mentioned method with varying reaction time at 12, 24 and 48 h. The appropriate reaction time was selected from the preparation with the highest thiol groups imply that this polymer will give stronger mucoadhesive than the other reaction time.



### 3.2.2 Chemical characterization

#### 3.2.2.1 Fourier Transformed Infrared Spectroscopy (FTIR)

Fourier transform infrared (FTIR) spectroscopy was employed to confirm changing of functional groups for chitosan and modified chitosan (pCA-chitosan and pCA-HT-chitosan), a dried sample was mixed with dry KBr and pressed into a pellet using a macro KBr die kit. The solid pellet was placed in a magnetic holder and the system was purged with air before testing. The FTIR spectra were acquired after 32 scans with a Nicolet 6700 spectrometer in the region from  $4000\text{ cm}^{-1}$  to  $400\text{ cm}^{-1}$ .

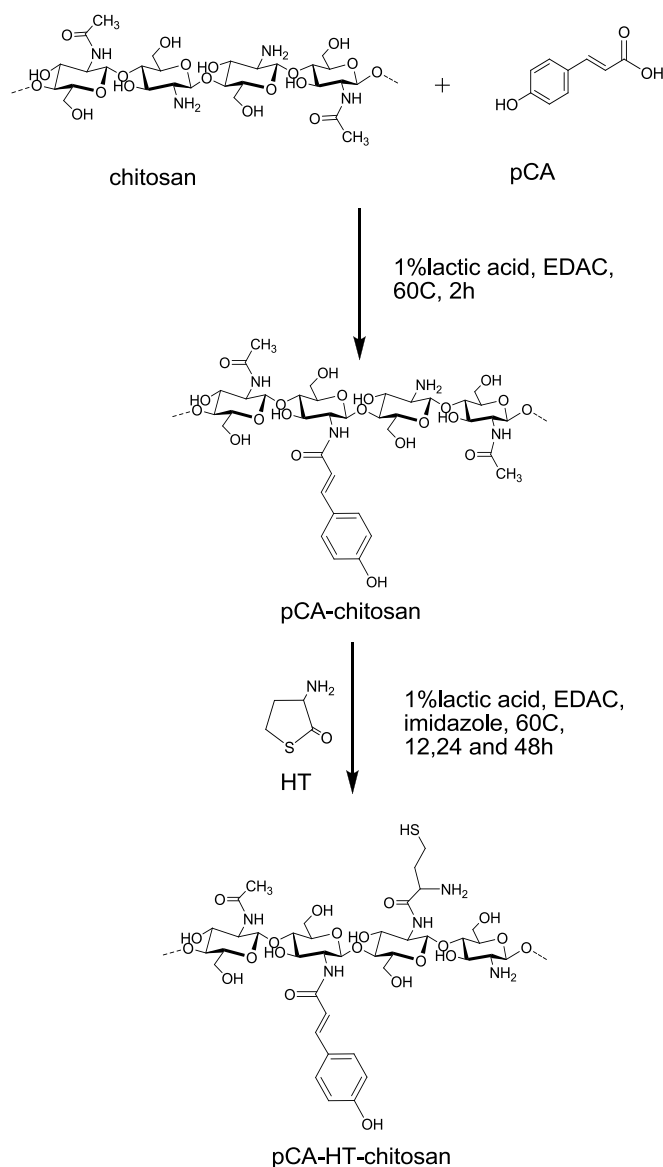


**Figure 3.1** Reaction scheme of the covalent attachment of pCA and HT onto chitosan

### 3.2.2.2 $^1\text{H}$ Nuclear Magnetic Resonance spectroscopy (NMR)

The  $^1\text{H}$  NMR spectra of chitosan and modified chitosan were obtained with a Varian XL-400 NMR Spectrometer. For acquiring the  $^1\text{H}$  NMR spectra of chitosan and modified chitosan their solutions were prepared at concentrations of 10 mg/ml. Both polymers were dissolved in  $\text{D}_2\text{O}/\text{CF}_3\text{COOH}$ .

### 3.2.2.3 Thermogravimetric analysis (TGA)

The thermal behavior of the chitosan, pCA-chitosan and pCA-HT-chitosan were studied using TGA analysis. TGA analysis was performed on a PerKinElmer Pyris Diamond TG/DTA machine under a nitrogen flow at a rate of 30 mL/min. Approximately 5 mg of samples were placed in the alumina pan, sealed and heated at  $10^\circ\text{C}/\text{min}$  from 25 to  $500^\circ\text{C}$ . This technique was used their thermal degradation behavior.

### Determination of the contents of phenol and thiol groups

#### - Determination of the content of phenol groups

The phenolic content in the modified chitosan was estimated by Folin-Ciocalteu (F-C) method. Briefly, a sample of modified chitosan was prepared in the concentration of 1 mg/ml into 1% (v/v) lactic acid solution, 20  $\mu\text{L}$  of sample is transferred into microlitre plate, then added 100  $\mu\text{L}$  of Folin-Ciocalteu's reagent and 80  $\mu\text{L}$  of sodium carbonate (75 g/L). The sample mixture was shaken for about 1 min and allowed to stand for 30 min at room temperature in the dark. Absorbance was measured at 765 nm with the spectrophotometric. A calibration curve was constructed using gallic acid standard solutions (0.02–0.1 mg/L), results were determined from equation of calibration curve ( $y = 7.265x - 0.0589$ ,  $R^2 = 0.9801$ ) and expressed in gallic acid equivalent (GAE) by the following Equation (1).

$$T = C \times V / M \quad (1)$$

T is the total phenolic content in  $\text{mg} \cdot \text{g}^{-1}$  of modified chitosan as GAE, C is the concentration of gallic acid established from the calibration curve in  $\text{mg} \cdot \text{ml}^{-1}$ , V is the

volume of the 1% lactic acid solution in ml and M is the weight of the modified chitosan in g. This method was calculated by using chitosan as controlled [45].

- Determination of the contents of thiol and disulfide groups

The amount of thiol groups conjugated on chitosan was determined with Ellman's reagent. First, 10 mg of the lyophilized modified chitosans was hydrated in 250  $\mu$ L of 0.5 M phosphate buffer (pH 8.0) and then 500  $\mu$ L of Ellman's reagent (3 mg in 10 mL of 0.5 M phosphate buffer pH 8.0) were added. The reaction was allowed to proceed for 2 h at room temperature and the absorbance was measured at a wavelength of 450 nm with a microtitration plate reader. The amount of thiol moieties was calculated from an according to standard curve obtained by chitosan solutions with increasing amounts of L-cysteine HCl.

The amount of disulfide bonds within the modified chitosans was tested according to the following. First, 10 mg of the conjugate was hydrated in 1 ml of 50 mM phosphate buffer pH 8.0 for 30 min. A 3% sodium-borohydride solution was freshly prepared, 600  $\mu$ L were added to the polymer solution, and the mixture was incubated for 2 h in an oscillating water bath at  $37 \pm 0.5$  °C. Thereafter, 500  $\mu$ L of 1 M HCl were added in order to destroy the remaining sodium-borohydride. After the addition of acetone (100  $\mu$ L) the mixture was agitated for 5 min then 1 ml of 1 M phosphate buffer pH 8.5 and 200  $\mu$ L of a 0.5% (m/v) DTNB dissolved in 0.5 M phosphate buffer pH 8.0 were added. After incubation for 15 min at room temperature aliquots of 200  $\mu$ L were transferred to a 96-well microtitration plate and the free sulfhydryl groups were determined as described above [46].

### 3.2.3 In vitro bioadhesion

Mucoadhesiveness was calculated as the amount of mucin adsorbed by 5 mg of pCA-chitosan, pCA-HT-chitosan and chitosan that differ in pH, namely SGF (pH 1.2), 0.1 N sodium acetate buffer (pH 4.0) and SIF (pH 6.4) media. Two modified chitosans and chitosan suspensions were mixed with type II mucin solution (1 mg/mL), vortexed, and incubated at 37°C for 2 h. After adsorption, the suspensions were centrifuged at  $12,000 \times g$  for 2 min and free mucin was measured in the

supernatant by a colorimetric method using periodic acid/Schiff (PAS) staining as reported. Schiff reagent was prepared by 100 mL of 1% (w/v) basic fuchsin (pararosaniline) in an aqueous solution and 20 mL of 1 M HCl. To this was added sodium metabisulphite (1.67% (w/v) final) just before use and the resultant solution was incubated at 37°C until it became colorless or pale yellow. Periodic acid solution was freshly prepared by adding 10 µL of 50% periodic acid to 7 mL of 7% acetic acid. Supernatants were mixed with 100 µL of dilute periodic acid and incubated for 2 h at 37°C. Then, 100 µL of Schiff's reagent was added at room temperature, and after 30 min the absorbance was measured at 555 nm. The amount of mucin adsorbed by the two modified chitosans and chitosan was determined by subtracting of concentration of mucin in solution after adsorption from that before. Mucin standards (0.1, 0.2, 0.3, 0.4 and 0.5 mg/mL) were measured by the same procedure and a standard calibration curve was prepared [47].

### 3.2.4 Swelling study

The dried films of chitosan and the two modified chitosans were prepared as follows. A 0.2 g of chitosan or modified chitosans (pCA-chitosan and pCA-HT-chitosan) was dissolved in 20 mL of 1% (v/v) aqueous lactic acid, poured into an 8 cm × 10 cm tray and air dried. The chitosan or modified chitosan films were then cut into 5.0 mm diameter circles and each one were carried out in three aqueous media: simulated gastric fluid (SGF, pH1.2), 0.1 N sodium acetate buffers (SIF, pH 4.0) and phosphate buffer saline (PBS, pH 6.4). The swelling properties were determined by measuring the change in the diameters of each film at various time intervals (0–6 h). The swelling ratio ( $S_w$ ) for each sample determined at time  $t$  was calculated from Eq. (2) as previously reported [43].

$$S_w = \frac{D_t - D_0}{D_0} \times 100 \quad (2)$$

where  $D_t$  is the film diameter at time  $t$  and  $D_0$  is the initial film diameter.

### **3.3 Pharmaceutical applications**

The pharmaceutical applications of polymers are becoming increasingly important in the field of drug delivery. Polymers can be used as of a drug, to enhance drug stability and to modify drug release characteristics. The microspheres were prepared by electrospray technique using piperine as hydrophobic drug is the representation model drug for studying the drug delivery system. The properties of drug loaded microspheres, e.g. morphology, particle size, zeta potential, encapsulation efficiency, and drug release profiles were investigated.

#### **3.3.1 Preparation of drugs-loaded polymer microspheres**

In order to study pharmaceutical application potential of modified chitosan as a drug delivery system, the microspheres using piperine as a model drug. The pCA-HT-chitosan reaction time at 24 h was used to prepared microspheres due to mucoadhesion at all pH showed the highest than all other reaction time. The thiolated chitosan microspheres were prepared by electrospray technique follows to Figure 3.2.

The electrospray experimental equipment consisted of a syringe pump, a stainless steel needle and a high voltage generator. A 10 mL of 0.1 mg/mL chitosan in 1% lactic acid with and without loading of piperine into polymeric matrix are ejected from a reservoir using a syringe pump into a syringe-nozzle system. The polymer matrix was sprayed from a stainless steel needle (cathode) into 5% TPP aqueous solution (anode) to form microspheres. A high electric field applied to the polymer solution in the syringe and stirred at 400 rpm by a magnetic stirrer bar during electrospraying for 2 h. To remove free piperine, the resultant solution was centrifuged at 12,000 for 5 min and washed by DI for 3 times [44].

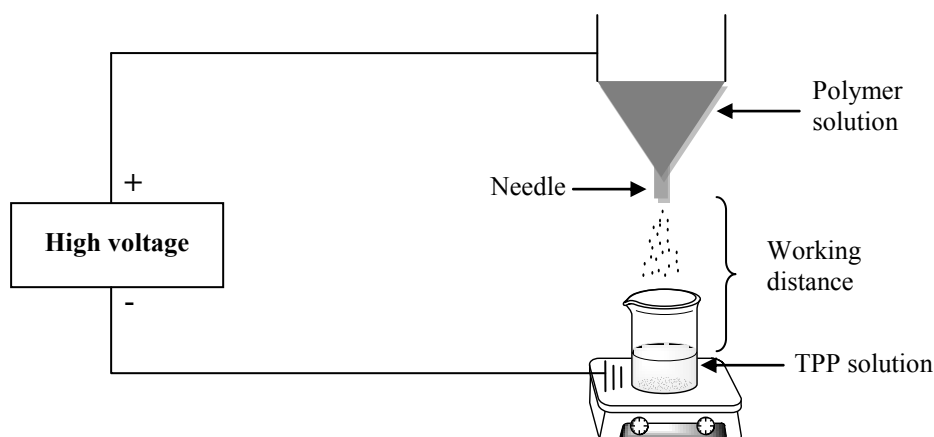


**Figure 3.2** Preparation of PIP loaded chitosan and modified chitosan microspheres

**Table 3.2 The conditions for the microspheres preparation**

Applied voltage (kv)	23
Flow rate (ml/h)	5
Needle gauge (G)	26
Working distance (cm)	10

### 3.3.2 Characterization of the microspheres

#### 3.3.2.1 Scanning Electron Microscope (SEM)

The morphology and surface appearance of the spheres (before and after the drug loading) were analyzed using scanning electron microscope. The sample was mounted onto an aluminum stub using double-sided carbon adhesive tape and coated with gold-palladium. Coating was achieved at 18 mA for at least 4 min. Scanning was performed under high vacuum and ambient temperature with beam voltage of 10-20 kV.

#### 3.3.2.2 Particle size measurement

The particle size and size distribution of microspheres were evaluated with a particle size analyzer after suspension of the microspheres in an aqueous 5% (w/v) sodium tripolyphosphate solution. The particle size calculation was based on

dynamic light scattering (DLS) method, as a software protocol. The scattered light was collected at an angle of 90° through fiber optics and converted to an electrical signal by an avalanche photodiode array (APDs). All samples were sonicated and run in triplicate with the number of runs set to five and run duration set to 10 seconds.

#### 3.3.2.3 Zeta potential

Zeta potential of the microspheres was determined using particle size. The analysis was performed at a scattering angle of 90°. All samples were sonicated and run in triplicate with the number of runs set to 5 and run duration set to 10 seconds.

#### 3.3.2.4 Fourier Transform Infrared (FTIR) Spectroscopy

The FTIR spectra of the microspheres were examined by using the potassium bromide disk (KBr) method with a Fourier transform infrared (FTIR) spectrometry in the range of 4000-400  $\text{cm}^{-1}$ .

### **3.3.3 Study of the drug behavior of the microspheres**

#### 3.3.3.1 Calibration curve of piperine

The standard stock piperine solution was prepared with ethanol solution. Piperine 5 mg was accurately weighed and dissolved with ethanol solution into 50 mL volumetric flask and adjusted to volume (100 ppm).

The stock piperine solution was diluted to 10, 20, 30, 40 and 50 ppm with ethanol solution in a volumetric flask. The absorbance of standard solution was determined by UV-Vis spectrophotometer at 342 nm. The ethanol was used as a reference solution.

#### 3.3.3.2 Calibration curve of piperine in various buffers (pH 1.2, 4.0, and 6.4)

The standard stock piperine solution was prepared in ethanol in pH 1.2, 4.0 and 6.4. Piperine 5 mg was accurately weighed and dissolved with ethanol solution into 50 mL volumetric flask and adjusted by various buffers to volume (100 ppm).

The stock piperine solution was diluted to 10, 20, 30, 40, and 50 ppm with three different buffers in volumetric flask. The absorbance of standard solution was

determined by UV-Vis spectrophotometer at 342 nm. The ethanol was used as a reference solution .

### 3.3.3.3 Determination of drug loading efficiency (EE)

The piperine content in the preparation was determined by extracting the drug from the chitosan and modified chitosan micrpspheres (2 mg) with 10 mL of ethanol. The mixture was stirred at room temperature for 3 h. The supernatant of solution was collected and analyzed by UV spectrophotometry at 342 nm. The amount of piperine loaded into the particles was calculated as the difference between the total amount used to prepare loaded particles and that recovered by ethanol extraction. The piperine EE% of the microspheres was calculated by the following equation [48]:

$$\text{Drug encapsulation efficiency} = \frac{\text{actual amount of drug loaded in microspheres}}{\text{theory amount of drug loaded in microspheres}} \times 100$$

### 3.3.3.4 In vitro drug release

In vitro release study on the microspheres (50 mg) was carried out in three difference buffers. An amount of drug containing 10 mg of particle was suspended in a dialysis bag diffusion technique, immersed into 50 mL of SGF pH 1.2, SIF pH 4.0, and SIF pH 6.4 in a flask and incubated on a shaking water-bath at  $37 \pm 1$  °C, 100 rpm. The incubated solution (5 ml) was collected at predetermined time intervals, for up to 12 h, for analysis. The medium was replenished with an equal volume of the dissolution medium after each sampling. The samples were analysed with a UV spectrophotometer at 342 nm. Total piperine concentration values were used to construct cumulative release profile. The percentages of cumulative piperince release were quantified as follows [49]:

$$\% \text{Cumulative release} = \frac{\text{Amount of piperine from release}}{\text{Amount of piperine before release}} \times 100$$



## CHAPTER IV

### RESULTS AND DISCUSSION

#### 4.1 Synthesis of pCA-CS-chitosan and pCA-HT-chitosan

The pCA and HT was conjugated onto amine group of chitosan using EDAC as a coupling agent via formation of amide bonds. The sulfhydryl compound homocysteine thiolactone (HT) was first formed a reactive intermediate (imidazole). The results in this work successfully were characterized by NMR, FTIR and TGA.

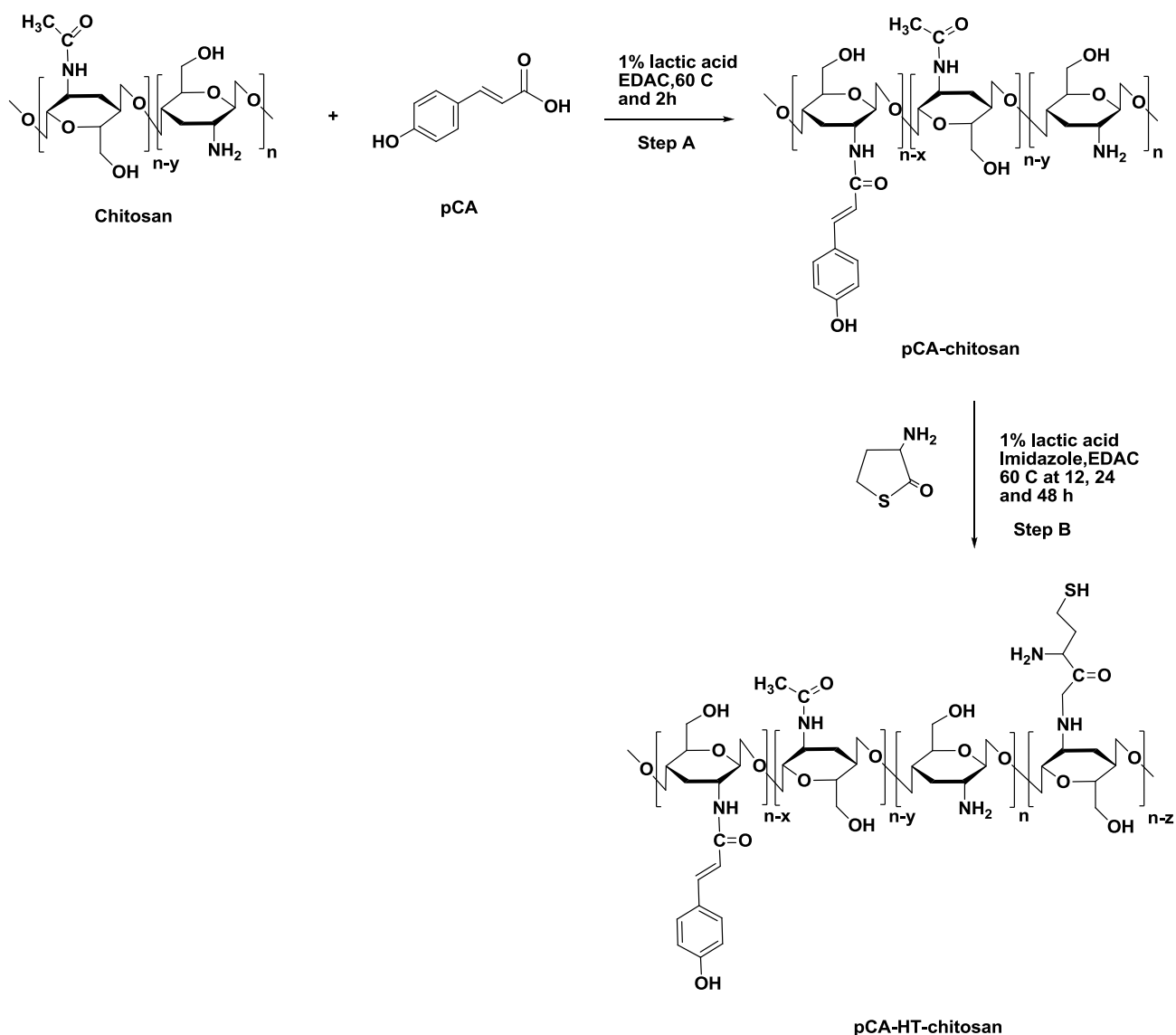


Figure 4.1 Synthesis scheme of pCA-chitosan (Step A) and pCA-HT chitosan (Step B).

## 4.2 Characterization and thermal properties of chitosan and modification of chitosan

### 4.2.1 $^1\text{H}$ NMR spectral of pCA-chitosan and pCA-HT-chitosan

The  $^1\text{H}$  NMR spectral of original chitosan and modified chitosans (pCA-chitosan and pCA-HT-chitosan) were shown in Fig.4.2. The signal centered at 1.73 ppm corresponds to the proton in the acetyl group of N-acetyl glucosamine units of chitosan, the signal observed 2.84 ppm corresponds to the  $\text{H}_2$  in the glucosamine ring, while the signals between 3.3 and 3.5 ppm can be attributed to  $\text{H}_3$ - $\text{H}_6$  of the polysaccharide backbone. The  $\text{H}_1$  of guluronic acid residue gives rise to the signal at 4.53 ppm. After grafting pCA onto chitosan, the new signals at 6.18, 6.73, 7.38 and 7.50 ppm were assigned to the aromatic protons of pCA (Fig. 4.2b) that shift of the signals in pure pCA (Appendix A). These results certified the successful synthesis of pCA-chitosan. In addition, the signal at 0.97 and 4.18 ppm correspond to the protons of lactic acid that reacted amino groups of chitosan. The proton signals of pCA-HT-chitosan spectrum (Fig. 4.2c) were not observed the aromatic proton of pCA and the new protons from the ring opened side chain of HT probably due to the small percent of substitution. This is also supported by IR result, the amount of grafted thiol group and phenol groups can be further investigated by Ellman's method and Folin-Ciocalteu method, respectively. However, the characteristic peaks of chitosan slightly shifted to a lower frequency when compared pure chitosan may be due to amino groups can be reached with lactic acid.

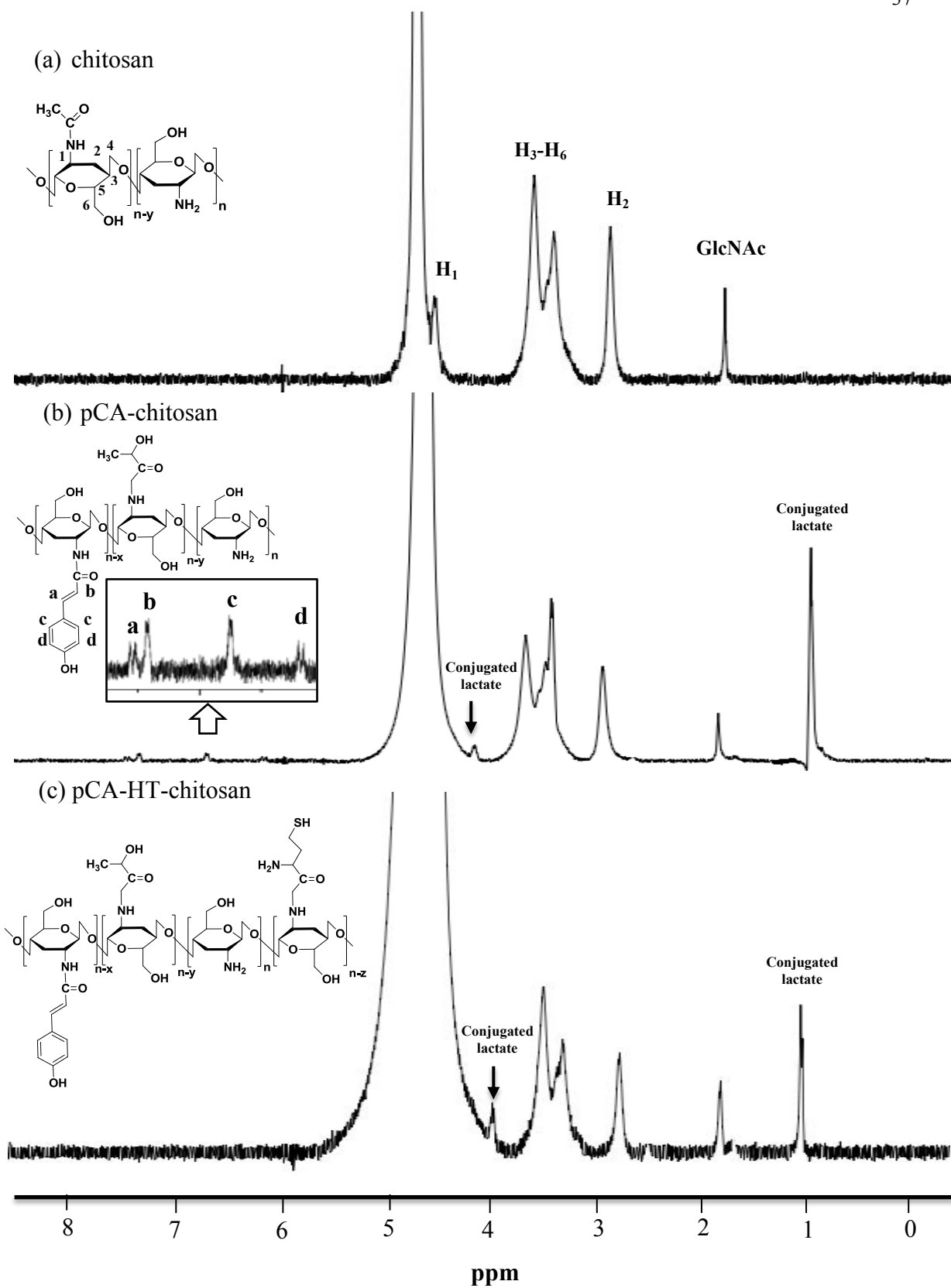
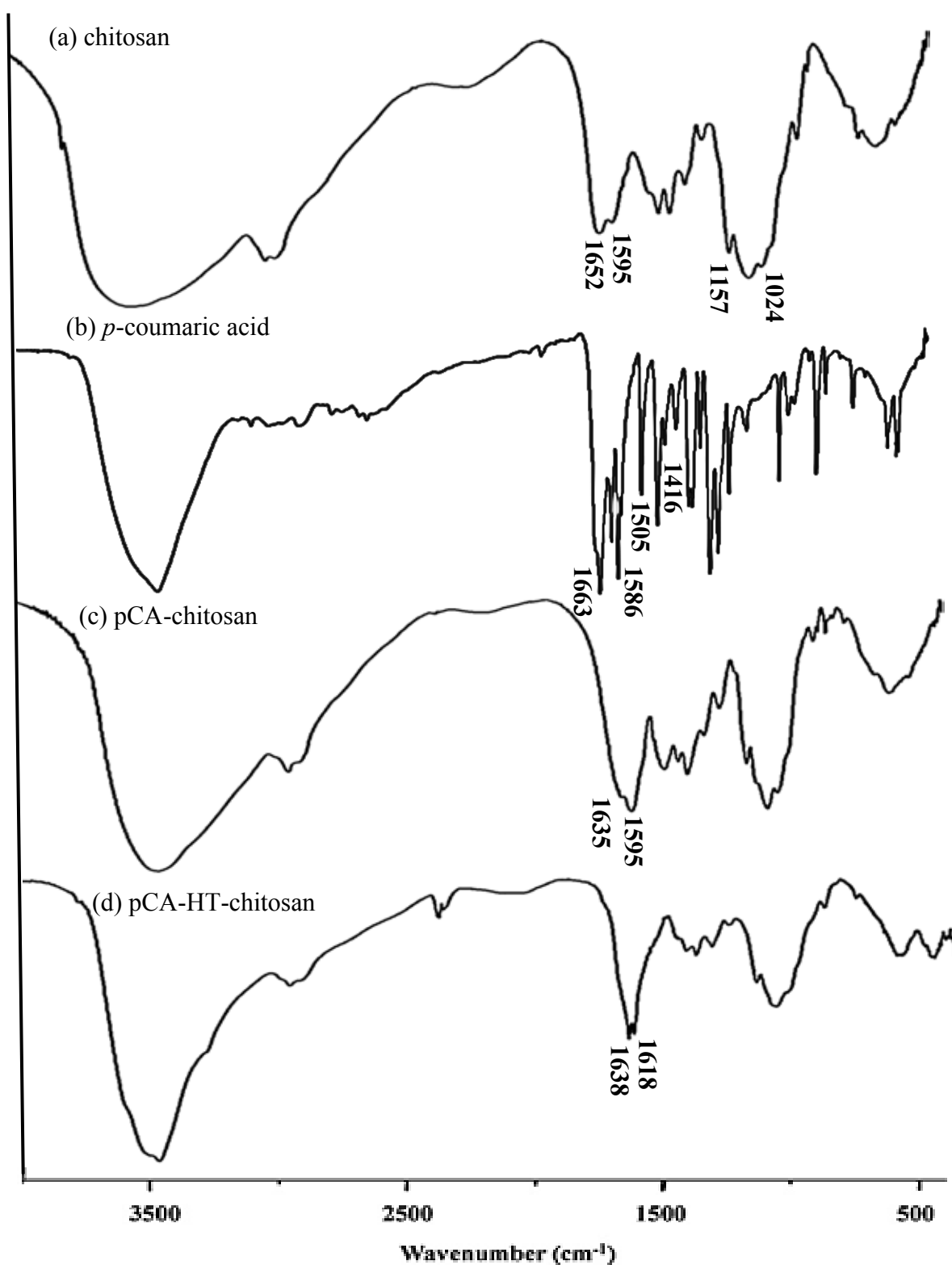


Figure 4.2 Representative  $^1\text{H}$  NMR spectra of (a) chitosan, (b) pCA-chitosan and (c) pCA-HT-chitosan.



**Figure 4.3** Representative FTIR spectra of (a) chitosan, (b) pCA, (c) pCA-chitosan and (d) pCA-HT-chitosan.

#### 4.2.2 FTIR spectra of pCA-chitosan and pCA-HT-chitosan

The structure of the chitosan and modified chitosan was confirmed by IR spectra (Fig. 3). The spectrum of chitosan shows peak at  $1652\text{ cm}^{-1}$  represent carbonyl group of acetylated amide of chitin, which indicates that the chitosan is not fully deacetylated. The peak at  $1595\text{ cm}^{-1}$  is assigned to the stretching vibration of amino group of band at  $1628\text{ cm}^{-1}$  is attributed to the C=C stretching from alkene group whereas the peaks at  $1586$ ,  $1505$ , and  $1416\text{ cm}^{-1}$  are assigned to the aromatic ring vibrations.

The IR spectrum of pCA-chitosan revealed a shift of the amide I band assigned to the C=O vibration of the acetamide group from  $1652$  to  $1635\text{ cm}^{-1}$ , indicating the formation of new amide bonds. The deformation vibration of the N-H bond of the amine and acetamide groups (amide II) at  $1597\text{ cm}^{-1}$  observably increased which confirmed the formation of an amide linkage between the primary amino groups of chitosan and the carboxyl groups of pCA.

After grafting HT onto pCA-chitosan, the absorption bands shift to  $1638\text{ cm}^{-1}$  and  $1618\text{ cm}^{-1}$  are characteristic of the amide I and II, respectively. The bands of acetamide group were more intense than that of unmodified chitosan and pCA-chitosan, owing to the overlapping of the peaks from the free amino band of chitosan and the amide that couples chitosan and HT. These results are all consistent with the successful preparation of pCA-chitosan and pCA-HT-chitosan conjugates.

#### 4.2.3 Thermogravimetric analysis (TGA)

The thermal properties of chitosan and modified chitosan were evaluated with thermogravimetry (TGA). Figure 4.4 shows the weight loss curves recorded with a heating rate of  $25^{\circ}\text{C}/\text{min}$  in nitrogen between  $50$  to  $600^{\circ}\text{C}$ . For chitosan, the initial thermal decompositions stage at  $326^{\circ}\text{C}$  with and the corresponding weight loss of about  $31.6\%$  is attributed to the decomposition of chitosan. The modified chitosan started to degrade at a lower temperature compared to chitosan that the pCA-chitosan and pCA-HT-chitosan exhibited their initial thermal decomposition at  $300^{\circ}\text{C}$  and  $280^{\circ}\text{C}$ , respectively. The results obtained from TGA curves indicate a decrease of thermal

stability by conjugated pCA and HT. This may be that pCA and HT might reduce the hydrogen bonding between chitosan chains.

A comparison of chitosan and two modified chitosan (pCA-chitosan and pCA-HT-chitosan), the weight loss of pCA-HT-chitosan (25% total weight) and pCA-chitosan (28.3% total weight) was lower than of chitosan (31.6% total weight). This may be due to the pCA and HT side chains into the polysaccharide structure should disrupt the crystalline structure of chitosan.

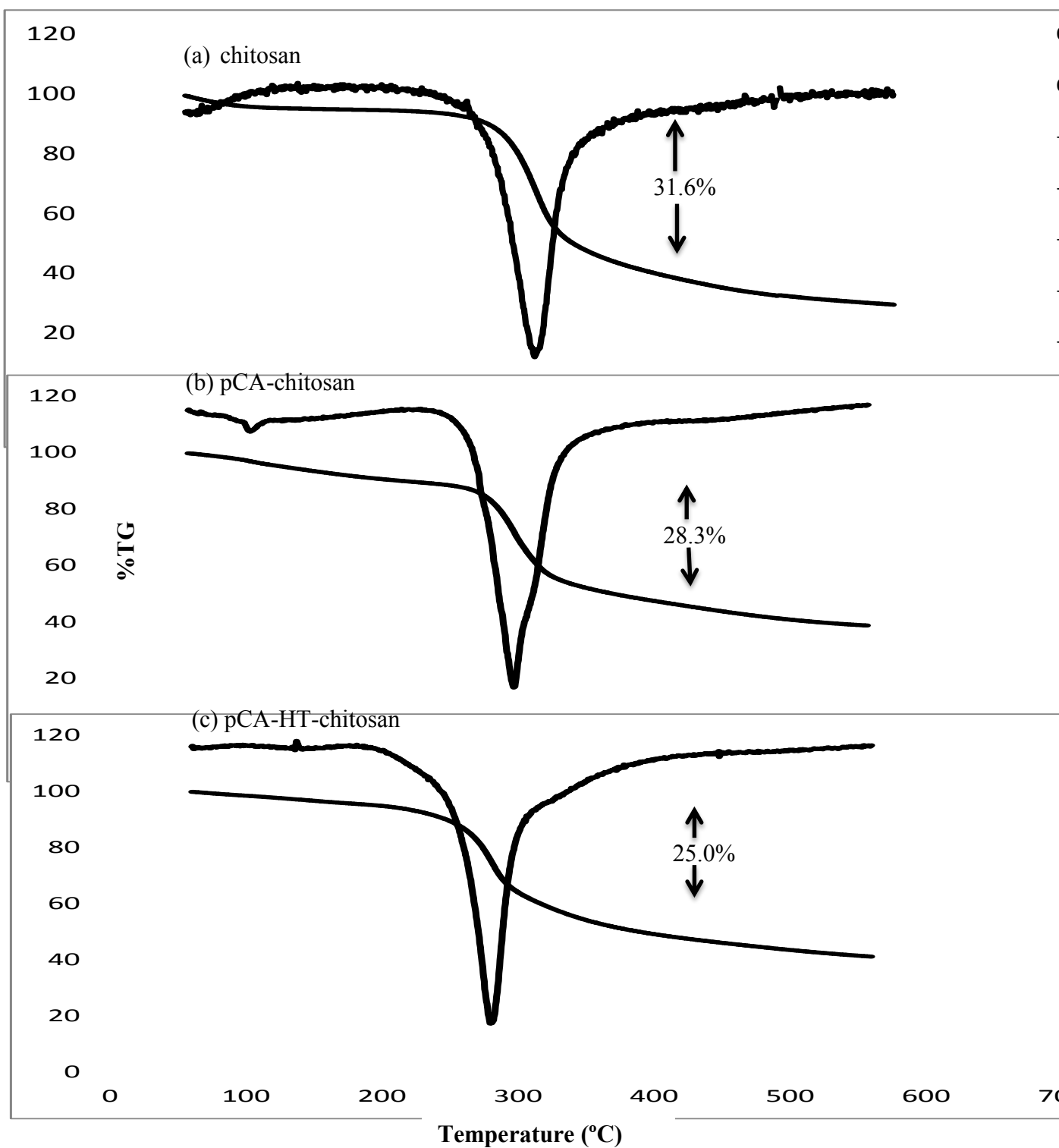


**Figure 4.4** Representative TG and DTG curves of (a) chitosan, (b) pCA-chitosan and (c) pCA-HT-chitosan

### 4.3 Degree of substitution of phenolic and thiol contents

#### 4.3.1 Degree of substitution of phenolic contents in pCA-CS and pCA-HT-chitosan

Phenolic content in modified chitosan was evaluated by using Folin–Ciocalteu method. Results in Table 4.1 shown that the mean total phenolic acids, it was calculated as gallic acid equivalent (GAE). The pCA-chitosan derived from a 1:0.2(w/w) ratio of chitosan:pCA found to be  $7.21 \pm 0.05$  mg GAE/g. Then grafted HT onto chitosan, the result was found to  $9.35 \pm 0.02$ ,  $8.16 \pm 0.07$  and  $8.49 \pm 0.01$  mg GAE/g at reaction time 12, 24 and 48, respectively. The total phenolic content higher than pCA-chitosan due to the reagent has also been shown to be reactive towards thiols, but results were not statistically significant ( $p > 0.05$ ).

**Table 4.1 Comparison of the levels of their phenolics content in modified chitosan**

<b>Compound</b>	<b>Total phenolic content (mg GAE /g)</b>
pCA-chitosan	$7.21 \pm 0.02$
pCA-HT-chitosan 12 h	$9.35 \pm 0.02^a$
pCA-HT-chitosan 24 h	$8.16 \pm 0.03^b$
pCA-HT-chitosan 48 h	$8.49 \pm 0.02^c$

<sup>a</sup>The mean difference is not significant ( $P > 0.05$ ) compared to pCA-chitosan using LSD method.

<sup>b</sup>The mean difference is not significant ( $P > 0.05$ ) compared to pCA-chitosan using LSD method.

<sup>c</sup>The mean difference is not significant ( $P > 0.05$ ) compared to pCA-chitosan using LSD method.



### 4.3.2 Degree of substitution of thiol and disulfide contents in pCA-HT-chitosan

Ellman's reagent is used for determine the thiol of pCA-HT-chitosan. It rapidly forms a disulfide bond with the thiol and releases a thiolate ion which is colored. The amount of free thiol groups and disulfide bonds in pCA-HT-chitosan under various reaction times (12, 24 and 48 h) are demonstrated in Table 4.2. The content of thiol groups on thiolated chitosan was found to be 13-17  $\mu\text{mol/g}$ . The sulphurs content are increase when increasing reaction time from 12 to 24 h but the total thiol groups decrease occurring with reaction time up to 48 h. This may be due to the moiety thiol containing chitosan being able to be formation disulfide bond within side chain chitosan that are reducing the amount thiol groups.

The rate of the amount disulfide bonds are increase when levels of the reaction time increases. Presumably due to higher density of thiol groups lead to oxidation and formation disulfide bond within side chains chitosan. In this work, the optimal condition from preparation pCA-HT-chitosan is 24 h.

**Table 4.2 Comparison of the levels of their thiol and disulfide content in thiolated chitosan**

<b>Compound</b>	<b>Total thiol groups(<math>\mu\text{mol/g}</math>)</b>	<b>Total disulfide groups(<math>\mu\text{mol/g}</math>)</b>
pCA-HT-chitosan 12 h	13.07 $\pm$ 0.02	8.32 $\pm$ 0.03
pCA-HT-chitosan 24 h	17.57 $\pm$ 0.01	8.48 $\pm$ 0.03
pCA-HT-chitosan 48 h	10.58 $\pm$ 0.01	11.85 $\pm$ 0.04

### 4.4 Mucoadhesive properties

In general, mucoadhesion is considered to occur in three major stages: wetting, interpenetration, and mechanical interlocking between mucus and polymer,

which are several general theories that have been presented to explain mucoadhesion phenomena. The mucoadhesive properties have traditionally been evaluated by many methods including tensile studies, flow retention techniques and spectroscopic. Periodic acid/Schiff colorimetric method was used for determining the amount of free mucin to estimate the amount of adsorbed mucins on the chitosan and modified chitosan.

Results of adhesion studies are shown in Table 4.3. The adhesion of pCA-chitosan was not statistically significant ( $p > 0.05$ ) that compared the unmodified chitosan owing to the pCA-chitosan form non-covalent bonds such as hydrogen bonding with mucus layer and the hydrophobic part of the aromatic phenol ring in pCA interact in part with the  $-\text{CH}_3$  groups on the mucin side chains. These interactions are weak in comparison to covalent bonds. After conjugated HT onto chitosan, the thiolated chitosan display significantly ( $p < 0.05$ ) higher mucoadhesive properties than that of the pCA-chitosan and unmodified chitosan. The mucoadhesive property of thiolated polymers are based on the formation of covalent bonds between thiol-bearing side chains of the polymer and cysteine-rich subdomains of mucus glycoprotein. In addition, pCA-HT-chitosan occurs hydrophobic interaction by the  $-\text{CH}_2$  moieties of HT with the  $-\text{CH}_3$  groups on the mucin side chains which, leading to increasing the mucoadhesive adsorption. The various reaction times are affecting the mucoadhesive properties of pCA-HT-chitosan that reaction times at 12, 24 and 48 h. The amount of mucin adsorbed onto polymer was increased by about 10% for all tested pHs, based on the value obtained from pCA-chitosan when the reaction time increased from 12 to 24 h. The result was also consistent with the number of thiol groups shown in Table 4.3. However, when the reaction time was increased to 48 h the amount mucin adsorbed was decreased about 1-fold compared to that of from pCA-chitosan. This may be the thiol groups were oxidized to be disulfides during the coupling procedure. Therefore, the highest mucoadhesiveness of pCA-HT-chitosan is obtained at the reaction time of 24 h, with the values about 9.87-, 2.01- and 1.58-fold more than chitosan in all tested three pH, respectively.

**Table 4.3 Comparison of the different reaction time to mucoadhesive property**

Batch	Total thiol groups( $\mu\text{mol/g}$ )	Total disulfide groups( $\mu\text{mol/g}$ )	Adsorbed mucin		
			pH 1.2	pH 4	pH 6.4
Chitosan	-	-	0.08 $\pm$ 0.02	0.41 $\pm$ 0.04	0.53 $\pm$ 0.02
pCA-chitosan	-	-	0.12 $\pm$ 0.01 <sup>a</sup>	0.44 $\pm$ 0.04 <sup>a</sup>	0.54 $\pm$ 0.02 <sup>a</sup>
pCA-HT-chitosan 12 h	13.07 $\pm$ 0.01	8.32 $\pm$ 0.02	0.62 $\pm$ 0.01 <sup>b</sup>	0.69 $\pm$ 0.03 <sup>b</sup>	0.78 $\pm$ 0.02 <sup>b</sup>
pCA-HT-chitosan 24 h	17.57 $\pm$ 0.01 <sup>d</sup>	8.48 $\pm$ 0.01	0.79 $\pm$ 0.02 <sup>b,c</sup>	0.83 $\pm$ 0.03 <sup>b,c</sup>	0.84 $\pm$ 0.02 <sup>b,c</sup>
pCA-HT-chitosan 48 h	10.58 $\pm$ 0.01	11.85 $\pm$ 0.01	0.45 $\pm$ 0.01 <sup>b</sup>	0.51 $\pm$ 0.01 <sup>b</sup>	0.63 $\pm$ 0.03 <sup>b</sup>

<sup>a</sup>The mean difference

is not significant ( $P > 0.05$ ) compared to chitosan using LSD method.

<sup>b</sup>The mean difference is significant ( $P < 0.05$ ) compared to chitosan using LSD method.

<sup>c</sup>The mean difference is significant ( $P < 0.05$ ) compared to pCA-HT-chitosan with reaction time at 12 h using LSD method.

<sup>d</sup>The mean difference is significant ( $P < 0.05$ ) compared to pCA-HT-chitosan with reaction time at 12 h using LSD method.

<sup>e</sup>The mean difference is not significant ( $P > 0.05$ ) compared to pCA-chitosan using LSD method

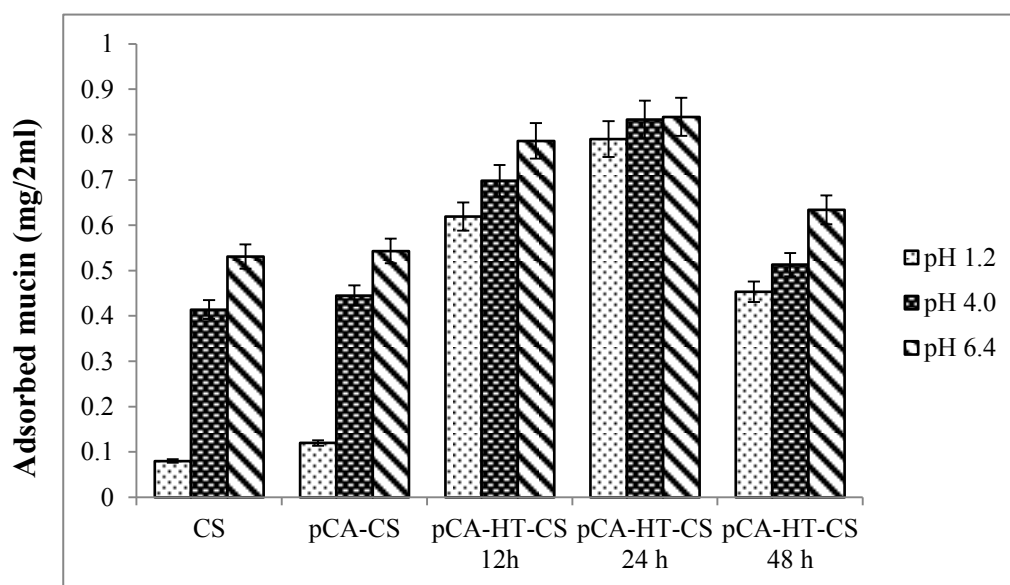


**Figure 4.5 Adsorption of mucin on CS, pCA-CS and pCA-HT-CS of different reaction time at pH 1.2, 4.0 and 6.4.**

In addition, the results indicate that mucoadhesive properties of chitosan and modified chitosan depend on the pH value (Fig. 4.5). The amount of mucins was adsorbed onto the chitosan and modified chitosan decreased at acidic condition because the degrees of the ionization of sialic acid or the different forms of the glycoprotein are influenced by the environment. The values of pKa and pI for sialic acid and mucin are 2.6 and ~3–5, respectively. Thus, the ionization of the sialic acid and the glycoprotein will be more sensitive to the acidic environment. As the pH value decreases, the amount of ionized sialic acid also decreases and so reduces the potential for interaction with chitosan and modified chitosan.

#### 4.5 Swelling study

The swelling of chitosan is an important characteristic in pharmaceutical applications. This behavior of mucoadhesive polymers greatly influences their adhesive, cohesiveness, and drug release. Swelling behavior of chitosan and modified chitosan with various the pH levels for the period up to 24 h, being SGF (pH 1.2), 0.1 M acetate buffer (pH 4.0) and SIF (pH 6.4) are well illustrated in Fig. 4.6 All modified chitosan had significant ( $p < 0.05$ ) changes in swelling ratios with

comparison the pure chitosan that showed essentially the same pattern, thus for the pCA-chitosan and pCA-HT-chitosan reaction time at 24 h is shown as an example. Degree of swelling of pCA-chitosan increases due to the dissociation hydrogen bonds occurred between acetylated units within chitosan chain, which allows the relaxation and decreasing crystallinity of polymer chains. These results swelling behavior of modified chitosan in spite of the hydrophobicity of pCA side chains. The pCA-HT-chitosan showed maximum degree of swelling in all conditions due to the presence of amino groups which interacted with hydrophilic of thiolated group and breaking of interaction producing intramolecular hydrogen bonding and creating more space for water within the polymer matrix.

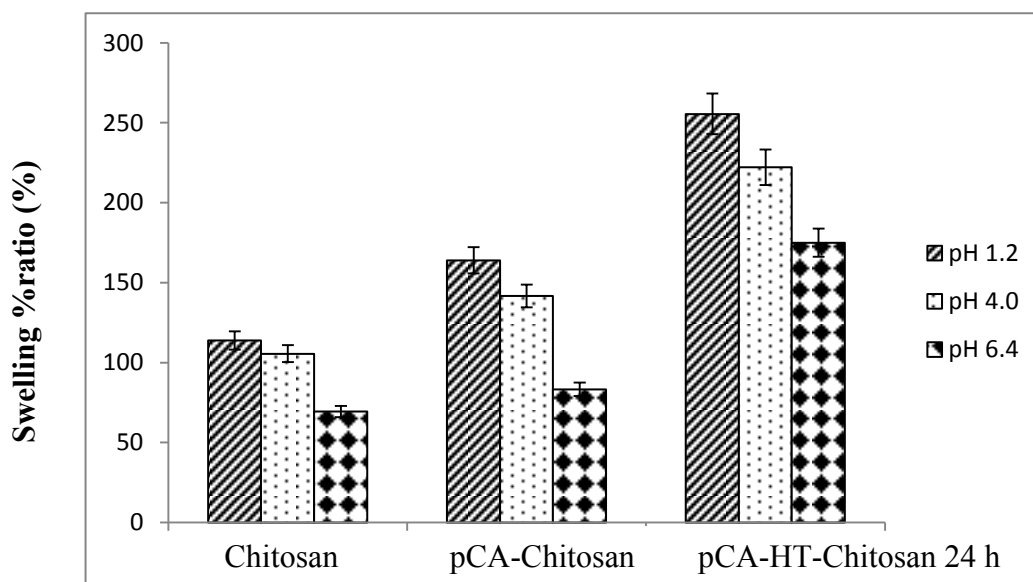


**Figure 4.6 Swelling behaviors of the chitosan and modified chitosan**

In addition, the results indicate that swelling behavior of chitosan and modified chitosan depend on the pH value (Fig. 4.7). Under acidic condition (pH 1.2), the swelling behavior of the chitosan and modified chitosan is controlled mainly by amino groups ( $-NH_2$ ) in the backbone of chitosan. It gets protonated and increased positively charge density on the chitosan that showed a high swelling ratio because the repulsive force between the positive charges within backbone chitosan. Degree of swelling of modified chitosan is slightly higher than that of unmodified chitosan and

increases significantly ( $p < 0.05$ ) with grafting the hydrophilic group (HT) onto chitosan by increasing up to 256%.

At pH 4, the degree of swelling decrease may be due to chitosan able to be formed hydrogen bonding between  $-NH_2$  and  $-CONH_2$  intramolecular chitosan.

In an alkaline condition (pH 6.4),  $-NH_3^+$  groups of chitosan can be changed into  $-NH_2$  as a result of a low concentration of  $H^+$ . The amino groups are fully deprotonated, thus reducing the swelling behavior of chitosan and modified chitosan.

However, the pCA-HT-chitosan is degree of swelling higher than the chitosan and other modified chitosan may be due to in this pH-range the concentration of thiolate anions increases, which electrostatic repulsive stronger force between the negative charges. But this swelling behavior lower than under acidic condition because the thiolate anions are a lower density within the polymer network and the local electrostatic repulsion weaker compared to amine groups in backbone of chitosan.

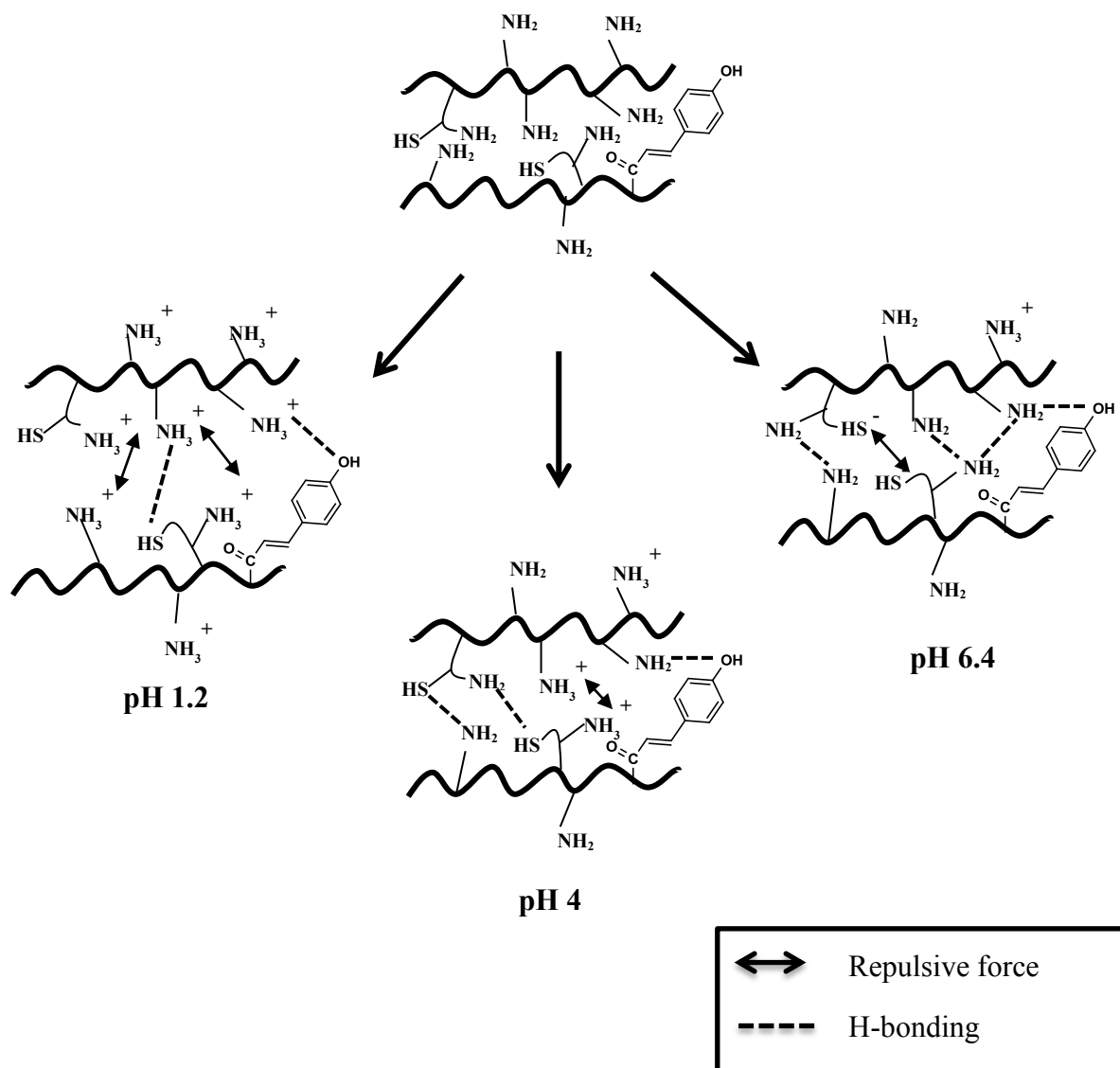


**Figure 4.7** Representative swelling mechanism of pCA-HT-chitosan in pH 1.2, 4.0 and 6.4

## 4.6 Fabrication microspheres

### 4.6.1. Morphology

#### 4.6.1.1. Chitosan and modified chitosan without piperine (PIP)

The electrospinning process use to produce the chitosan and modified chitosan microspheres. The advantages are the ability to obtain a uniform particle size, the narrow size distribution, simplicity, fast preparation, and one-step technique. Electrospinning parameters chosen in this work to prepare formed particles are as follow: working distance of 10 cm, needle gauge of 26 G, flow rate of 5 mL/h, stirring rate of 400 rpm a electrospinning voltage of 23 kV.

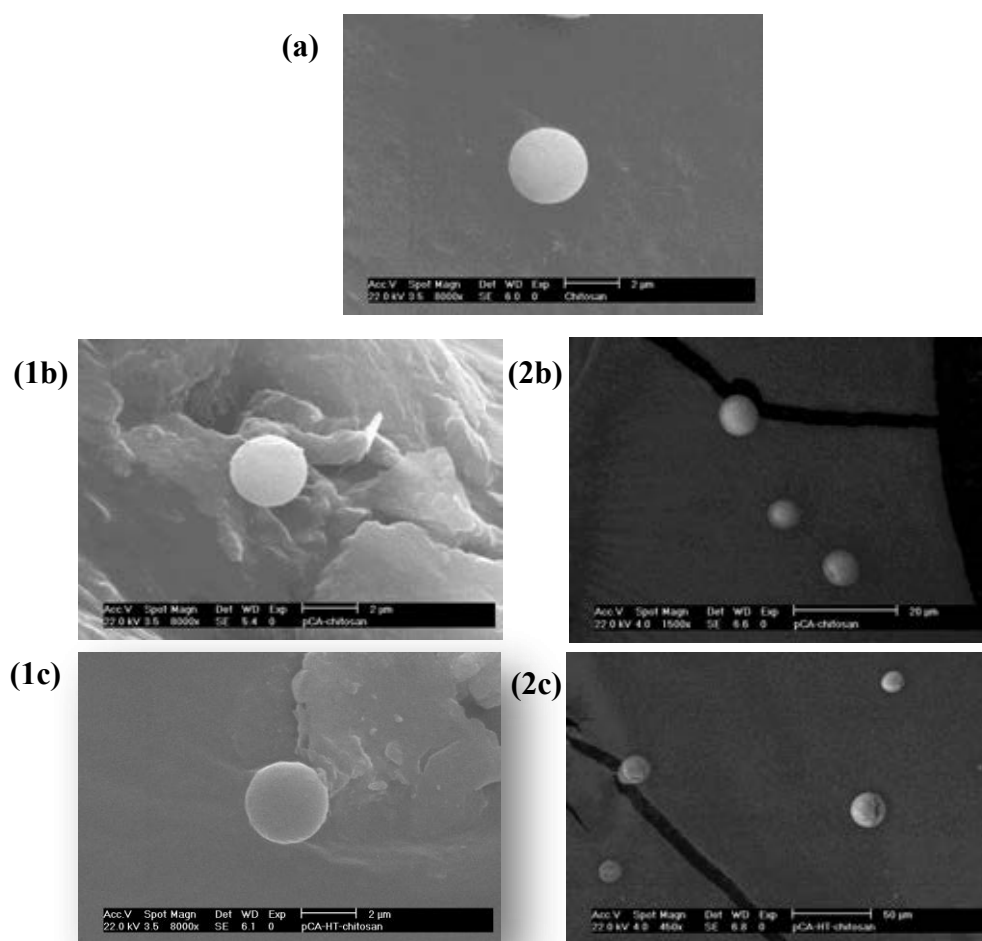


**Figure 4.8 Scanning electron micrographs of (a) chitosan, (b) pCA-chitosan and (c) pCA-HT-chitosan without PIP**



The morphology and microstructure of electrosprayed microspheres were characterized with a scanning electron microscope (SEM). The SEM micrographs of microsphere without PIP were shown in Figure 4.8. This result exhibited good morphological characteristics, a spherical shapes with smooth surface, no aggregation was visible between the particles and they did not show any internal or external porosity.

#### 4.6.1.2. Chitosan and modified chitosan loading PIP

The SEM micrographs of chitosan and modified chitosan microspheres loading PIP formulations are presented in Figure. 4.9. It can be seen that microspheres are spherical with wrinkles on their surface. This may be indicated PIP loading on chitosan and modified chitosan microspheres.

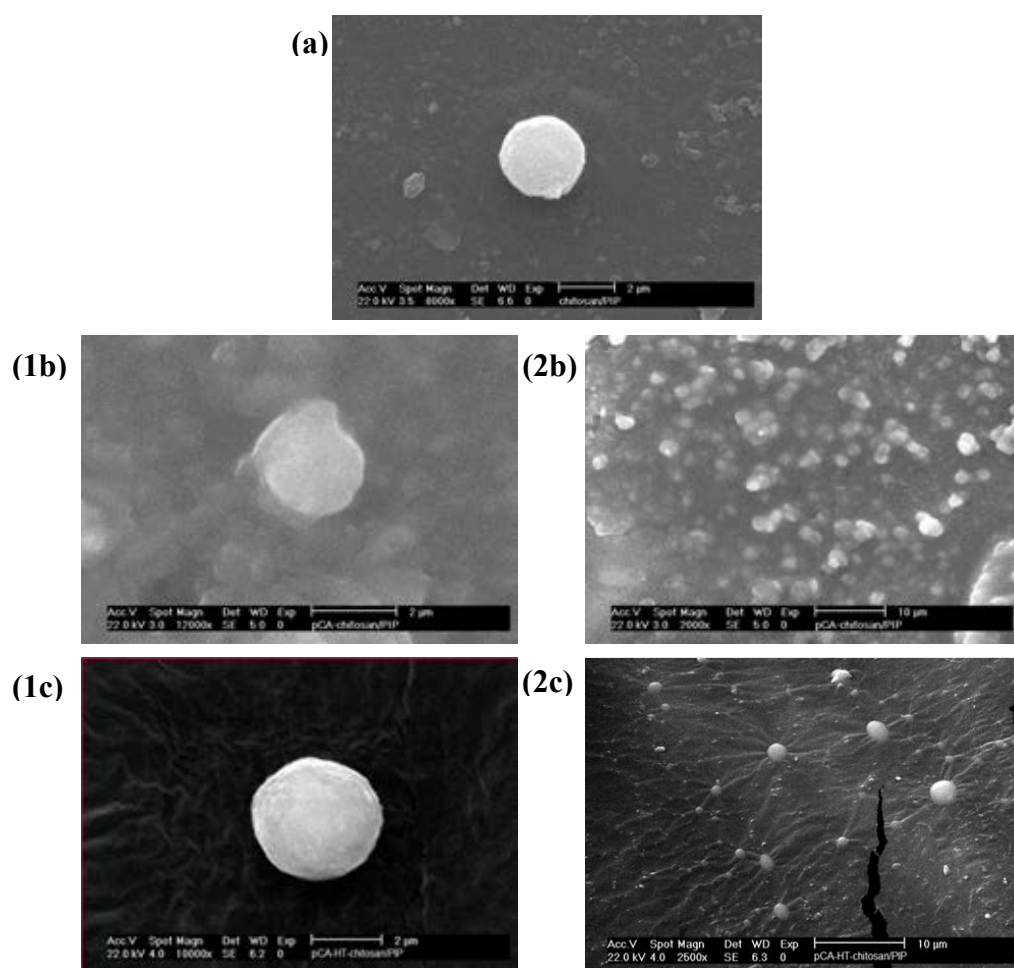


**Figure 4.9 Scanning electron micrographs of (a) chitosan/1%PIP, (b) pCA-chitosan/1%PIP and (c) pCA-HT-chitosan/1%PIP**

#### 4.6.2 Particle size and size distribution

The size distributions of chitosan and modified chitosan microspheres with/without loaded-1%PIP, and 5%PIP were presented in Table 4.4. The size of chitosan, pCA-chitosan and pCA-HT-chitosan without PIP particles size was approximately 2.69, 2.83 and 2.92  $\mu\text{m}$ , respectively with PDI approximately 0.62, 0.67 and 0.77, respectively.

In case of the size distributions of chitosan and modified chitosan with 1%PIP microspheres showed that they were in the range approximately from 3.12-4.66  $\mu\text{m}$  with PDI from about 0.64 to 0.86. In addition, when PIP was loaded onto polymer it results in increasing the mean size of spheres.

#### 4.6.3 Zeta potential (Zp)

The zeta potential, that is the average net surface charge density, can greatly influence particle stability in suspension through electrostatic repulsion between particles and how this is affected by changes in the environment (e.g. pH, presence of counter-ions, adsorption).

Zeta potential values are also of interest for the characterization of the microspheres since 1% PIP-loaded microspheres display Zp values -14.35, -11.61 and -19.71 mV as chitosan, pCA-chitosan and pCA-HT-chitosan, respectively. As shown in Table 4.4, the Zeta potential values indicating the surface charge of microsphere dispersions. It is commonly used to predict and control dispersion stability. The surface charge on these chitosan and modified chitosan microspheres were negative because of the effect of the stabilizing TPP. These results reveal that the pCA-HT-chitosan microsphere is negative charge higher than chitosan and pCA-chitosan due to include thiolated anion on the surface of polymer.

**Table 4.4 Effect of composition on morphology of the microsphere**

<b>Compound</b>	<b>shape</b>	<b>Bead size <math>\pm</math> SD(<math>\mu\text{m}</math>)by nanosizer</b>	<b>Zetapotential (mV)</b>	<b>Polydispersity (PDI)</b>
Chitosan	Spherical	2.69 $\pm$ 0.26	-19.61 $\pm$ 0.05	0.622
pCA-chitosan	Spherical	2.73 $\pm$ 0.30	-16.13 $\pm$ 0.05	0.671
pCA-HT-chitosan	Spherical	2.82 $\pm$ 0.10	-25.24 $\pm$ 0.90	0.772
Chitosan/1%PIP	Spherical	3.12 $\pm$ 0.04	-14.35 $\pm$ 0.10	0.799
pCA-chitosan/1%PIP	Spherical	3.55 $\pm$ 0.05	-11.61 $\pm$ 0.03	0.868
pCA-HT-chitosan/1%PIP	Spherical	3.63 $\pm$ 0.02	-19.71 $\pm$ 0.40	0.692
pCA-HT-chitosan/3%PIP	Spherical	4.66 $\pm$ 0.04	-16.70 $\pm$ 0.05	0.641
pCA-HT-chitosan/5%PIP	Spherical	5.01 $\pm$ 0.05	-13.70 $\pm$ 0.05	0.817

#### **4.6.4 Characterization of microspheres**

##### **4.6.4.1 Fourier transform infrared spectroscopy (FTIR)**

Fourier transform infrared spectroscopy (FT-IR) spectra of chitosan and modified chitosan microspheres loaded piperine(PIP) are shown in Figure 4.10. For the FTIR spectrum of PIP (Fig. 4.10a), the absorption band at 2940  $\text{cm}^{-1}$  is ascribed to aromatic C-H stretching. The most intense bands appearing at 1631 and 1608  $\text{cm}^{-1}$  can be assigned to C=C stretching of the aromatic and diene aliphatic chain, whereas

bands at  $1030\text{ cm}^{-1}$  are due to  $=\text{C}-\text{O}-\text{C}$  stretching and the most characteristic peaks related to C-O stretching at  $927\text{ cm}^{-1}$ .

The FTIR spectrum of chitosan/PIP microspheres was shown in Figure 4.10b. The absorption band at  $3510\text{ cm}^{-1}$  attributed to N-H bending. This is broadened due to formation electrostatic interactions with TPP. The characteristic peaks of piperine were observed in the spectra. The band at  $970\text{ cm}^{-1}$  and  $917\text{ cm}^{-1}$  are assigned to  $=\text{C}-\text{O}-\text{C}$  stretching and C-O stretching. The spectra obtained from the drug loaded microspheres indicate characteristic peaks of PIP were shifted to lower absorption in the formulations suggesting definite interactions between PIP and chitosan. This behavior was confirmed the occurring of encapsulation PIP onto chitosan microspheres.

The FTIR spectrum of pCA-chitosan/PIP was shown in Figure 4.10c. The pCA-chitosan/PIP microspheres revealed of the amide band assigned to the  $\text{C}=\text{O}$  vibration. The intensity of amide absorption increased comparison with chitosan microspheres (Fig. 4.10b) due to coupling pCA onto amine group of chitosan. The spectrum of pCA-chitosan/PIP microspheres appeared the characteristic peak of PIP at  $980$  and  $920\text{ cm}^{-1}$  corresponding to  $=\text{C}-\text{O}-\text{C}$  stretching and C-O stretching, indicating that PIP was loaded on pCA-chitosan microspheres.

The FTIR spectrum of pCA-HT-chitosan/PIP was shown in Figure 4.10d. The bands of amide were more intense comparison with pCA-chitosan/PIP (Fig. 4.10c) that confirmed HT coupling onto chitosan. The pCA-HT-chitosan/PIP spectrum was additional absorption peaks at  $983$  and  $924\text{ cm}^{-1}$  corresponding to  $=\text{C}-\text{O}-\text{C}$  stretching and C-O stretching of PIP that confirmed the presence of PIP loaded on pCA-HT-chitosan.

#### 4.6.4.2 Thermogravimetric analysis (TGA)

The results of thermogravimetric analysis of chitosan and modified chitosan were shown in Figure 4.11. Pure PIP is shown thermograms in Figure 4.11a. As can be seen, the temperature of highest decomposition rate is  $363^\circ\text{C}$ .

The TGA thermograms chitosan/PIP microspheres (Fig 4.11b) showed two degradation stages. The first stage started around  $60^\circ\text{C}$  with a weight loss of 5.0%

ascribed to the volatile low molecular products and water content in the microspheres. The second stage started at 260°C then reached the maximum of 293°C with a weight loss of 11.7%. Comparing to that of pure chitosan(Fig. 4.4a), the temperature of decomposition shifted to lower temperature after loading PIP on chitosan microspheres, which indicated that chitosan microsphere was more thermally stable than chitosan.

The pCA-chitosan/PIP (Fig. 4.11c) showed three degradation stages, The first stage started at 60 °C attributed to the water content. The second degradation stages of the solvent resident and impurity started at 140 °C. The final decomposition temperature 305 °C with a weight 10.2% attributed to the decomposition of chitosan. Comparision that of pCA-chitosan (Fig. 4.4b), The final decomposition temperature shifted to higher stage due to decomposition of PIP. Indicate the pCA-chitosan/PIP more thermally stable than pCA-chitosan.

TGA thermograms of pCA-HT-chitosan/PIP microspheres (Figure 4.11d) showed wo stages of weight loss. The frist degradation stages of the water and impurity. The final stage of degradation at 250-350 °C with weight loss 8.9%. The final stage of pCA-HT-chitosan/PIP shifted to higher stage with comparision pCA-HT-chitosan (Fig. 4.4c) due to microsphere encapsulation of PIP. Incicated the pCA-HT-chitosan/PIP more thermally stable than pCA-HT-chitosan.

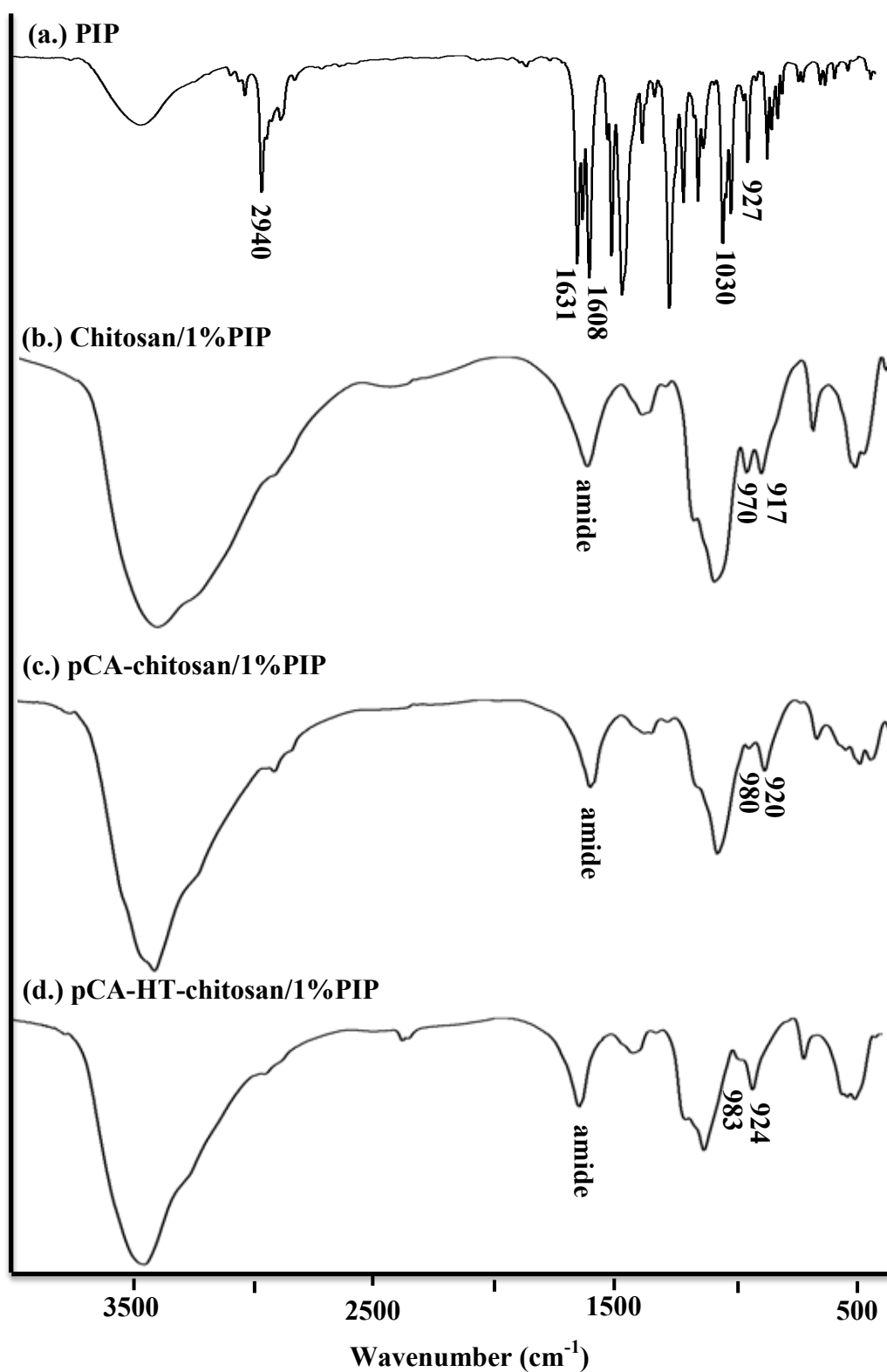
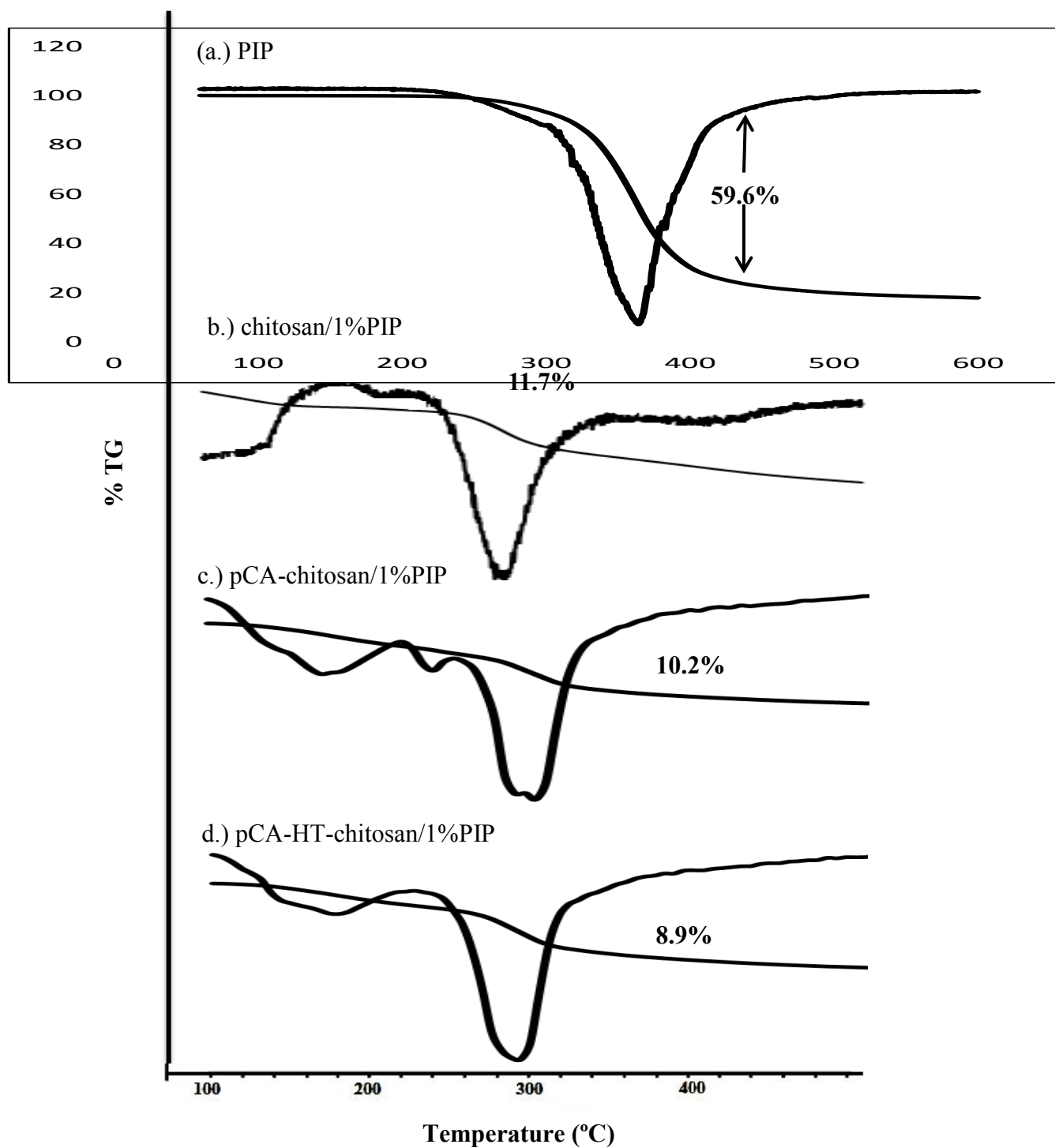


Figure 4.10 Representative FTIR spectrums of (a) PIP, (b) chitosan/1%PIP, (c) pCA-chitosan/1%PIP and (d) pCA-HT-chitosan/1%PIP.



**Figure 4.11** TGA thermograms of (a) PIP, (b) chitosan/1%PIP, (c) pCA-chitosan/1%PIP and pCA-HT-chitosan/1%PIP microspheres

### 6.5 Evaluation of drug encapsulation efficiency (%EE)

The percentages of encapsulation efficiency (%EE) of the PIP loaded chitosan and modified chitosan microspheres were given in Table 4.5. The encapsulation efficiency were analyzed using UV/Vis microplate reader spectroscopy at  $\lambda_{\text{max}} = 342 \text{ nm}$ .

In this work, Percentage entrapment loading of PIP on pCA-chitosan microsphere investigated to achieve the percentage of encapsulation efficiency higher than chitosan microsphere. This could be due to increased hydrogen bonding and hydrophobic interaction by the *p*-coumaric acid chains which ensures strong entrapment of PIP in pCA-chitosan microspheres. In addition, the pCA-HT-chitosan microspheres had a highest percent encapsulation due to  $-\text{CH}_2$  moieties of HT increasing hydrophobic part onto the side chain of chitosan.

The entrapment loading of 1.0% PIP onto chitosan, pCA-chitosan and pCA-HT-chitosan microspheres are about 54.02%, 60.44% and 67.97% respectively. The percent encapsulation is increased after that increasing %PIP loading onto pCA-HT-chitosan microspheres. Furthermore, the percent encapsulation had highest when increase %PIP loading onto microspheres up to 5%.

**Table 4.5 Encapsulation of PIP loaded polymer microspheres**

<b>Formulations</b>	<b>% Encapsulation</b>
Chitosan/1%PIP	54.84% $\pm$ 0.11
pCA-chitosan/1%PIP	61.36% $\pm$ 0.20
pCA-HT-chitosan/1%PIP	69.01% $\pm$ 0.22
pCA-HT-chitosan/3%PIP	77.80% $\pm$ 0.20
pCA-HT-chitosan/5%PIP	84.32% $\pm$ 0.30



#### 4.6.6 Mucoadhesiveness of microspheres

The best approach to evaluate mucoadhesive microspheres is to evaluate the effectiveness of mucoadhesive polymer to prolong the residence time of drug at the site absorption, thereby increasing absorption and bioavailability of the drug.

**Table 4.6 Effect of composition on mucoadhesive property of the chitosan and modified chitosan microspheres**

Abbreviation	Adsorbed of mucin at pH 1.2 (mg) ( $\pm$ SD, n=3)	Adsorbed of mucin at pH 4.0 (mg) ( $\pm$ SD, n=3)	Adsorbed of mucin at pH 4.0 (mg) ( $\pm$ SD, n=3)
Chitosan	0.08 $\pm$ 0.02	0.41 $\pm$ 0.04	0.53 $\pm$ 0.05
pCA-HT-chitosan	0.79 $\pm$ 0.02	0.83 $\pm$ 0.03	0.84 $\pm$ 0.03
Chitosan/PIP	0.11 $\pm$ 0.01	0.42 $\pm$ 0.02	0.45 $\pm$ 0.03
pCA-HT-chitosan/PIP	0.63 $\pm$ 0.02	0.67 $\pm$ 0.07	0.70 $\pm$ 0.04

The mucoadhesive properties of pCA-HT-chitosan are showed the values about 9.87-, 2.01- and 1.58-fold more than chitosan in all tested three pHs. After fabrication of microspheres, the amount absorbed mucin of pCA-HT-chitosan/PIP are about 5.72-, 1.59- and 1.55-fold higher than chitosan/PIP microsphere.

In these work, the pCA-HT-chitosan/PIP microsphere showed strongly mucoadhesive ability than chitosan/PIP microsphere. There are different factors increased the mucoadhesive properties, including (1) the hydrophobic interaction between the aromatic group of pCA and  $-\text{CH}_3$  groups on the mucin side chains; (2) the disulfide covalent bond between thiol groups of HT and cysteine-rich domains of mucin; (3) the electrostatic interaction between the remaining  $\text{NH}_3^+$  moieties of chitosan backbone and the  $\text{COO}^-$  or  $\text{SO}_3^-$  groups on the mucin carbohydrate side chain.

However, the pCA-HT-chitosan/PIP microspheres showed reducing mucoadhesion level compared to pCA-HT-chitosan at all tested pH, indicating after the pCA-HT-chitosan/PIP formed particles with TPP, the amino groups of chitosan

were interacted with TPP through electrostatic interaction, which is likely to be due to the fact that the influence of the positive charge of pCA-HT-chitosan/PIP was not enough to increase the mucoadhesion when compared with pCA-HT-chitosan. This may be due to the amount thiol moieties onto side chain chitosan were oxidized during form particles.

#### 4.6.7 In vitro PIP release profiles

The release of piperine from chitosan and modified chitosan was carried out in buffers pH 1.2, 4.0, and 6.4 (SGF, vaginal fluids, and SIF, respectively) at 37°C (Figs. 4.12-4.14).

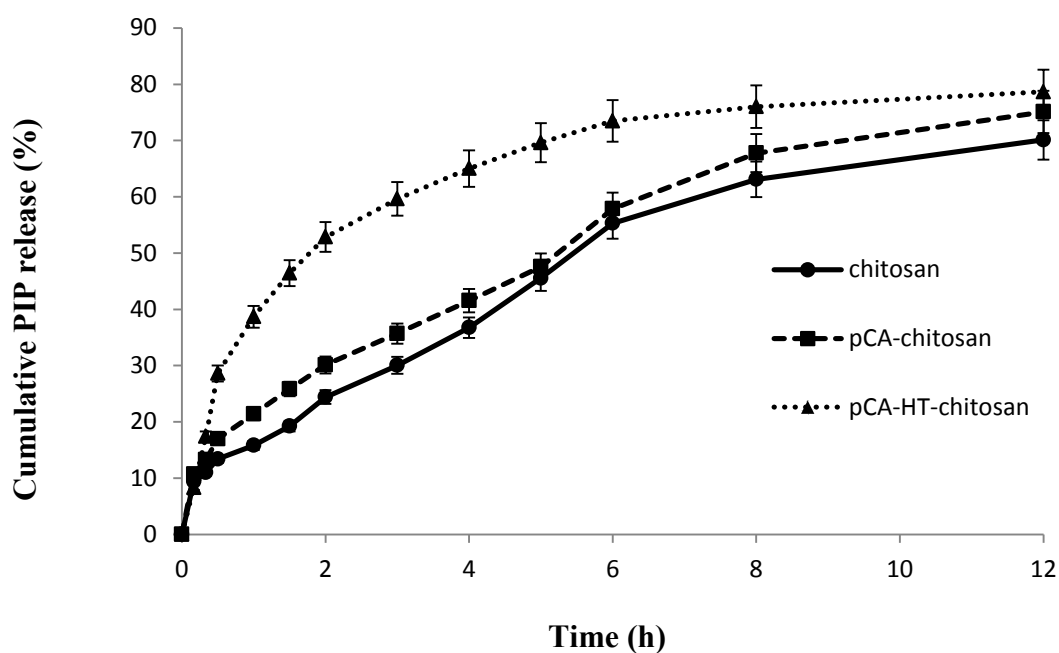


**Figure 4.12 Release profiles of piperine (PIP) from chitosan and modified chitosan in pH 1.2**

In Figs.4.12-4.14 shown the release profiles of piperine from chitosan and modified chitosan loaded with 1%wt of PIP as a function of time in three pH condition. The results showed that the drug release rate from all types of the polymer was quite fast during the initial period of time. About 10% of the drug was released in about 30 min. Such release was due to the free drug remaining at the surface that was not entrapped efficiently within the polymer matrix. After that the all polymer encapsulated with the drug presented a slow.

The cumulative drug release percentage are about 75%, 79% and 81% for chitosan, pCA-chitosan and pCA-HT-chitosan microspheres in pH 1.2 respectively and about 60-70% for all polymer in pH 4.0. Moreover, the release behavior in pH 6.4 (Figure 4.14) was lower than that in either pH condition. Most of PIP released from the spheres in the first 12 h.

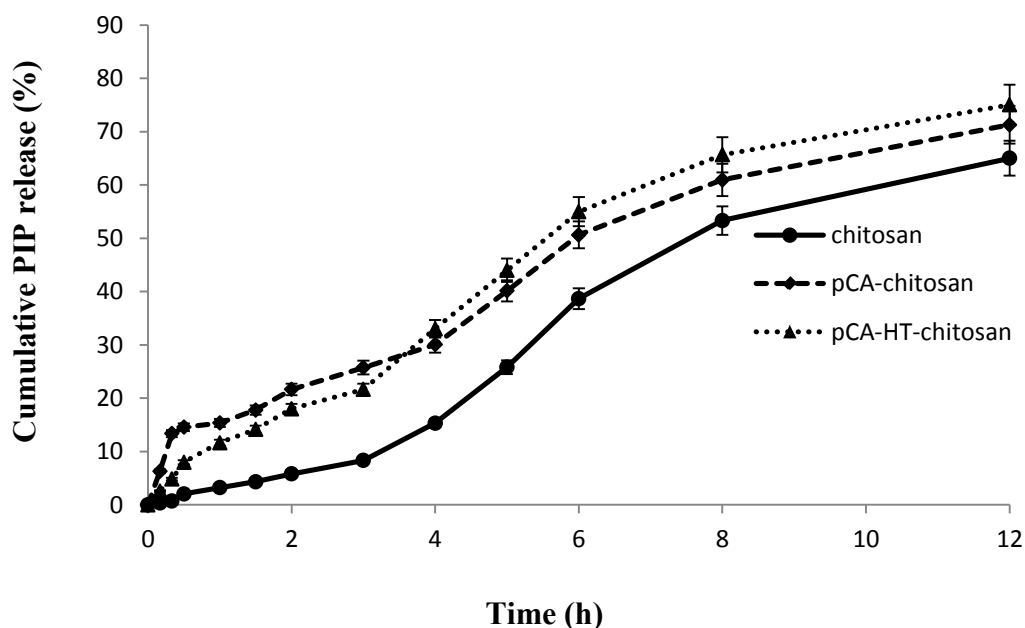


**Figure 4.13 Release profiles of piperine (PIP) from chitosan and modified chitosan in pH 4.0**

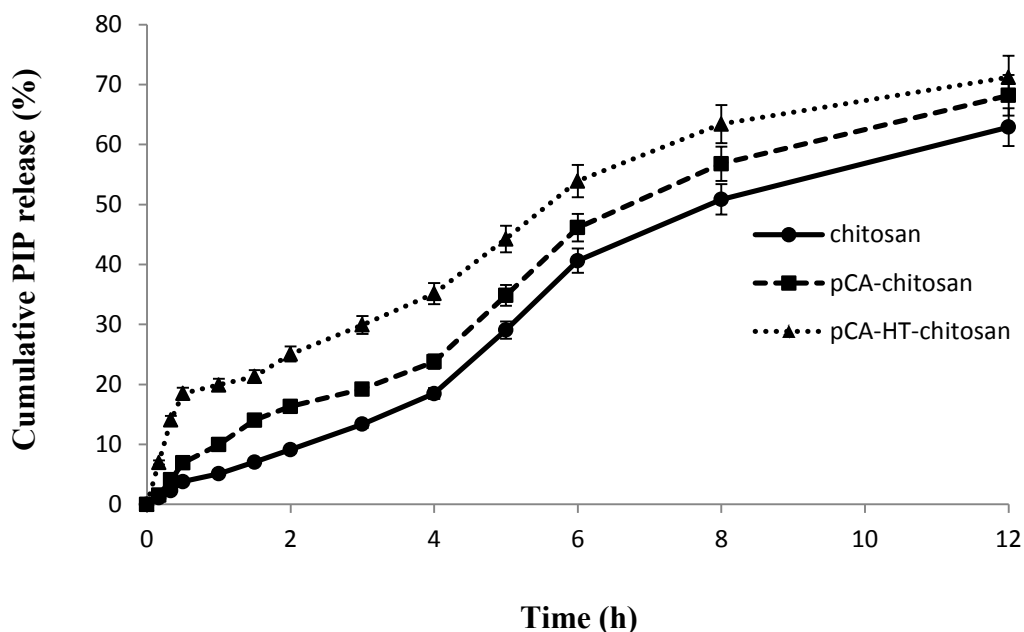


**Figure 4.14 Release profiles of piperine (PIP) from chitosan and modified chitosan in pH 6.4**

Controlled release of chitosan and modified chitosan microspheres, it was observed that drug release is faster during the initial period of time. Thereafter, a slower release rate is observed. It seems that the release obeys a swelling controlled release mechanism, especially at this initial period of release. After this initial period, in which the swelling equilibrium is achieved, the release is most probably followed by a diffusion-controlled mechanism. In this work, diffusion step the release of the PIP from the modified chitosan was higher than in chitosan that are not significant due to the interaction with hydrogen bond and hydrophobic between thiolated polymer and drug. And the ability of HT present in the thiolated polymers could be formation disulfide cross-linking between the polymer chains the main reasons for reduce swelling ratio of thiolated polymer lead to the steady release of drug.

Compared two modified chitosans in all pHs, the rate of drug release from microspheres depends on the contents of their thiol groups. The rate of release from pCA-HT-chitosan was found to be slightly higher than pCA-chitosan microspheres. This can be explained by considering the rate of diffusion from the swollen microsphere. As previously discussed, due to the higher thiol density, there is a

swelling of pCA-HT-chitosan more than when compared with pCA-chitosan which inhibits the diffusion of drugs at a faster rate.

In vitro release behaviors of 5%PIP from pCA-HT-chitosan is shown in Fig. 4.15. The cumulative release percentage increases up to 86% at pH 1.2. And shows percentage about 60%-70% at pH 4.0 and 6.4

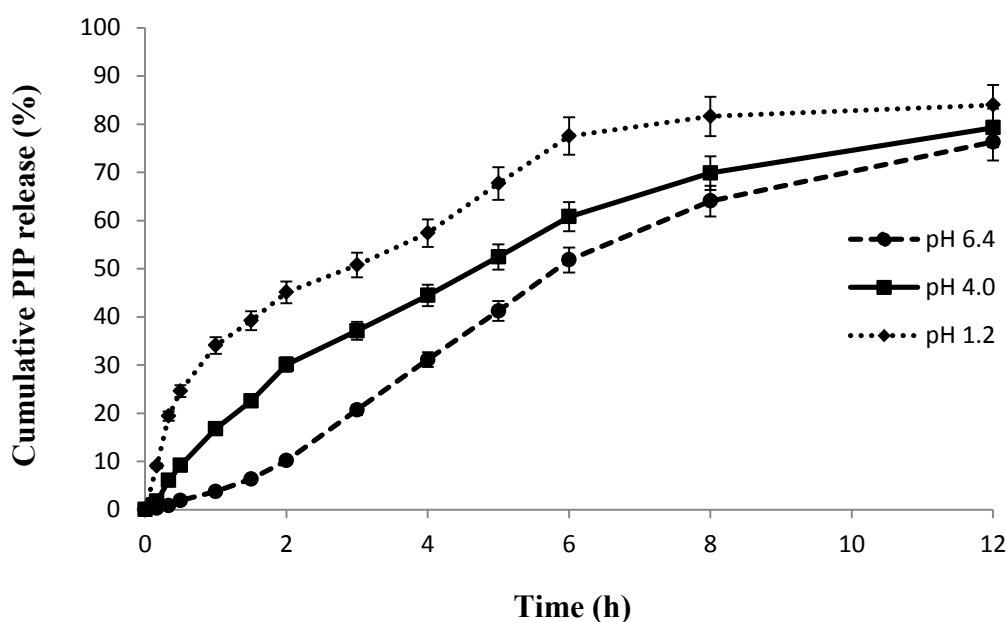


**Figure 4.15 Release profiles of 5%wt piperine (PIP) from pCA-HT- chitosan in different pHs**

The effect of pH on the release rate of 5%PIP from the pCA-HT-chitosan microsphere shows in Figure 4.15. At pH 1.2, the cumulative release of PIP from the spheres is 30% within the first hour, and below 10% and 5% in pH 4.0 and 6.4, respectively. In acid condition amino groups of chitosan are protonated. The positive charge repulsion force within side chain of chitosan. This results indicated that the higher swelling ratios of the polymer create larger surface areas to diffuse the drug. At pH 4.0 and 6.4, the density of positive charge are reduced that leading to decrease the cumulative release PIP of polymer.

## CHAPTER V

### CONCLUSION

In this work, the hydrophobic mucoadhesive thiolated chitosan was successfully synthesized, by conjugated pCA and HT on chitosan. The thiolated chitosan leads to strongly improved mucoadhesive properties by forming inter and/or intramolecular disulfide bonds and a good swelling behavior. The results of thiolated polymer indicated that this system seems to be a very promising vehicle for the administration of controlled release of drugs.

The piperine (PIP) loaded thiolated chitosan microspheres were successfully prepared using an electrospray ionization method. The morphology and size of these spheres can be manipulated by fixing the parameters as follows: working distance of 10 cm, needle gauge of 26G, flow rate of 5 mL/h, stirring rate of 400 rpm and electrospraying voltage of 23 kV. The thiolated chitosan of 5%PIP-polymer (w/w) microspheres were spherical in shape with a narrower size distribution and a high PIP-loaded (%EE) of over 80%. The microsphere prolonged the release of PIP for up to 12 h. Thus, the electrospray technique is a promising technique for the preparation of microsphere-based drug carrier systems.

The ability of *p*-coumaric acid and homocysteine thiolactone present in the thiolated polymers to form entrapped hydrophobic drug molecules (PIP) and able be formed disulfide bond with mucus membranes. The amount of mucin absorbed onto thiolated microsphere displayed 5.72-, 1.59- and 1.55-fold stronger than the unmodified chitosan at pH 1.2, 4.0, and 6.4 respectively. The PIP encapsulation efficiencies were significantly ( $p < 0.05$ ) affected by the aromatic group of thiolated microsphere and the highest piperine EE% values 84%. The mechanisms of drug release from thiolated polymer can be controlled by swelling followed by a diffusion-controlled mechanism. The PIP presented a slow, steady release and prolongs release into the buffer for up to 12 h. These results suggest that thiolated chitosan with improved mucoadhesive properties may potentially become an effective hydrophobic drug carrier system with controlled drug release capability.

**Suggestion**

The aim of the further work will prepare polyelectrolyte of thiolated chitosan-carrageenan hydrogel beads. It is believed that polyelectrolyte controlled release hydrophobic drug slower than thiolated chitosan.

## REFERENCES

- [1] Zhang, Y.; Chan, H. F.; Leong, K. W., Advanced materials and processing for drug delivery: The past and the future. *Advanced Drug Delivery Reviews* 65, 1 (2013) : 104-120.
- [2] Denkbaz, E. B., Perspectives on: Chitosan Drug Delivery Systems Based on their Geometries. *Journal of Bioactive and Compatible Polymers* 21, 4 (2006) : 351-368.
- [3] Acharya, G.; Park, K., Mechanisms of controlled drug release from drug-eluting stents. *Advanced Drug Delivery Reviews* 58, 4 (2006) : 387-401.
- [4] Iqbal, J.; Shahnaz, G.; Dünnhaupt, S.; Müller, C.; Hintzen, F.; Bernkop-Schnürch, A., Preactivated thiomers as mucoadhesive polymers for drug delivery. *Biomaterials* 33, 5 (2012) : 1528-1535.
- [5] Ludwig, A., The use of mucoadhesive polymers in ocular drug delivery. *Advanced Drug Delivery Reviews* 57, 11 (2005) : 1595-1639.
- [6] Ugwoke, M.; Agu, R.; Verbeke, N.; Kinget, R., Nasal mucoadhesive drug delivery: Background, applications, trends and future perspectives. *Advanced Drug Delivery Reviews* 57, 11 (2005) : 1640-1665.
- [7] Riva, R.; Ragelle, H.; Rieux, A.; Duhem, N.; Jérôme, C.; Pr at, V., Chitosan and Chitosan Derivatives in Drug Delivery and Tissue Engineering. 244, (2011) : 19-44.
- [8] Jain, G. K.; Pathan, S. A.; Akhter, S.; Ahmad, N.; Jain, N.; Talegaonkar, S.; Khar, R. K.; Ahmad, F. J., Mechanistic study of hydrolytic erosion and drug release behaviour of PLGA nanoparticles: Influence of chitosan. *Polymer Degradation and Stability* 95, 12 (2010) : 2360-2366.
- [9] Park, J. H.; Saravanakumar, G.; Kim, K.; Kwon, I. C., Targeted delivery of low molecular drugs using chitosan and its derivatives. *Advanced Drug Delivery Reviews* 62, 1 (2010) : 28-41.
- [10] Vipin Bansal, P. K. S., Nitin Sharma, Om Prakash Pal and Rishabha Malviya, Applications of Chitosan and Chitosan Derivatives in Drug Delivery. *Advances in Biological Research* 5, 1 (2011) : 28-37.



- [11] Bernkop-Schnürch, A.; Dünnhaupt, S., Chitosan-based drug delivery systems. *European Journal of Pharmaceutics and Biopharmaceutics* 81, 3 (2012) : 463-469.
- [12] Yang, J.; Chen, J.; Pan, D.; Wan, Y.; Wang, Z., pH-sensitive interpenetrating network hydrogels based on chitosan derivatives and alginate for oral drug delivery. *Carbohydrate Polymers* 92, 1 (2013) : 719-725.
- [13] Nina Langoth, J. K., Andreas Bernkop-Schurch, Development of buccal drug delivery systems based on a thiolated polymer. *International Journal of Pharmaceutics* 252, (2003) : 141-148.
- [14] Yin, L.; Ding, J.; He, C.; Cui, L.; Tang, C.; Yin, C., Drug permeability and mucoadhesion properties of thiolated trimethyl chitosan nanoparticles in oral insulin delivery. *Biomaterials* 30, 29 (2009) : 5691-5700.
- [15] Prabakaran, M.; Gong, S., Novel thiolated carboxymethyl chitosan-g- $\beta$ -cyclodextrin as mucoadhesive hydrophobic drug delivery carriers. *Carbohydrate Polymers* 73, 1 (2008) : 117-125.
- [16] Petchsangsa, M.; Sajomsang, W.; Gonil, P.; Nuchuchua, O.; Sutapun, B.; Puttipipatkachorn, S.; Ruktanonchai, U. R., A water-soluble methylated N-(4-N,N-dimethylaminocinnamyl) chitosan chloride as novel mucoadhesive polymeric nanocomplex platform for sustained-release drug delivery. *Carbohydrate Polymers* 83, 3 (2011) : 1263-1273.
- [17] Lou, Z.; Wang, H.; Rao, S.; Sun, J.; Ma, C.; Li, J., p-Coumaric acid kills bacteria through dual damage mechanisms. *Food Control* 25, 2 (2012) : 550-554.
- [18] Derrick L. Sauls, E. L., Maria Esteban Warren, Angela Lenkowski, Susan E. Wilhelm and Maureane Hoffman, Modification of Fibrinogen by Homocysteine Thiolactone Increases Resistance to Fibrinolysis: A Potential Mechanism of the Thrombotic Tendency in Hyperhomocysteinemia. *Biochemistry* 45, (2006) : 2480-2487.
- [19] Raffaele Capasso, A. A. I., Francesca Borrelli, Alessandra Russo, Lidia Sautebin, Aldo Pinto, Francesco Capasso and Nicola Mascolo, Effect of piperine, the active ingredient of black pepper, on intestinal secretion in mice. *Life Sciences* 71, (2002) : 2311-2317.

- [20] Sunila, E. S.; Kuttan, G., Immunomodulatory and antitumor activity of Piper longum Linn. and piperine. *Journal of Ethnopharmacology* 90, 2-3 (2004) : 339-346.
- [21] Joshi, H., Recent advances in drug delivery systems: polymeric prodrugs. *Pharmaceutical Technology* (1988) : 118-130.
- [22] Almería, B.; Fahmy, T. M.; Gomez, A., A multiplexed electrospray process for single-step synthesis of stabilized polymer particles for drug delivery. *Journal of Controlled Release* 154, 2 (2011) : 203-210.
- [23] Arya, N.; Chakraborty, S.; Dube, N.; Katti, D. S., Electrospraying: A facile technique for synthesis of chitosan-based micro/nanospheres for drug delivery applications. *Journal of Biomedical Materials Research Part B: Applied Biomaterials* 88B, 1 (2009) : 17-31.
- [24] Jaworek, A., Micro- and nanoparticle production by electrospraying. *Powder Technology* 176, 1 (2007) : 18-35.
- [25] Acharya, G.; Park, K., Mechanisms of controlled drug release from drug-eluting stents. *Advanced Drug Delivery Reviews* 58, 3 (2006) : 387-401.
- [26] Fredenberg, S.; Wahlgren, M.; Reslow, M.; Axelsson, A., The mechanisms of drug release in poly(lactic-co-glycolic acid)-based drug delivery systems—A review. *International Journal of Pharmaceutics* 415, 1-2 (2011): 34-52.
- [27] Abruzzo, A.; Bigucci, F.; Cerchiara, T.; Cruciani, F.; Vitali, B.; Luppi, B., Mucoadhesive chitosan/gelatin films for buccal delivery of propranolol hydrochloride. *Carbohydrate Polymers* 87, 1 (2012) : 581-588.
- [28] Salamatmiller, N.; Chittchang, M.; Johnston, T., The use of mucoadhesive polymers in buccal drug delivery. *Advanced Drug Delivery Reviews* 57, 11 (2005) : 1666-1691.
- [29] Svensson, O.; Thuresson, K.; Arnebrant, T., Interactions between chitosan-modified particles and mucin-coated surfaces. *Journal of Colloid and Interface Science* 325, 2 (2008) : 346-350.
- [30] Zambito, Y.; Felice, F.; Fabiano, A.; Di Stefano, R.; Di Colo, G., Mucoadhesive nanoparticles made of thiolated quaternary chitosan crosslinked with hyaluronan. *Carbohydrate Polymers* 92, 1 (2013) : 33-39.

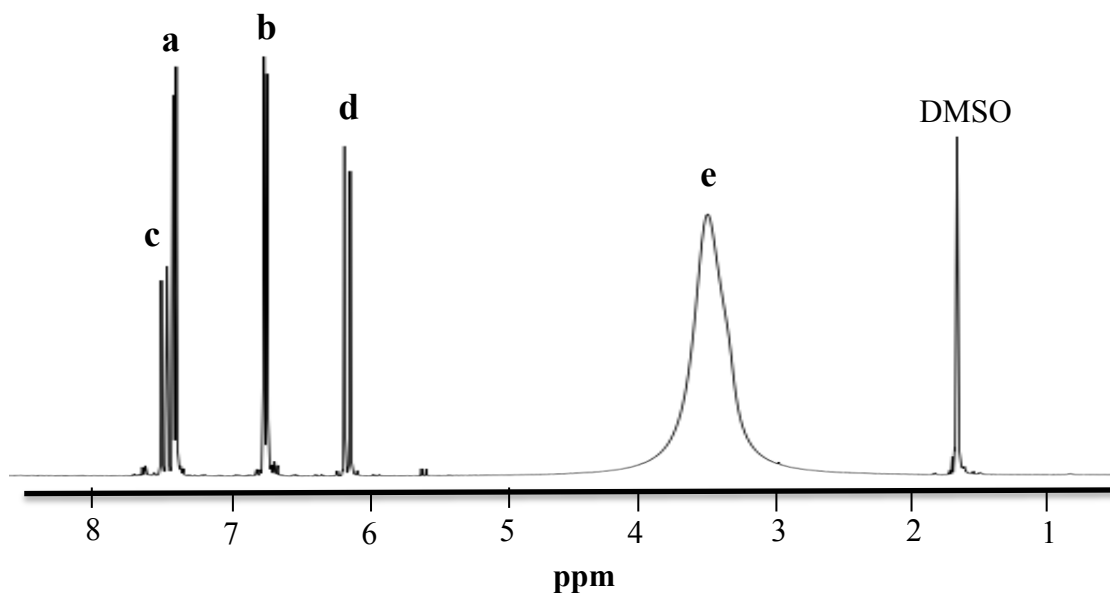
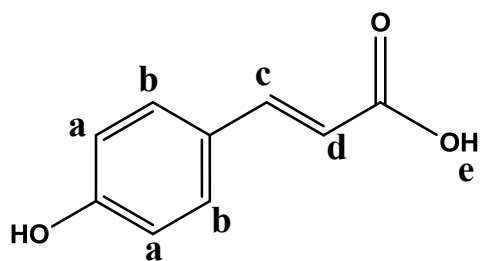
- [31] Smart, J., The basics and underlying mechanisms of mucoadhesion. *Advanced Drug Delivery Reviews* 57, 11 (2005) : 1556-1568.
- [32] Sogias, I. A.; Williams, A. C.; Khutoryanskiy, V. V., Chitosan-based mucoadhesive tablets for oral delivery of ibuprofen. *International Journal of Pharmaceutics* 436, 1-2 (2012) : 602-610.
- [33] Khutoryanskiy, V. V., Advances in Mucoadhesion and Mucoadhesive Polymers. *Macromolecular Bioscience* 11, 6 (2011) : 748-764.
- [34] Salamat-Miller, N.; Chittchang, M.; Johnston, T. P., The use of mucoadhesive polymers in buccal drug delivery. *Advanced Drug Delivery Reviews* 57, 11 (2005) : 1666-1691.
- [35] Flaherty, J. D.; Bax, J. J.; De Luca, L.; Rossi, J. S.; Davidson, C. J.; Filippatos, G.; Liu, P. P.; Konstam, M. A.; Greenberg, B.; Mehra, M. R.; Breithardt, G.; Pang, P. S.; Young, J. B.; Fonarow, G. C.; Bonow, R. O.; Gheorghide, M., Acute Heart Failure Syndromes in Patients With Coronary Artery Disease: Early Assessment and Treatment. *Journal of the American College of Cardiology* 53, 3 (2009) : 254-263.
- [36] Yalonetsky, S.; Horlick, E. M.; Osten, M. D.; Benson, L. N.; Oechslin, E. N.; Silversides, C. K., Clinical characteristics of coronary artery disease in adults with congenital heart defects. *International Journal of Cardiology* 164, 2 (2013) : 217-220.
- [37] Badmaev, V.; Majeed, M.; Prakash, L., Piperine derived from black pepper increases the plasma levels of coenzyme q10 following oral supplementation. *The Journal of Nutritional Biochemistry* 11, 2 (2000) : 109-113.
- [38] Kesarwani, K.; Gupta, R., Bioavailability enhancers of herbal origin: An overview. *Asian Pacific Journal of Tropical Biomedicine* 3, 4 (2013) : 253-266.
- [39] Wilhelm, O., L. Midler, and S.E. Pratsinis, Electrospray evaporation and deposition. *Journal of Aerosol Science*, 34, 7 (2003) : 815-836.
- [40] Oh, H., K. Kim, and S. Kim, Characterization of deposition patterns produced by twin-nozzle electrospray. *Journal of Aerosol Science*, 39, 9 (2008) : 801-813.

- [41] Juntapram, K.; Praphairaksit, N.; Siraleartmukul, K.; Muangsin, N., Synthesis and characterization of chitosan-homocysteine thiolactone as a mucoadhesive polymer. *Carbohydrate Polymers* 87, 4 (2012) : 2399-2408.
- [42] Everette, J. D.; Bryant, Q. M.; Green, A. M.; Abbey, Y. A.; Wangila, G. W.; Walker, R. B., Thorough Study of Reactivity of Various Compound Classes toward the Folin–Ciocalteu Reagent. *Journal of Agricultural and Food Chemistry* 58, 14 (2010) : 8139-8144.
- [43] Schmitz, T.; Grabovac, V.; Palmberger, T. F.; Hoffer, M. H.; Bernkop-Schnürch, A., Synthesis and characterization of a chitosan-N-acetyl cysteine conjugate. *International Journal of Pharmaceutics* 347, 1-2 (2008) : 79-85.
- [44] Kilcoyne, M., et al., Periodic acid-Schiff's reagent assay for carbohydrates in a microtiter plate format. *Analytical Biochemistry* 416, 1 : 18-26.
- [45] Juntapram, K.; Praphairaksit, N.; Siraleartmukul, K.; Muangsin, N., Electrospayed polyelectrolyte complexes between mucoadhesive N,N,N,-trimethylchitosan-homocysteine thiolactone and alginate/carrageenan for camptothecin delivery. *Carbohydrate Polymers* 90, 4 (2012) : 1469-1479.
- [46] Briones, A. V.; Sato, T., Encapsulation of glucose oxidase (GOD) in polyelectrolyte complexes of chitosan–carrageenan. *Reactive and Functional Polymers* 70, 1 (2010) : 19-27.
- [47] Xu, Y.; Zhan, C.; Fan, L.; Wang, L.; Zheng, H., Preparation of dual crosslinked alginate–chitosan blend gel beads and in vitro controlled release in oral site-specific drug delivery system. *International Journal of Pharmaceutics* 336, 2 (2007) : 329-337.

## **APPENDICES**

# APPENDIX A

## NMR spectrum *p*-coumaric acid



## APPENDIX B

### Standard curve of gallic acid

The concentrations versus peak absorbance of gallic acid are presented in Table 1B. The plot of calibration curve of gallic acid is illustrated in Figure 1B.

**Table 1B** Absorbance of various concentrations of Gallic acid by UV spectrometer

Concentration (mg/ml)	Abs.
0.02	0.106
0.04	0.234
0.06	0.355
0.08	0.481
0.10	0.709

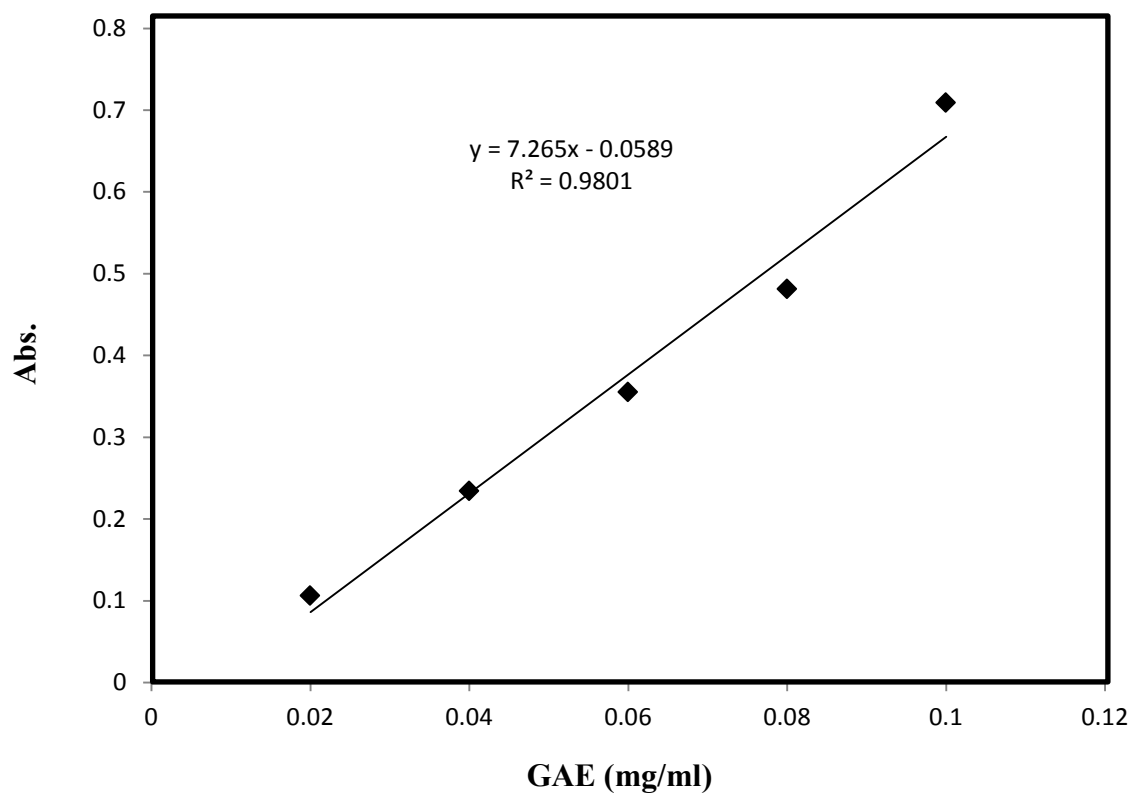


**Figure 1B** Standard curve of Gallic acid by UV spectrometer

**Table 2B Absorbance phenol groups by UV spectrometers**

<b>Bath</b>	<b>Abs.</b>	<b>Abs.</b>	<b>Abs.</b>	<b>GAE(mg/ml)</b>	<b>SD</b>
Chitosan	0.143	0.184	0.175	-	-
pCA-chitosan	0.330	0.215	0.252	7.21	0.06
pCA-HT-chitosan 12 h	0.313	0.303	0.267	9.35	0.02
pCA-HT-chitosan 24 h	0.297	0.247	0.315	8.16	0.04
pCA-HT-chitosan 48 h	0.288	0.357	0.236	8.49	0.06



## APPENDIX C

### Standard curve of L-cysteine Hydrochloride

The concentrations versus peak absorbance of L-cysteine are presented in Table 1C. The plot of calibration curve of L-cysteine hydrochloride is illustrated in Figure 1C

**Table 1C** Absorbance of various concentrations of L-cysteine Hydrochloride by UV spectrometer

Concentration ( $\mu\text{mol/g}$ )	Abs.
100	0.017
200	0.164
400	0.533
600	0.901
800	1.289
1000	1.642

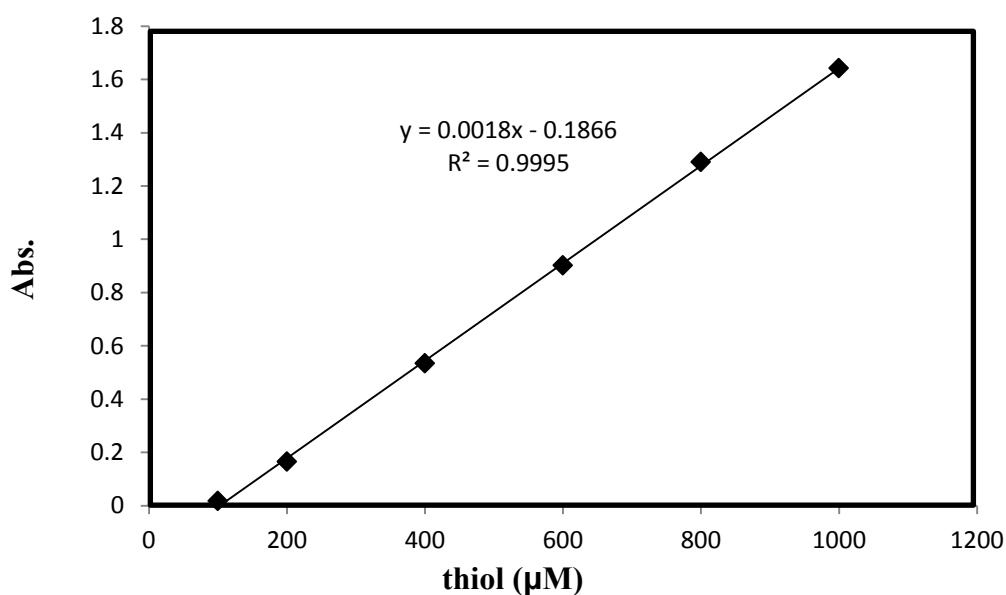


**Figure 1C** Standard curve of L-cysteine Hydrochloride by UV spectrometer

**Table 2C** Absorbance thiol groups by UV spectrometer

<b>Compound</b>	<b>Abs.</b>	<b>Abs.</b>	<b>Abs.</b>	<b>thiol (<math>\mu\text{M}</math>)</b>	<b>SD</b>
pCA-HT-chitosan 12 h	0.201	0.213	0.223	13.07	0.01
pCA-HT-chitosan 24 h	0.290	0.201	0.279	17.57	0.01
pCA-HT-chitosan 48 h	0.191	0.172	0.183	10.58	0.01

**Table 3C** Absorbance disulfide groups by UV spectrometer

<b>compound</b>	<b>Abs.</b>	<b>Abs.</b>	<b>Abs.</b>	<b>thiol (<math>\mu\text{M}</math>)</b>	<b>SD</b>
pCA-HT-chitosan 12 h	0.137	0.147	0.190	8.32	0.03
pCA-HT-chitosan 24 h	0.133	0.171	0.188	8.48	0.03
pCA-HT-chitosan 48 h	0.321	0.251	0.283	11.85	0.04

## APPENDIX D

### Calibration curve of mucin (type II)

The concentration versus peak absorbance mucin glycoprotein (type II) determined by UV is presented in Table 1D. The plot of calibration curve of mucin is illustrated in Figure 1D.

Table 1D Absorbance concentrations of mucin (type II) at pH 1.2, 4.0 and 6.4 by UV spectrometer

Concentration (mg/ 2mL)	HCl (pH 1.2)	Acetate buffer (pH 4.0)	PBS (PH 6.4)
0.2	0.063	0.121	0.236
0.4	0.131	0.293	0.609
0.6	0.184	0.466	0.869
0.8	0.224	0.640	1.122
1.0	0.275	0.844	1.371

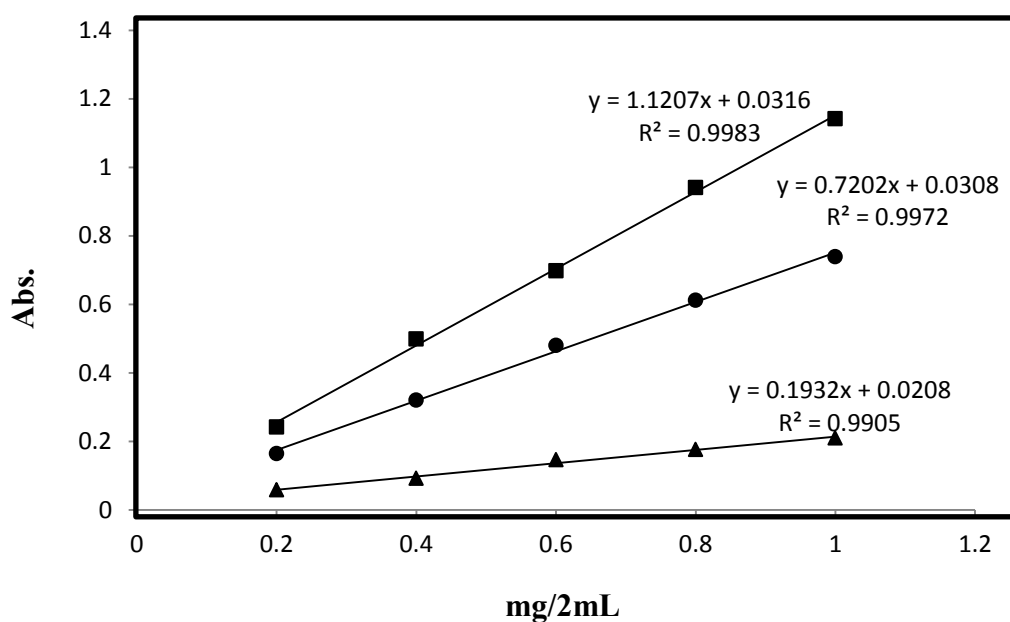


Figure 1D Standard curve of mucin at pH 1.2, 4.0, and 6.4

**Table 2D** Absorbance of adsorped mucin of chitosan and modified chitosan at pH 1.2 by UV spectrophotomer

<b>compound</b>	<b>Abs.</b>	<b>Abs.</b>	<b>Abs.</b>	<b>Adsorped mucin(mg/2ml)</b>	<b>SD</b>
Chitosan	0.240	0.267	0.285	0.081	0.02
pCA-chitosan	0.244	0.263	0.259	0.126	0.01
pCA-HT-chitosan 12 h	0.163	0.178	0.154	0.593	0.01
pCA-HT-chitosan 24 h	0.124	0.139	0.115	0.795	0.01
pCA-HT-chitosan 48 h	0.158	0.162	0.221	0.514	0.03

**Table 3D** Absorbance of adsorped mucin of chitosan and modified chitosan at pH 4.0 by UV spectrophotomer

<b>compound</b>	<b>Abs.</b>	<b>Abs.</b>	<b>Abs.</b>	<b>Adsorped mucin(mg/2ml)</b>	<b>SD</b>
Chitosan	0.502	0.586	0.534	0.414	0.04
pCA-chitosan	0.497	0.569	0.488	0.445	0.04
pCA-HT-chitosan 12 h	0.342	0.299	0.365	0.699	0.03
pCA-HT-chitosan 24 h	0.251	0.222	0.281	0.815	0.03
pCA-HT-chitosan 48 h	0.456	0.490	0.461	0.513	0.02

**Table 4D** Absorbance of adsorbed mucin of chitosan and modified chitosan at pH 6.4 by UV spectrophotometer

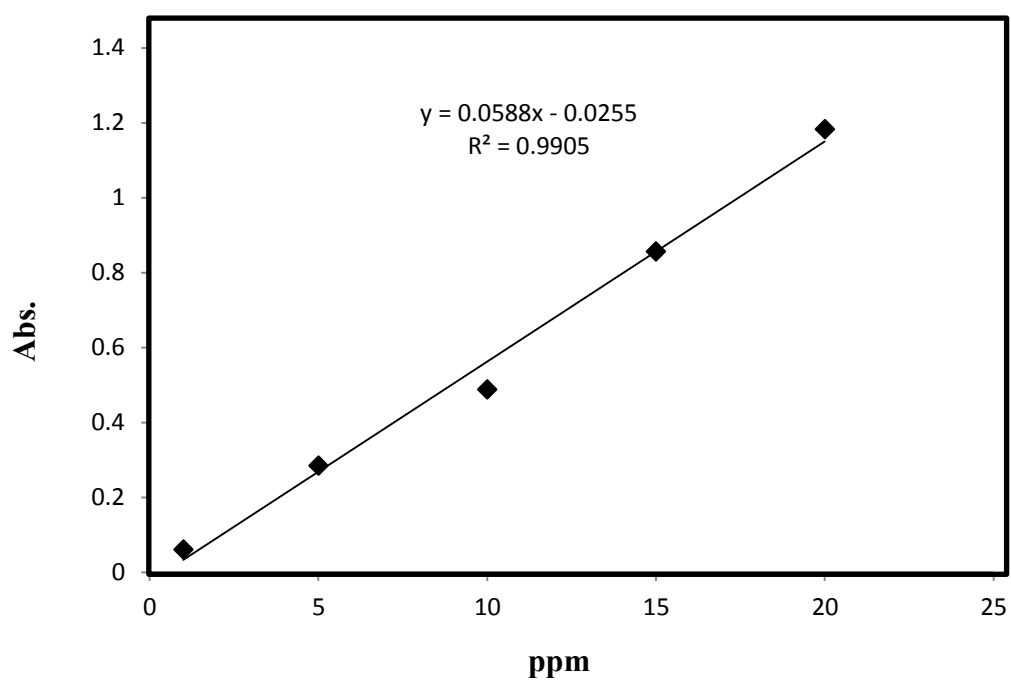
<b>compound</b>	<b>Abs.</b>	<b>Abs.</b>	<b>Abs.</b>	<b>Adsorbed mucin(mg/2ml)</b>	<b>SD</b>
Chitosan	0.659	0.697	0.599	0.543	0.05
pCA-chitosan	0.595	0.675	0.650	0.543	0.04
pCA-HT-chitosan 12 h	0.394	0.339	0.371	0.786	0.03
pCA-HT-chitosan 24 h	0.269	0.323	0.290	0.852	0.03
pCA-HT-chitosan 48 h	0.474	0.541	0.601	0.634	0.06

## APPENDIX E

### Calibration curve of PIP

**Table 1E** Absorbance of piperine drug in ethanol determined in 342 nm

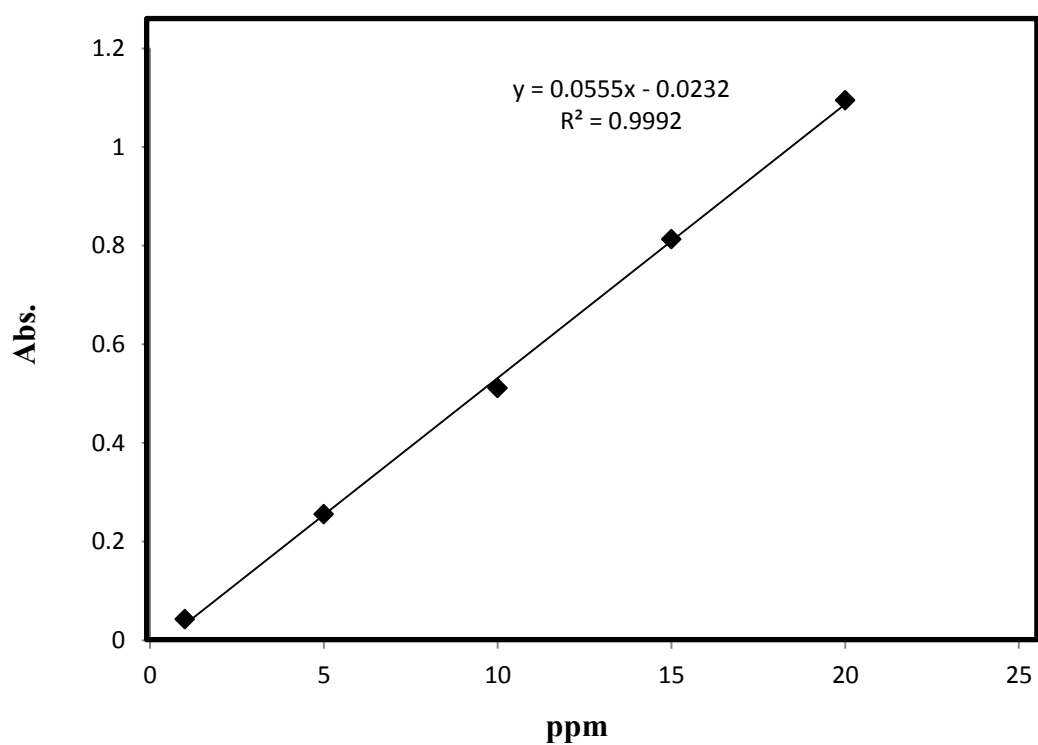
Concentration (ppm)	Absorbance (avg.)
1	0.060
5	0.284
10	0.487
15	0.855
20	1.182



**Figure 1E** Calibration curve of piperine in ethanol

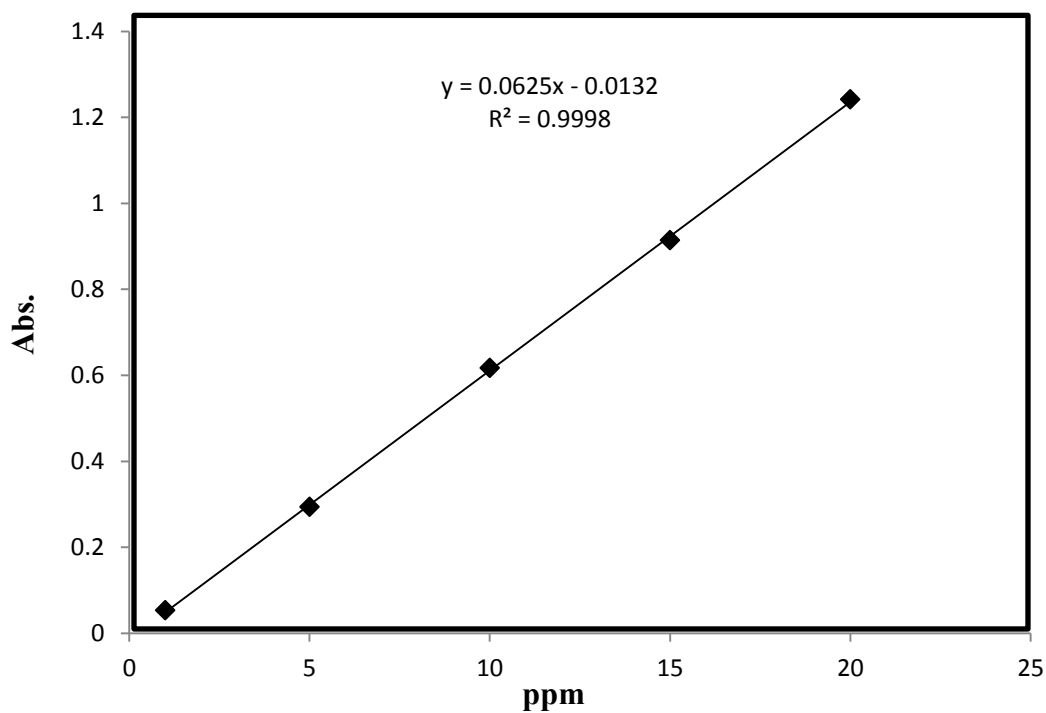
**Table 2E** Absorbance of piperine drug in pH 1.2 determined in 342 nm

Concentration (ppm)	Abs.	Abs.	Abs.	Avg.	SD
1	0.144	0.149	0.141	0.144	0.01
5	0.348	0.368	0.357	0.357	0.01
10	0.618	0.591	0.632	0.613	0.02
15	0.910	0.872	0.963	0.915	0.05
20	1.195	1.250	1.146	1.197	0.05

**Figure 2E** Calibration curve of piperine in pH 1.2

**Table 3E** Absorbance of piperine drug in pH 4.0 determined in 342 nm

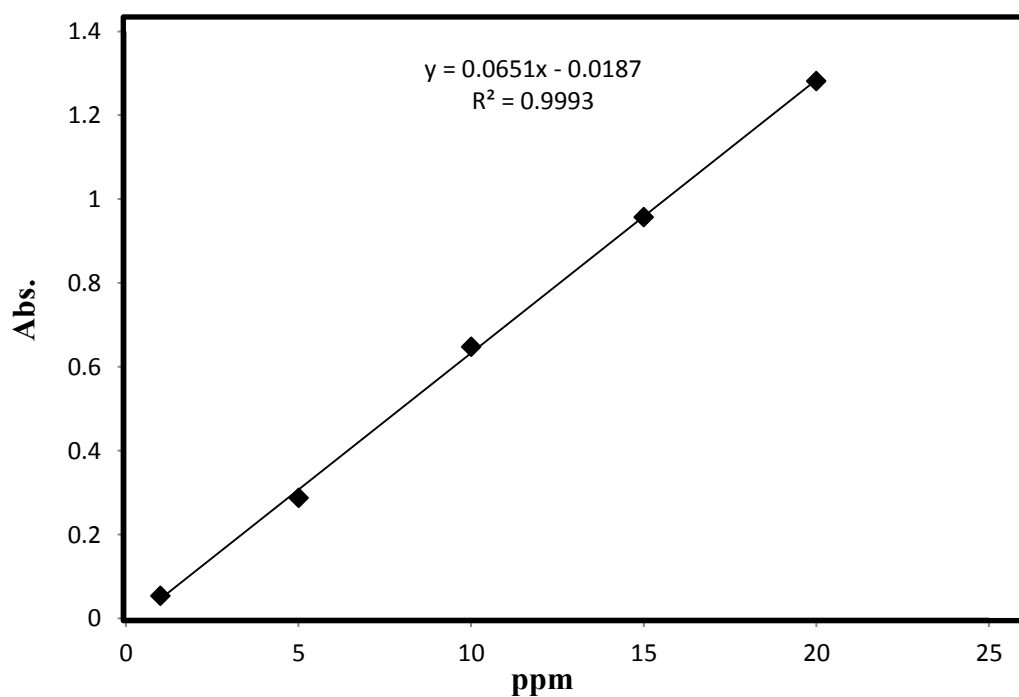
<b>Concentration (ppm)</b>	<b>Abs.</b>	<b>Abs.</b>	<b>Abs.</b>	<b>Avg.</b>	<b>SD</b>
1	0.149	0.145	0.148	0.147	0.01
5	0.411	0.367	0.385	0.387	0.02
10	0.717	0.741	0.674	0.711	0.03
15	1.001	0.970	1.053	1.008	0.04
20	1.359	1.274	1.374	1.335	0.05

**Figure 3E** Calibration curve of piperine in pH 4.0



**Table 4E** Absorbance of piperine drug in pH 6.4 determined in 342 nm

Concentration (ppm)	Abs.	Abs.	Abs.	Avg.	SD
1	0.156	0.159	0.152	0.155	0.01
5	0.379	0.396	0.394	0.389	0.01
10	0.759	0.745	0.744	0.749	0.01
15	1.049	1.071	1.057	1.059	0.01
20	1.344	1.413	1.394	1.383	0.04

**Figure 4E** Calibration curve of piperine in pH 6.4

## APPENDIX F

### Cumulative Drug Release

**Table 1F Cumulative 1% PIP release from chitosan microspheres in pH 1.2**

Time(min)	Amount of PIP release				
	1	2	3	Mean	SD
0	0	0	0	0	0
10	9.8031	9.6705	8.6895	9.387721	0.608283
20	12.0904	10.5981	10.3428	11.01045	0.943948
30	15.4037	12.9313	11.8644	13.39979	1.815606
60	17.5075	16.8368	13.0839	15.80942	2.384057
90	21.0294	19.5996	17.0896	19.23952	1.994417
120	26.5866	23.3217	23.3225	24.41024	1.884768
180	31.6099	28.7204	29.8056	30.04532	1.459613
240	37.5676	35.0033	37.6485	36.7398	1.504361
300	48.8555	42.1121	45.6498	45.53915	3.373067
360	59.0674	53.2332	53.6094	55.30336	3.265179
480	66.1929	61.2154	61.8694	63.09254	2.704797
720	78.0998	74.1567	73.8096	75.35536	2.383054

**Table 2F Cumulative 1% PIP release from chitosan microspheres in pH 4.0**

Time(min)	Amount of PIP release				
	1	2	3	Mean	SD
0	0	0	0	0	0
10	0.3579	0.3061	0.2764	0.313481	0.041243
20	0.7751	0.6492	0.6418	0.688691	0.074933
30	2.2145	1.9627	1.9701	2.049086	0.143316
60	3.4687	2.9724	3.1799	3.207012	0.24926
90	4.6785	4.0341	4.2489	4.320494	0.328135
120	6.7698	5.1920	5.4142	5.792	0.854039
180	8.5721	8.1351	8.2092	8.305481	0.233891
240	15.6856	14.9079	15.3597	15.31773	0.390584
300	28.0658	26.1769	23.1917	25.81146	2.4575
360	41.1867	39.2237	35.5719	38.66074	2.849427
480	55.8631	54.0113	50.1172	53.33052	2.932827
720	67.9493	64.4234	62.2553	64.876	2.873891

**Table 3F Cumulative 1% PIP release from chitosan microspheres in pH 6.4**

Time(min)	Amount of PIP release				
	1	2	3	Mean	SD
0	0	0	0	0	0
10	1.1073	0.9878	1.1571	1.08404	0.086986
20	2.2736	2.1484	2.4905	2.304147	0.173071
30	3.7883	3.6006	3.9704	3.786435	0.184908
60	4.9809	4.8145	5.4546	5.083348	0.332082
90	6.9345	6.7859	7.3925	7.037606	0.316182
120	8.5751	9.1945	9.5878	9.119161	0.510535
180	12.4787	13.6265	13.9927	13.36595	0.789932
240	17.0258	18.6807	19.7254	18.47727	1.36122
300	27.4990	29.3530	30.3337	29.06189	1.439581
360	39.1840	40.2230	42.4497	40.6189	1.66842
480	49.3941	49.8073	51.8917	50.36435	1.338741
720	63.7618	63.7139	63.9145	63.79675	0.10474

**Table 4F Cumulative 1% PIP release from pCA-chitosan microspheres in pH 1.2**

Time(min)	Amount of PIP release				
	1	2	3	Mean	SD
0	0	0	0	0	0
10	11.5286	10.6646	10.0000	10.73106	0.766453
20	13.4869	13.8340	12.4383	13.25309	0.72662
30	17.2619	18.2440	15.4527	16.98617	1.415932
60	21.2066	23.2816	19.6411	21.37646	1.826196
90	26.6061	28.2750	22.5890	25.82336	2.922706
120	31.8579	32.1607	26.3270	30.1152	3.284181
180	38.0180	37.4790	31.5640	35.687	3.58076
240	44.0230	43.7720	36.8158	41.53695	4.090532
300	49.4152	50.3013	42.9538	47.55674	4.010831
360	60.1167	59.9985	53.4212	57.84547	3.831977
480	69.6515	69.0385	64.6101	67.7667	2.750819
720	81.9790	80.5538	75.6823	79.40506	3.3018

**Table 5F Cumulative 1% PIP release from pCA-chitosan microspheres in pH 4.0**

Time(min)	Amount of PIP release				
	1	2	3	Mean	SD
0	0	0	0	0	0
10	5.8505	5.5816	7.3849	6.27235	0.972845
20	12.6780	12.4551	14.9338	13.35563	1.37125
30	13.8203	13.6236	16.1875	14.54383	1.426894
60	14.6807	14.3987	16.9757	15.35169	1.413512
90	16.7869	17.2197	19.2656	17.75738	1.323941
120	20.1062	21.6341	23.1882	21.64284	1.541002
180	24.3830	24.5797	28.2321	25.73158	2.167769
240	28.0826	28.7515	33.2761	30.03672	2.825218
300	37.5725	38.6020	44.2151	40.12984	3.575178
360	48.1311	48.8000	54.9705	50.63388	3.770477
480	57.5882	57.1816	63.4439	59.40459	3.504076
720	70.0957	69.8859	75.6498	71.87716	3.268919

**Table 6F Cumulative 1% PIP release from pCA-chitosan microspheres in pH 6.4**

Time(min)	Amount of PIP release				
	1	2	3	Mean	SD
0	0	0	0	0	0
10	1.6142	1.4611	1.5802	1.551816	0.080364
20	4.0707	3.9655	4.2003	4.078824	0.117655
30	6.7129	6.9036	7.0755	6.897312	0.181391
60	9.8505	10.0683	9.9255	9.948104	0.110632
90	14.0540	14.1257	13.9590	14.04626	0.083656
120	16.2361	16.7447	15.9830	16.32123	0.387924
180	18.9097	19.7470	18.9866	19.21443	0.462803
240	21.9291	22.7543	22.2394	22.30761	0.416841
300	33.5109	33.8180	32.7686	33.36584	0.53952
360	44.6224	44.8704	44.5267	44.67316	0.17737
480	54.2085	54.7587	54.4780	54.48173	0.2751
720	64.4494	65.0399	64.4041	64.63111	0.354708
1440	68.4200	69.2937	68.6139	68.77584	0.458845

**Table 7F Cumulative 1% PIP release from pCA-HT-chitosan microspheres in pH 1.2**

Time(min)	Amount of PIP release				
	1	2	3	Mean	SD
0	0	0	0	0	0
10	8.2661	8.2530	8.4358	8.318318	0.101975
20	18.9411	19.7049	13.5749	17.40697	3.340592
30	30.1972	31.1176	24.5176	28.61078	3.574589
60	38.9268	41.8645	35.2579	38.68303	3.31004
90	47.5029	49.7454	42.0590	46.43578	3.95275
120	53.5690	56.5296	48.4450	52.84785	4.090265
180	59.9288	64.1037	54.8440	59.6255	4.637294
240	65.6685	69.4320	59.9765	65.02568	4.760434
300	70.0437	74.0945	64.7239	69.62071	4.699639
360	73.0154	78.4371	69.0142	73.48892	4.729263
480	74.6423	80.9453	72.4820	76.0232	4.397373
720	81.2711	88.3967	80.2866	83.3181	4.425618



**Table 8F Cumulative 1% PIP release from pCA-HT-chitosan microspheres in pH 4.0**

Time(min)	Amount of PIP release				
	1	2	3	Mean	SD
0	0	0	0	0	0
10	2.8707	2.9229	1.9026	2.565411	0.574596
20	4.8023	4.9994	4.7038	4.835169	0.150539
30	8.1948	7.9513	7.8064	7.984155	0.196276
60	12.1072	11.6730	11.1119	11.63072	0.499029
90	14.8272	13.8249	13.7235	14.12522	0.610087
120	18.8180	18.2412	16.9867	18.01527	0.936317
180	22.8464	21.6962	20.3930	21.64522	1.227462
240	34.2475	32.8858	31.9072	33.01353	1.175362
300	45.4777	43.4957	42.9559	43.97643	1.327836
360	56.2788	54.2272	54.4290	54.97836	1.130759
480	67.0974	64.8661	64.9925	65.65198	1.253356
720	75.5925	75.0713	75.0933	75.25237	0.294738

**Table 9F Cumulative 1% PIP release from pCA-HT-chitosan microspheres in pH 6.4**

Time(min)	Amount of PIP release				
	1	2	3	Mean	SD
0	0	0	0	0	0
10	6.8829	7.2280	6.8774	6.996112	0.20085
20	13.9551	14.2456	13.9941	14.06495	0.157695
30	18.5250	18.7743	18.2111	18.50349	0.282234
60	19.8107	20.0216	19.9086	19.91362	0.105557
90	21.2393	21.4564	21.2488	21.31485	0.122678
120	25.0000	25.8627	24.2859	25.04953	0.78953
180	30.2300	30.5973	28.9521	29.92646	0.863566
240	35.5523	35.6102	34.2473	35.1366	0.770736
300	44.6782	44.2407	43.8072	44.24206	0.43548
360	54.4669	54.0345	53.2337	53.91169	0.62574
480	64.5824	63.1108	62.5087	63.40064	1.066812
720	70.8459	69.9698	70.6923	70.50268	0.467808

**Table 10F Cumulative 5% PIP release from pCA-HT-chitosan microspheres in pH 1.2**

Time(min)	Amount of PIP release				
	1	2	3	Mean	SD
0	0	0	0	0	0
10	8.9468	8.9522	9.3479	9.082297	0.230052
20	19.5592	19.0208	19.6777	19.41924	0.350105
30	24.6439	24.2063	25.0408	24.63034	0.417369
60	33.9597	33.6508	34.6353	34.08194	0.503537
90	39.0524	38.7961	39.7710	39.20653	0.505386
120	45.5681	44.7727	44.9657	45.10216	0.414901
180	51.1140	49.8585	51.3514	50.77461	0.802218
240	57.6981	57.8390	56.6795	57.40553	0.632662
300	68.4349	67.9516	66.7224	67.70297	0.882885
360	79.2103	76.7043	76.7015	77.5387	1.447664
480	83.1469	81.4699	80.2499	81.62225	1.454515
720	88.1845	85.7889	84.3651	86.11281	1.93019

**Table 11F Cumulative 5% PIP release from pCA-HT-chitosan microspheres in pH 4.0**

Time(min)	Amount of PIP release				
	1	2	3	Mean	SD
0	0	0	0	0	0
10	1.5771	1.9962	1.6867	1.753333	0.217333
20	5.7162	6.4543	5.9810	6.050476	0.373927
30	8.1981	9.3695	10.0143	9.193968	0.920734
60	15.6467	16.7705	17.4438	16.62032	0.907932
90	22.1733	23.3614	21.5814	22.37205	0.906493
120	28.3426	29.9982	28.1880	28.84294	1.003501
180	34.9940	36.7231	34.4270	35.38141	1.196057
240	42.6071	43.7828	41.7423	42.71071	1.024177
300	50.4772	50.9440	48.7851	50.06878	1.135936
360	58.8068	58.8621	57.6165	58.42846	0.703704
480	68.1839	67.9345	65.8546	67.32434	1.278908
720	80.5239	79.6816	78.4660	79.55719	1.03456

**Table 12F Cumulative 5% PIP release from pCA-HT-chitosan microspheres in pH 6.4**

Time(min)	Amount of PIP release				
	1	2	3	Mean	SD
0	0	0	0	0	0
10	0.3323	0.2933	0.2710	0.298871	0.030988
20	0.7091	0.6144	1.1654	0.829642	0.294625
30	1.8539	1.6619	2.2279	1.914557	0.287845
60	3.4145	3.0394	3.7551	3.402977	0.358005
90	5.4999	5.0124	5.7364	5.416231	0.36922
120	8.1241	7.8213	8.6066	8.18399	0.396066
180	17.4726	17.3329	18.0052	17.60354	0.354782
240	27.7728	27.7889	28.5670	28.04288	0.453948
300	38.2338	37.0534	39.0507	38.11264	1.004185
360	49.1518	47.7098	49.2508	48.70411	0.862549
480	61.2553	59.9980	61.5528	60.93535	0.825292
720	77.7260	74.7713	77.2611	76.58611	1.588814

## VITA

Name : Miss. Thatthai Pengpong

Date of birth : March 26, 1988

Nationality : Thai

University Education : Bachelor's Degree from Department of Chemistry, Faculty of Science, Prince of Songkla University, 2006-2009  
Master's Degree from Program of Petrochemistry and Polymer Science, Faculty of Science, Chulalongkorn University, 2010-2012

Conference attendance: Poster presentation "A novel mucoadhesive hydrophobic polymer of *p*-coumaric acid thiolated chitosan" at the 9th SPSJ International Polymer Conference (IPC 2012), Polymer Science and Technology, Kobe, Japan